

**Development of novel dyes and fluorescence-imaging based
approaches for cellular localization and dynamics of lipid droplets**

PhD thesis

Soujanya Kuntam

Supervisor: Dr. Ferhan Ayaydin

Biological Research Centre of the Hungarian Academy of Sciences,
Institute of Plant Biology
Cellular Imaging Laboratory

Doctoral School of Biology
University of Szeged

Szeged, 2016

TABLE OF CONTENTS

LIST OF ABBREVIATIONS	4
LIST OF FIGURES	5
1. INTRODUCTION	7
1.1. Lipid droplets	7
1.1.1. LD structure and size	8
1.1.2. LD biogenesis	10
1.1.3. LDs are highly conserved structures.....	12
1.1.4. Economic importance	13
1.1.5. Visualizing LDs.....	14
1.1.6. Dye discovery	16
1.1.7. LDs and plant cell cycle	18
1.2. Detection of DNA replication (S-phase) in plants	19
1.2.1. Labeling with tritiated thymidine.....	21
1.2.2. Labeling with thymidine analog 5-bromo-2-deoxyuridine (BrdU)	22
1.2.3. EdU and click chemistry	22
2. OBJECTIVES	25
3. MATERIALS AND METHODS.....	26
3.1. Chemicals.....	26
3.2. Cell culturing.....	27
3.3. Cell treatment	28
3.3.1. Treatment of human HeLa cells with selected compounds	28
3.3.2. Plant cell treatment with fluorochromes	28
3.4. Colocalization of novel dyes	29
3.4.1. Co-localization of chemicals with fluorescent markers on human HeLa cells	29
3.4.2. Co-localization on rice Unggi 9 cells	29
3.5. Detecting S-phase of cell cycle in tobacco BY-2 cells using EdU	30
3.5.1. EdU labeling on BY-2 cells	30
3.5.2. Detection of EdU using fluorescence microscopy	30

3.6. Blocking BY-2 cells in S-phase using hydroxyurea	31
3.7. Confocal laser scanning microscopy	31
3.8. Three dimensional image analysis and LD quantification	33
4. RESULTS AND DISCUSSION	34
4.1. Novel fluorochrome discovery through combinatorial chemistry	34
4.1.1. Small molecule microarray (SMM) prescreening	35
4.1.2. <i>In vivo</i> microscopy studies of the prescreened potential fluorochromes	36
4.1.3. Intracellular localization confirmation by colocalization with known markers.....	42
4.1.4. Unusual spectral behavior of chemical C2	45
4.1.5. Effect of selected chemicals on long-term viability of cells.....	47
4.2. Characterizing blue-fluorescent LD markers in plants	50
4.2.1. Localization and toxicity of Ac chemicals on plant suspension cultures	51
4.2.2. Ac chemicals and Nile Red colocalization	55
4.2.3. Spectral emission characteristics of Ac chemicals	57
4.2.4. LD detection on various plant cultures.....	59
4.2.5. LD labeling on intact Arabidopsis seedlings	62
4.3. Monitoring LD behavior during plant cell cycle	67
4.3.1. LD variability in BY-2 cells across the culture's growth curve.....	68
4.3.2. LDs in hydroxyurea synchronized BY-2 cells	71
5. CONCLUSIONS.....	77
REFERENCES	79
ACKNOWLEDGEMENTS	92
SUMMARY	93
ÖSSZEFOGLALÁS	96
PUBLICATION LIST	99

LIST OF ABBREVIATIONS

BY-2	<i>Nicotiana tabacum</i> cultivar BY-2 (Bright Yellow – 2)
CLSM	Confocal Laser Scanning Microscopy
DAG	Diacylglycerol
DAPI	4',6- diamidino-2-phenylindole
DMEM	Dulbecco's modified Eagle's medium
DMSO	Dimethyl sulfoxide
EdU	5-ethynyl-2'-deoxyuridine
EGFP	Enhanced Green Fluorescence Protein
ER	Endoplasmic reticulum
FDA	Fluorescein diacetate
FP	Fluorescent protein
H33342	Hoechst 33342
HeLa	Human cervical cancer cells originating from Henrietta Lacks
HTS	High-throughput screening
HU	Hydroxyurea
LD	Lipid droplet
OA	Object Analyzer tool
PI	Propidium iodide
SMM	Small molecule microarray
S-phase	DNA synthesis (replication) phase of the cell division cycle
TAG	Triacylglycerol
Unggi 9	<i>Oryza sativa</i> subspecies japonica cultivar 'Unggi 9'

LIST OF FIGURES

Figure 1. Schematic representation of the structures of oleosin, caleosin, and steroleosin on the surface of LDs	9
Figure 2. Schematic representation of models for oleosin-dependent/independent LD formation from the ER	11
Figure 3. EdU detection utilizing click-chemistry	24
Figure 4. Pseudocolored images of an SMM block excited by 532 and 633 nm lasers	35
Figure 5. Fluorescence emission and intracellular localization of selected chemicals	39
Figure 6. Fluorescence emission of selected chemicals after 24-hours	41
Figure 7. Colocalization of chemicals with fluorescent markers.....	43
Figure 8. Laser scanning-induced relocalization of chemical C2 from mitochondria to cytoplasm and nucleoli	45
Figure 9. Stability of chemical C2 using low laser intensity settings	46
Figure 10. Viability analyses of 24-hour treated HeLa cells	48
Figure 11. Nuclear morphology analyses of 24-hour treated HeLa cells	49
Figure 12. Localization of B2, B3 and C4 dyes on Unggi 9 cells	51
Figure 13. LD labeling efficiency and analysis of cell viability using various treatment durations and doses of Ac chemicals on rice culture	52
Figure 14. Ac chemicals and LD dye Nile Red colocalization.....	56

Figure 15. Comparison of spectral emission characteristics of Ac chemicals, LD540 and Nile Red using spectral imaging and live cell microscopy on rice cell cultures	58
Figure 16. Detection of LDs, EGFP and cell borders on live rice cell cultures.....	59
Figure 17. LD detection on various plant cultures using Ac chemicals	60
Figure 18. Application of low concentration of Ac chemicals on alfalfa cultures	61
Figure 19. LD labeling on seedlings using Ac chemicals.....	62
Figure 20. LD labelling on Arabidopsis cotyledon using Ac-202.....	64
Figure 21. Optical z-section of Arabidopsis cotyledon labelled with Ac-202.....	66
Figure 22. Ac-1041 labeling on Arabidopsis seedling.....	67
Figure 23. Detection of LDs and S-phase nuclei on fixed BY-2 cells.....	70
Figure 24. 3D reconstruction of BY-2 cells using 3D analysis software.....	71
Figure 25. Change in total LD, S-phase and mitotic index count of BY-2 cells during growth	72
Figure 26. Re-emergence of LDs after HU removal in BY-2 cells	73
Figure 27. Re-emergence of LDs after HU removal confirmed with multiple optical z-sections.....	74
Figure 28. Comparing cell viability of control and HU treated culture.....	75
Table 1. Hormone concentrations and media used for plant cultures.....	27
Table 2. Chemical structures and labeling characteristics of the selected molecules.....	38

1. INTRODUCTION

1.1. Lipid droplets

Lipid droplets (LDs) are one of the two major forms of macromolecular lipid assemblies in cells, with the other being the lipid bilayer, which forms the matrix of cellular membranes. LDs are responsible for intracellular storage of neutral lipids, serving as the long-term energy storage compartments, as well as a reserve of components for the synthesis of membrane phospholipids.

Lipotoxicity becomes a significant danger at relatively lower concentrations, potentially triggering cell death, requiring cells to have compartments for lipid storage rather than simply allowing lipids to diffuse in the cytoplasm (Maxfield & Tabas, 2005). Cells can effectively buffer themselves against this toxicity with the effectively compartmentalized storage of lipids within LDs, and store far larger quantities of lipids, giving them a larger reserve of energy and membrane components, than would be possible without such structures (Farese & Walther, 2009). The evolutionary advantage of this strategy is significant enough that even prokaryotes, which lack most intracellular membrane-bound compartments, appear to have membrane-bound LDs, even though they most likely are subdomains of the plasma membrane (Ding *et al.*, 2012; Murphy, 2012). LDs thus are key structures for survival and growth. Their principal contents are triacylglycerols (TAGs), diacylglycerols (DAGs), sterol esters (SEs) and wax esters (WEs). They are of significant medical interest due to their role in lipid metabolism-related disorders such as diabetes and obesity (Walther & Farese, 2009). Despite their importance, they have only been

studied intensively in recent years, and are among the least well-understood organelles (Farese & Walther, 2009; Kühnlein, 2012).

LDs were first observed in non-seed plant tissue, in the 19th century by Hanstein. Their neutral lipid content provides a different refractive index from the surrounding aqueous environment making them clearly visible and distinguishable by light microscopy, facilitating their early discovery (Farese & Walther, 2009). LDs when first discovered, were termed “microsomes” or “liposomes” (Wilson, 1896). These names became obsolete over the 20th century and were later taken up by other structures. Depending on the organism and scientific field, LDs have been referred to as adiposomes, granules, oleosomes, oil bodies, lipid bodies or lipid droplets. The term now emerging as preferred by the majority of authors is “lipid droplet” (Martin & Parton, 2006; Farese & Walther, 2009; Murphy, 2012), which will be used throughout this thesis.

1.1.1. LD structure

Mammalian white adipocyte lipid droplets are probably the most extensively studied type of LDs. They are often considerably large, of the order of 100 µm in diameter. Usually one or a few of these LDs typically take up majority of the internal volume of these cells. In contrast, LDs in other cells are primarily small and numerous, of the order of 1-20 µm in diameter (Thiele & Spandl, 2008). The smallest LDs identified in fungi were less than 0.1 µm in diameter; no lower limit on the size of LDs is firmly established (Long *et al.*, 2012). Plant LDs are typically 1-5 µm in diameter.

LDs are made up of a hydrophobic core of neutral lipids such as TAGs which are highly

reduced, concentrated energy storage molecules consisting of three fatty acid chains bound to a glycerol backbone (Chapman *et al.*, 2012); and sterol esters (SEs), a heterogeneous category of neutral lipid which are important as membrane lipid components. LDs are bound by a monolayer, single leaflet, phospholipid membrane composed of amphipathic phospholipids, glycolipids and/or sterols. This single leaflet membrane as opposed to the more familiar bilayer membranes with two leaflets, is possible because of the highly hydrophobic core dominated by non-polar neutral lipids (Tauchi-Sato *et al.*, 2002). The LD membrane is highly similar to the endoplasmic reticulum (ER) membrane (Fujimoto *et al.*, 2008), which is consistent with the hypothesis that LD biogenesis occurs in the ER. Most LDs contain a specific population of proteins, which are either more or less tightly bound to their surface or embedded in the monolayer (Murphy, 2001; Purkrtova *et al.*, 2008; Chapman & Ohlrogge, 2012).

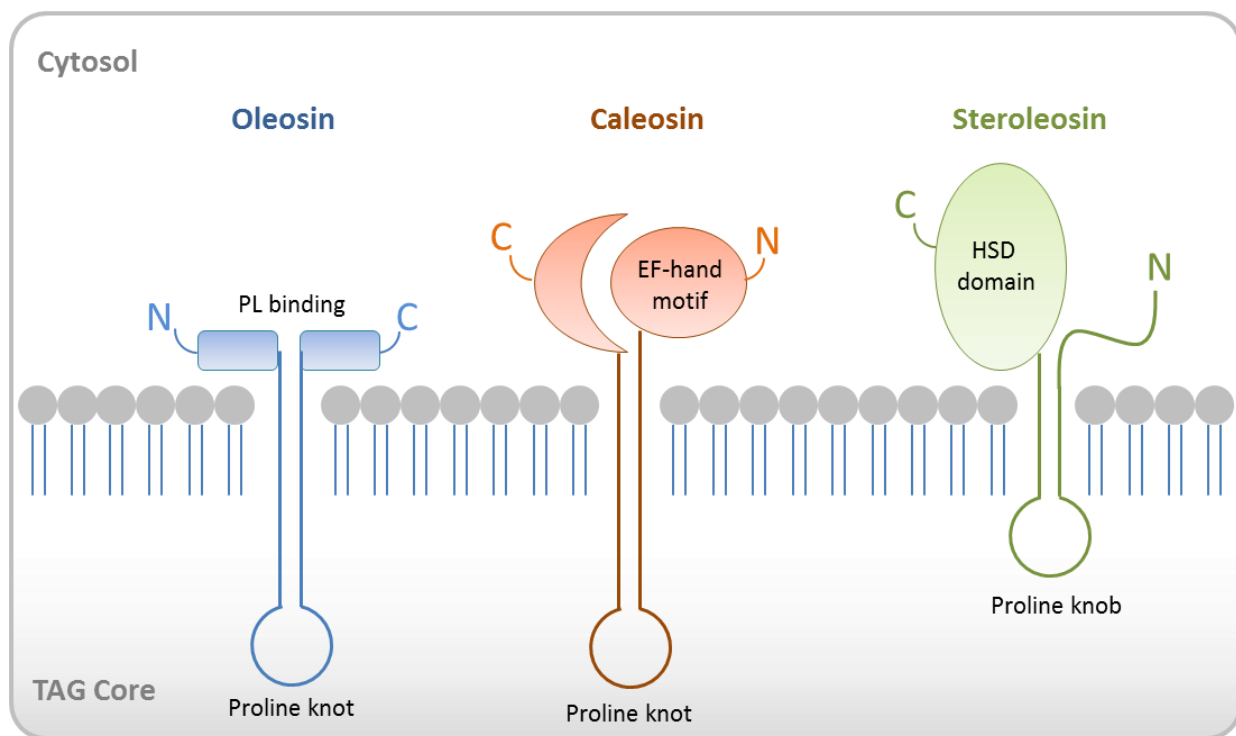


Figure 1. Schematic representation of the structures of oleosin, caleosin, and steroleosin on the surface of LDs. Cytosol-facing N- and C-terminal domains of oleosin (including the phospholipid, PL binding region), caleosin (including its calcium-binding EF-hand motif) and steroleosin (including its hydroxysteroid dehydrogenase, HSD domain) are shown. Illustration is drawn based on Chapman *et al.*, (2012).

A large number of LD associated proteins have been identified which have greatly enhanced our knowledge of LD function in both seed and non-seed tissues (Fig. 1). Some of the major LD associated proteins studied extensively thus far are, oleosins, caleosins and sterol dehydrogenases (steroleosins) (Chapman *et al.*, 2012).

1.1.2. LD biogenesis

As in all other eukaryotes, LDs in plants are thought to arise from the ER. The most substantial and earliest evidence supporting this concept comes from ultrastructural studies of developing seeds, including those showing frequent and close relation between the ER and LDs (Frey-Wyssling *et al.*, 1963; Wanner & Theimer, 1978). The commonly held theory is that, LD assembly begins with the accumulation of TAG between the two leaflets of the ER bilayer, followed by the expansion and eventual pinching off of the LD into the cytoplasm. This theory was formulated primarily from the ultrastructural studies of plant embryos (Wanner *et al.*, 1981). There is also some evidence from studies in plants for the idea that LDs form a specific subdomain of the ER; that the ER is a dynamic and intricate network containing specialized regions for LD biogenesis (Sparkes *et al.*, 2009; Park & Blackstone, 2010; Lynes & Simmen, 2011). For example, oleosins, the structural protein that stabilize LDs and diacylglycerol acyltransferase (DGAT), an enzyme responsible for synthesizing the final step in TAG biosynthesis, have both been found to localize within specific regions of the ER (Shockey *et al.*,

2006; Gidda *et al.*, 2009). These results with those obtained from recent studies in yeast (Adeyo *et al.*, 2011) and mammals (McFie *et al.*, 2010), have helped formulate the concept that a localized partitioning of DGAT and/or DAG within the ER serves as the initiator for TAG accumulation and eventual LD formation (Fig. 2a).

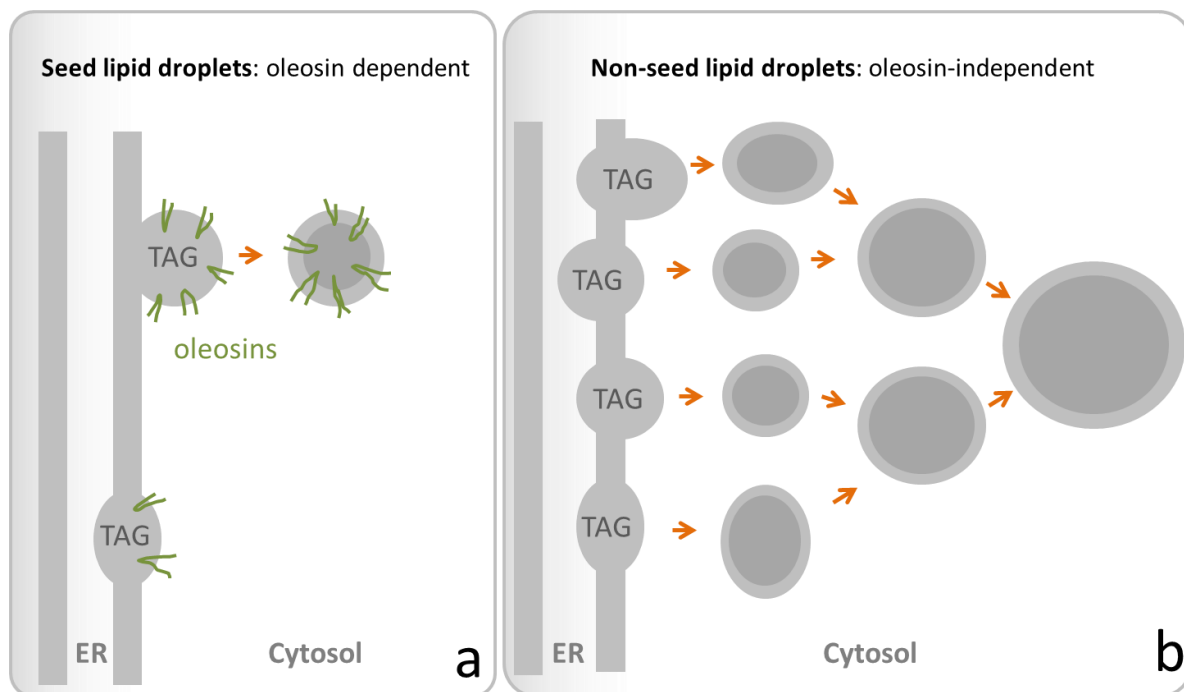


Figure 2. Schematic representation of models for oleosin-dependent/independent LD formation from the ER. Oleosins while being translated are inserted into the ER in seed tissues. The inserted oleosins partition into domains in which TAG gets accumulated between two leaflets. This promotes orientation of the hydrophobic/hydrophilic regions of the oleosins. They also help stabilize the LDs in the cytosol and keep them from fusing during the rapid dehydration and rehydration that seed tissues undergo. Illustrations drawn based on Chapman *et al.*, (2012).

However, little is known about the actual mechanism of LD biogenesis, i.e., the induction, growth and disassociation from ER microdomains. But some headway is being made to identify the protein machinery through homology based searches in plants. It is also uncertain whether small LDs emerge from the ER, which then coalesce to form larger LDs (Fig. 2b) or

whether they emerge from the ER budding off in their final size or a combination of the above two processes occur. Theories have been proposed at the biophysical level that the thermodynamics of lipid demixing aids in the formation of small, 12 nm droplets that would bud from the surface of the ER and then fuse in the cytosol (Zanghellini *et al.*, 2010). But this theory calls into question the participation of protein machinery in the process of LD biogenesis. One more alternative model for LD biogenesis predicts that the LDs are formed from coatomer (COP) transport vesicles (Kalantari *et al.*, 2010). Alternatively, they are proposed to not even detach from the ER, but instead remain as an integral part of the ER, growing and shrinking depending on the needs of the cell/organism (Goodman, 2009). The notion that there is also a likelihood of LD biogenesis being species and even cell-type specific, and may involve different classes of proteins that bind to LD and mediate LD formation, size, and interaction, cannot be disregarded (D J Murphy, 1993; Napier *et al.*, 1996; Schmidt & Herman, 2008). Hence, with the data currently available, a unified concept of LD biogenesis tends to draw from several proposed mechanisms that may not be mutually exclusive.

1.1.3. LDs are highly conserved structures

Cytosolic lipid inclusions are found in many and perhaps all eukaryotic and bacterial cells in varying amounts. Similar structures are found in several types of archaea too. These structures mostly occur as spheroidal macromolecular assemblies having a neutral lipid ester or lipid based polymer core bound by a phospholipid monolayer membrane (Ding *et al.*, 2012; Murphy, 2012). This is despite the finding of Jacquier *et al.*, (2011) that *Saccharomyces cerevisiae* cells can continue to grow and reproduce even when lipid droplet formation is

blocked, which indicates that they are not absolutely required for life. But their wide evolutionary conservation must represent a large selective advantage, most likely conferred by the ability to store energy and thus survive periods of nutrient starvation.

LDs are structurally similar between different groups of organisms, and the enzymes that are responsible for lipid synthesis and degradation are predominantly conserved; for example, monoacylglycerol lipase appears to be conserved between bacteria and humans (Rengachari *et al.*, 2012). LD regulatory proteins are not as widely conserved: for example, the perilipin family, proteins with major roles in LD regulation in animals, are absent from many fungi (Bickel *et al.*, 2009). Certain viral proteins have plant LD associated protein, oleosin-like proline knot motifs that mediate their localization to LDs in mammalian cells (Hope *et al.*, 2002). And also, ectopic expression of plant oleosins in either mammalian or yeast cells resulted in their proper targeting to LDs in the heterologous system (Hope *et al.*, 2002; Beaudoin & Napier, 2002).

In general, the high level of structural and functional homology that is believed to exist between LDs across the tree of life, supports the use of even evolutionarily distant organisms as models for human LD function and dysfunction.

1.1.4. Economic importance

Lipid droplets are the major sites of cellular lipid metabolism and storage, and are thus the immediate source of oils and fats produced agriculturally for human consumption. Historically, selective breeding to produce improved crops and better breeds of animals, has produced breeds with increased LD production (Pang *et al.*, 2006). This enhancement of nutritional value can be further amplified by genetic engineering, with relevance to almost all

food sources. Overall, a thorough understanding of LD biology could have a wide-range of food security implications (Farese & Walther, 2009).

Biodiesel production also relies on oils from LDs. Plants such as *Brassica carinata* have been cultivated in recent times for this purpose (Bouaid *et al.*, 2005). More recent approaches focus on engineering microorganisms to produce increased yields of oil (Farese & Walther, 2009). Hence, a detailed understanding of lipid synthesis is critical for this economically and environmentally important field.

1.1.5. Visualizing LDs

In recent times, progress in genomics, proteomics and technical advances in cell biology have helped in broadening our understanding of the nature and function of LDs. Techniques such as genome/transcriptome sequencing of whole organism/specific cell types, generating gene knockout/overexpression lines and developments in mass spectrometry have enabled researchers to extend their knowledge of LD composition, function and remodeling in live cells (de Kroon, 2007). But some of the most important insights have come from the use of new imaging techniques. They have helped us understand the real-time dynamics of LDs in live cells and following such behavior during processes such as inflammatory responses (Melo *et al.*, 2011). Examples of such imaging techniques include vibrational imaging of LDs in live fibroblast cells (Nan *et al.*, 2003), novel fixation methods for LDs in immunofluorescence microscopy (DiDonato & Brasaemle, 2003), multiples CARS (Coherent Anti-Stokes Raman Spectroscopy) microscopy (Müller & Schins, 2002), freeze-fracture replica immunogold labeling (Robenek *et al.*, 2011), stimulated Raman scattering microscopy (Bewersdorf *et al.*, 2011), quantitative

electron microscopy (Cheng *et al.*, 2009) and confocal reflection microscopy (Gáspár & Szabad, 2009).

However, in the past few years, there have been particular advances in the use of live imaging systems including live microscopy (Digel *et al.*, 2010; Somwar *et al.*, 2011), time-lapse adaptive harmonic generation microscopy (Watanabe *et al.*, 2010) and vital staining in combination with fluorescence activated cell sorting (Cooper *et al.*, 2010). Such imaging tools in combination with photostable genetically encoded fluorescent proteins can be used in multiplexed tracking of protein remodeling on LDs (Tsien, 2009). Photo-switchable fluorescent proteins as well as fluorescent timers can be used for the quantitative assessment of LD protein dynamics (Terskikh *et al.*, 2000; Chudakov *et al.*, 2007). Protein conformational changes or protein–protein interactions relevant to LDs can be observed using fluorescent sensors, such as those based on Fluorescence Resonance Energy Transfer (FRET) (Giepmans *et al.*, 2006). Combining a reliable LD marker with these tools can create a versatile scheme for investigating LD biology. Yet, many commercially available live cell LD dyes have limited ability to penetrate plant cell wall.

Moreover, the available cell wall permeable dyes such as Nile Red and BODIPY 493/503 have certain drawbacks. Not only does Nile Red have a broad emission range occupying the orange and red regions of the spectrum, but also its absorption significantly overlaps with widely used green and red reporters such as EGFP (Enhanced Green Fluorescence Protein) and mCherry, hindering the use of most ready-made fluorescent reporters in colocalization experiments (Miquel *et al.*, 2014). Although BODIPY 493/503 (which fluoresces in green) can be combined with red fluorescent constructs for two-color imaging, its lesser photostability and photoconvertible properties limit its ability to be utilized in long-term imaging experiments

(Ohsaki *et al.*, 2010). Even though there are other live cell staining LD dyes with better photostability, such as BODIPY 505/515 and LD540 (Spandl *et al.*, 2009), they still fluoresce in the green to orange region of the visible spectrum. Recently, a new blue-red emission live cell dye monodansylpentane (MDH) has also been reported (Yang *et al.*, 2012). Due to its dansyl moiety, this dye shows strong solvatochromatic behavior (ability of a chemical substance to change color due to change in solvent polarity) and shows blue emission on LDs and red emission (550–650 nm) in aqueous cellular compartments (Yang *et al.*, 2012). This dual behavior necessitates proper configuration of microscope settings in multicolor experiments. Therefore, the identification of a live cell dye that can stain LDs while being spectrally well separated from most green, orange and red fluorescence reporters will be a great asset for live cell imaging in studying LD biology.

1.1.6. Dye discovery

Fluorescent proteins (FPs), small molecule dyes (SMDs), chromophoric agents and nanoparticles are commonly used in fluorescence imaging studies, to label cellular compartments, subcellular moieties for both basic and applied research including clinical investigations (Tsien, 2005; Weissleder & Pittet, 2008). SMDs or fluorochromes, are substantially smaller in size in comparison to other fluorescent labels such as FPs. Their high membrane permeability, less or no toxicity, minimal technical limitations and moderate cost also make them a prominent tool to analyze cellular processes in an unperturbed environment. Although a large number of fluorochromes are known and commercially available by now, there is still a demand for novel molecules marking new targets or having improved spectral

characteristics. However, designing molecules with a particular objective in mind, is a time-consuming and expensive process requiring high computational power, expertise and often elaborate chemical synthesis (Henrich *et al.*, 2010). Alternatively, random libraries can be subjected to high-throughput screening (HTS) methods, by which novel dyes with extraordinary characteristics can be identified in a relatively inexpensive and rapid way by simultaneous testing of a large number of compounds, up to hundreds of thousands, in amounts as low as microliters (Manning *et al.*, 2008). While these techniques are routinely used in pharmaceutical research, they have only a limited number of applications in basic science for fluorescent probe discovery (Li *et al.*, 2006; Simeonov *et al.*, 2008; Lea & Simeonov, 2011; Yun *et al.*, 2012)

Microarrays are a powerful HTS tools. Similar to DNA or protein microarray, small molecule microarray (SMM) is a collection of molecules spotted or synthesized on a solid surface in order to examine possible binding partners (Hackler *et al.*, 2003; Darvas *et al.*, 2004; Molnár *et al.*, 2006). This format enables a rapid screen of drug candidates from thousands of small organic compounds that specifically bind to certain proteins marked fluorescently to detect their interaction (Barnes-Seeman *et al.*, 2003; Darvas *et al.*, 2004; Vegas *et al.*, 2007; Shi *et al.*, 2009; Chen *et al.*, 2010; Lee & Park, 2011). Nevertheless, applicability of the selected compounds under *in vivo* conditions cannot be assured in advance. In the course of the quality control process of SMMs, autofluorescent molecules are to be eliminated or ignored at the subsequent data analysis stage as false positives, since they might interfere with the labeling of the studied protein sample. Thus, compounds showing strong autofluorescence drop out of drug screening, although they still have the potential to be fluorescent probes.

Confocal laser scanning microscopy (CLSM) is one of the most ubiquitous research tools in basic cell biology. Mobility, dynamics, interaction and localization of living cells, organelles

and even single molecules can be recorded with high precision due to its high resolution, sensitivity and optical sectioning capability. However, time-consuming manual analysis of images had rendered traditional microscopy a non-scalable method, until the advent of high content microscopy systems, which has opened an accelerated way for screening multitudinous samples (Oheim, 2011). Still, this technique has some drawbacks like difficulties in automated image analysis and higher cost compared to SMMs. Thus, the advantages of these two approaches, SMM and CLSM, can be combined and applied for the discovery of new fluorescent dyes (Molnár and Kuntam *et al.*, 2013).

1.1.7. LDs and plant cell cycle

One of the fundamental characteristics of living organisms is their ability to grow and reproduce. At the cellular level, growth is accomplished by gain of mass, followed by division into two daughter cells. These cell division activities need to be strictly regulated in order to avoid incorporation of mistakes into the genome. As in all eukaryotic life forms, plant cell cycle comprises of four phases, where the DNA synthesis phase (S) and mitotic phase (M) are preceded by gap phases, G1 prior to S-phase and G2 prior to M-phase. These gap phases separate the two highly dynamic phases allowing the monitoring of the cell cycle progression ensuring that critical events such as DNA replication and chromosome segregation are completed with high fidelity (Elledge *et al.*, 1996).

In the past decade, along with an increasing appreciation for the prevalence of LDs throughout biological systems, a broader range of functions associated with LDs has been reported including stress response and pathogen resistance (Coca & San Segundo, 2010),

dormancy release in shoot apical meristems (Rinne *et al.*, 2001), dormancy process in root nodules, photoperiod signaling (Grefen *et al.*, 2008), lipid homeostasis, hormone metabolism/signaling and a specialized role in anther development (Hsieh & Huang, 2004). In growing cells, high energy load and excess fatty acid is thought to trigger TAG synthesis, the main component of LDs. Under conditions of nutrient limitation or rapidly growing cells, TAG is thought to serve two crucial roles: (1) the provision of fatty acids which are then oxidized to generate energy in the absence of other carbon sources; and (2) the production of lipid precursors such as fatty acids and DAG for membrane lipid synthesis, mainly sphingolipids and glycerophospholipids.

In the past years, the neutral lipid content of cells has been linked to cell cycle progression; (Guckert & Cooksey, 1990; Gocze & Freeman, 1994; Kwok & Wong, 2005). This is exciting because the role of lipid droplets in cells may be broader than previously believed. The major TAG lipase in budding yeast, Tgl4p, is phosphorylated and activated by cyclin-dependent kinase 1/cell division cycle protein 28 (Cdk1p/Cdc28p) (Kurat *et al.*, 2009). The resulting lipolysis contributes to bud formation in late G1 phase of the budding yeast cell cycle and lack of lipolysis of TAG delays the same bud formation. Also, recent evidence demonstrates that the major enzymes of the patatin-domain containing family of lipases are structurally and functionally conserved between yeast (Tgl4) and Arabidopsis (SUGAR DEPENDENT 1) (Eastmond, 2006). Other earlier work has shown that the BODIPY 493/503-stained neutral lipid intensity of MA-10 Leydig tumor cells was a function of the cell cycle, although the cells in that study were cultured in high amounts of oleic acid (Gocze & Freeman, 1994). Neutral lipid biosynthesis has also been reported to be coordinated with cell cycle progression in heterotrophic dinoflagellates (Kwok & Wong, 2005). Thus, there appear to be links between cell cycle

progression and neutral lipid turnover, but they are just beginning to be appreciated, and the role of lipid droplets in these processes is yet to be fleshed out.

1.2. Detection of DNA replication (S-phase) in plants

A detailed analysis of the cell cycle is necessary to understand the changes in the structure and metabolic processes of plant cells. Studying cell proliferation is also crucial in assessing cell health, characterizing cellular responses to various treatments or genetic modifications. But such assays become difficult to perform since only a minor fraction of the cells are cycling (e.g. meristematic tissues) and the cell cycle progression in most somatic tissues is asynchronous. Hence, different methods have been developed to enrich cells in a single stage of the cell cycle, synchronizing them artificially. Different plant tissues and cell cultures can be used to obtain synchronously dividing cell populations. Plant tissues such as leaf mesophyll protoplasts (Kapros *et al.*, 1992; Carle *et al.*, 1998) and root meristems (Doležel *et al.*, 1999) have been used successfully to obtain synchronous cell populations. Since the fast growing, suspension culture cells can be grown in large quantities under well-defined conditions and they can be exposed uniformly to synchronizing treatments, they are highly suitable to follow cell cycle-associated changes in most biochemical or cytological parameters. High degree of synchrony has been achieved in various cell cultures such as *Arabidopsis* (Menges & Murray, 2002), alfalfa (Magyar *et al.*, 1997), tobacco BY-2 (Kumagai-Sano *et al.*, 2006), carrot (Ghosh *et al.*, 1999), tomato (Arumuganathan *et al.*, 1991), maize (Peres *et al.*, 1999) and wheat (Wang *et al.*, 1992). Most of the chemical methods used for synchronizing above mentioned cultures are both reproducible and effective.

Chemical methods for synchrony are based on two approaches: deprivation of an essential growth compound or chemical agents which block cell cycle progression at specific stage of the cell cycle (Menges & Murray, 2002). For example, hydroxyurea (HU) reversibly inhibits the ribonucleotide reductase enzyme and consequently the production of deoxyribonucleotides, leading to the accumulation of cells in G1 and early S-phase (Young & Hodas, 1964). On the other hand, aphidicolin, a fungal toxin derived from *Cephalosporium aphidicola*, inhibits the eukaryotic DNA polymerase and the plant α -like DNA polymerase blocking the cells in G1/S phase (Ghosh *et al.*, 1999). Alternatively, mimosine a plant amino acid blocks the cells in the G1/S border by suppressing the formation of the amino acid hypusine in the eukaryotic translation initiation factor 4D (Watson *et al.*, 1991).

The next step in assaying cell proliferation is determining the degree of synchronicity in cell division cycle synchronization experiments. To this effect, most assays estimate the number of cells by either incorporating a modified nucleotide during cell proliferation or by measuring the total nucleic acid content of lysed or isolated cells using flow cytometry. One of the most accurate methods is the direct measurement of new DNA synthesis. A few of the approaches employed to this effect will be explored in detail in the following sections.

1.2.1. Labeling with tritiated thymidine

Autoradiography was the major methodology utilized to measure DNA replication and transcriptional activity during the 1950s and 60s. The cells were pulse labeled with ^3H -thymidine followed by the analysis of the percentage of labeled cells moving through mitosis (Quastler & Sherman, 1959). Tritiated thymidine is detected by the radioactive decay of the ^3H tag. However,

this weak decay can only travel through tissues over a short distance. Hence, detection necessitates thin tissue sections (1-30 μm), covered in photographic emulsion and dark exposure to detect exposed silver grains in the overlaying emulsion. Although *in vitro* and *in vivo* applications of ^3H -thymidine autoradiography has yielded significant information on cell cycle distribution and cell proliferation, it has several drawbacks; dealing with radioactive isotopes, sectioning tissues and the fact that the signal is not detected in the tissue itself but in the overlying emulsion. Also the necessity to exclude extraneous light which would ruin the emulsion during exposure can be cumbersome.

1.2.2. Labeling with thymidine analog 5-bromo-2-deoxyuridine (BrdU)

In the mid-1980s, instead of radioactive markers, the incorporation of halogenated nucleotide analogs such as 5-bromo-2-deoxyuridine (BrdU) into DNA followed by immunodetection with a specific antibody raised against BrdU was developed (Gratzner, 1982; Leif *et al.*, 2004). Although effective and sensitive, it does require DNA denaturation or digestion (using hydrochloric acid, heat or DNase) to expose BrdU to the antibody (Dolbeare *et al.*, 1983; Moran *et al.*, 1985). Antibody-based detection method of BrdU assay also necessitates cell wall digestion in experiments carried out on plant cells. Therefore protoplasts or partially cell-wall-digested cells/organs/tissue sections are often used for BrdU-based detection of proliferative activity in plants (Stroobants *et al.*, 1990). However, a significant wounding and osmotic stress is imposed on live plant cells due to treatment with cell wall digesting enzymes (Fowke, 1994).

1.2.3. EdU and click chemistry

Recently, a new agent 5-ethynyl-2'-deoxyuridine (EdU) has emerged as a remarkable alternative to the above mentioned methods. EdU is a terminal alkyne containing nucleoside analog of thymidine and is incorporated into DNA during active DNA synthesis (Salic & Mitchison, 2008). The EdU detection method is based on click chemistry (Fig. 3). "Click" chemistry (Huisgen 1,3-dipolar cycloaddition) is a type of chemical reaction that occurs at room temperature and is catalyzed by copper Cu(I), resulting in the formation of a strong covalent bond between an azide (present in the structure of the fluorochrome) and an alkyne group (present in EdU) (Kolb & Sharpless, 2003; Darzynkiewicz *et al.*, 2011).

The alkyne group is fairly un-reactive in biological systems and thus allows use in living cells (Agard *et al.*, 2006; Best, 2009). The small molecular size of the detection fluorochrome, compared to that of antibodies required for BrdU based immunodetection, enables efficient penetration into plant cells, without the need for cell wall digestion or harsh DNA denaturation treatments (Kotogány *et al.*, 2010). This considerably simplifies the procedure and reduces the duration of the assay. In addition, the mild non-caustic EdU proliferation assay components keep the proteins intact, allowing their parallel immunocytochemical detection with fluorescence-labeled antibodies. Although initially developed for application in cultured mammalian cells, the EdU assay has been successfully applied in a wide variety of species including bacteria (Ferullo *et al.*, 2009), yeast (Hua & Kearsey, 2011; Lopez-Serra *et al.*, 2013) and a broad spectrum of animals (Kaiser *et al.*, 2009; Warren *et al.*, 2009; Diermeier-Daucher *et al.*, 2009; Limsirichaikul *et al.*, 2009) and plants (Kotogány *et al.*, 2010).

The EdU-based assay has already been applied in several plant tissues and organs such as *Arabidopsis* root tips (Zhu *et al.*, 2011; Notaguchi *et al.*, 2012; Xu *et al.*, 2012; Kakar *et al.*, 2013; Perilli *et al.*, 2013; Xiong *et al.*, 2013), leaf/petiole junction (Ichihashi *et al.*, 2011) and inflorescence (She *et al.*, 2013). The assay was also used to differentiate cells in early and late S-phase in root tips of *Arabidopsis* seedlings (Hayashi *et al.*, 2013).

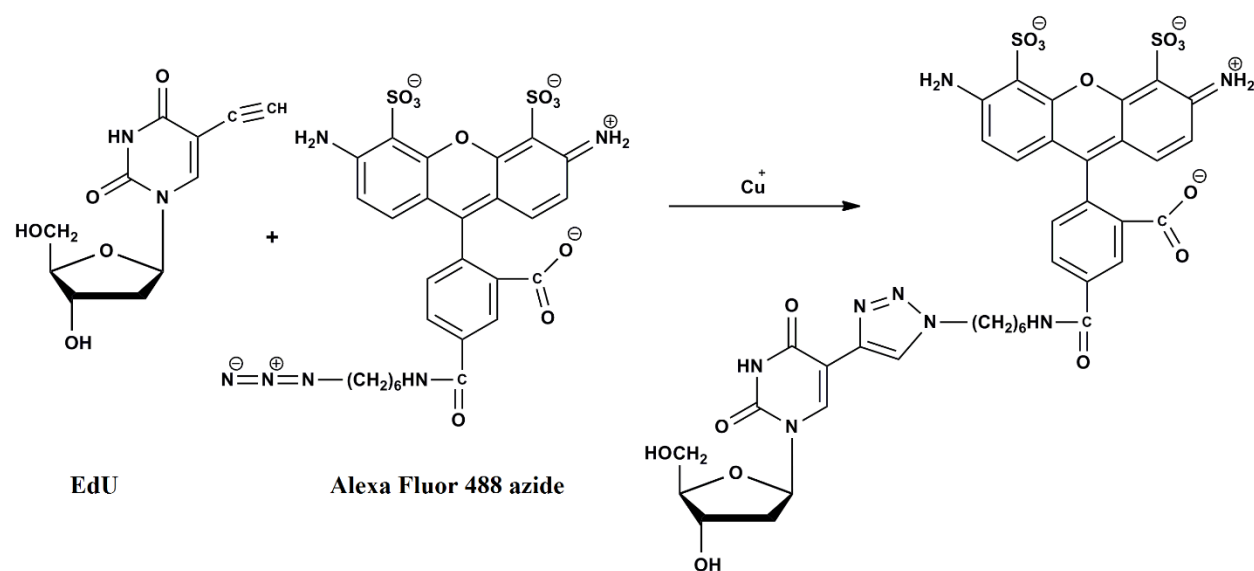


Figure 3. EdU detection utilizing click-chemistry. EdU incorporated into DNA during the S-phase of the cell cycle is detected by copper (I) - catalyzed click coupling to an azide-derivatized fluorophore such as Alexa Fluor 488 azide.

The assay was successfully applied in alfalfa suspension cultured cells (Ayaydin *et al.*, 2011) and root tips (Bazin *et al.*, 2013), tomato root tips (Ron *et al.*, 2013; Kuznetsova & Sheval', 2013), field bean root tips (Schubert *et al.*, 2011), asparagus cladodes (Nakayama *et al.*, 2012), tobacco suspension cultured cells (Tresch *et al.*, 2011), rice suspension cultured cells (Dudits *et al.*, 2011) and maize root tips (Bass *et al.*, 2014). Further, this assay was used to

determine the proliferation activity of different cell types of the anther locule of maize (Kelliher & Walbot, 2011).

2. OBJECTIVES

Although SMDs or fluorochromes have various advantages such as their small size and high membrane permeability in comparison to other fluorescent markers, designing a fluorochrome with a specific target in mind (e.g. LD localizing dyes) is a tedious and expensive process (Henrich *et al.*, 2010). Discovering new fluorochromes is significantly advanced by HTS methods, by which novel dyes can be identified in a relatively inexpensive and rapid way by simultaneous testing of a large number of compounds, up to hundreds of thousands, in amounts as low as microliters (Manning *et al.*, 2008). While these techniques are routinely used in pharmaceutical research, there are only a limited number of applications in basic science for fluorescent probe discovery (Simeonov *et al.*, 2008). Through the course of this work, a method was developed to combine SMM prescreening and CLSM in order to discover novel cell staining fluorescent dyes.

The goals of this work are as follows:

- Characterizing the potential novel, cell compartment specific, fluorochromes in human HeLa cells and potential LD fluorochromes in several plant cell suspension cultures.
- Analyzing their intracellular labeling, spectral properties, optimal working concentration and assessing their toxicity to confirm their use for long-term live cell analysis.
- Employing EdU based S-phase cell cycle detection in combination with LD dyes to study LD variability during cell cycle.

3. MATERIALS AND METHODS

The thesis involves variety of methods ranging from vertebrate and plant culturing conditions to microscopy and cytology techniques. Hence, focus is limited to methods that are specifically adapted to the present experimental system and includes details that are necessary to reproduce results presented in the current work. Relevant citations are given for commonly used methods and protocols not to exceed the size limitation of the thesis.

3.1. Chemicals

All chemicals used in this study were purchased from Sigma (Sigma, St. Louis, MO) unless stated otherwise. Hoechst 33342 and MitoTracker Orange were purchased from Invitrogen (Grand Island, NY, USA), Dulbecco's modified Eagle's medium (DMEM), antibiotics and trypsin from Lonza (Basel, Switzerland), RedDot 1 from Biotium (Hayward, CA, USA).

The 14,585-member small molecule collection screened during the discovery of eleven live cell staining fluorescent dyes, consisted of two commercially available libraries: 8,800 compounds from Nanosyn (Santa Clara, CA, USA) and 5,120 compounds from Enamine (Kiev, Ukraine), and a 665-member library of Avidin Ltd. (Szeged, Hungary).

The three chemicals characterized as plant lipid droplet dyes, Ac-201, Ac-202 and Ac-1041, were in-house synthesized thalidomide analogs (Puskás *et al.*, 2010) (The code “Ac” represents a group of in-house synthesized compounds: 2,6- diisopropylphenyl- 4/5- amino- substituted- 4/5,6,7-trifluorophthalimides (AC-201: 4-ethylamino-; AC-202: 5-ethyl-; AC-1041: 4-morpholine-).

3.2. Cell culturing

Human HeLa cervical carcinoma cells were cultured using standard conditions in Dulbecco's modified Eagle's medium (DMEM <http://www.sigmaaldrich.com/life-science/cell-culture/learning-center/media-formulations/dme.html>) supplemented with 10% fetal bovine serum, 2 mM glutamine and an antibiotic mixture (100 units/mL penicillin and 100 µg/mL streptomycin) at 37 °C under 5% CO₂ and 85% humidity.

Rice, Arabidopsis, alfalfa, maize and tobacco suspension cultures were grown in liquid plant culture medium. The culture medium and hormone concentrations of each culture are shown in Table 1. Suspension cultures were maintained in a shaker incubator at 22°C, 140 rpm and subcultured every week. Arabidopsis seedlings (7 days old) were grown on half-strength MS medium with 0.7 % plant agar (Duchefa Biochemie BV, Haarlem, The Netherlands).

	Growth medium	2,4-D (mg/L)	NAA (mg/L)	Kinetin (mg/L)
Alfalfa (<i>M. sativa</i> ssp. Varia A2)	MS ¹	1	-	0.2
Arabidopsis (<i>A. thaliana</i> , ecotype Landsberg erecta, cell line MM1)	MS ¹	-	0.5	0.05
Maize (<i>Z. mays</i> , cv. H1233)	N6M (LP40) ²	0.5		
Rice (<i>O. sativa</i> ssp. japonica cv. 'Unggi 9')	G1 ³	1		
Tobacco SR1 (<i>N. tabacum</i> cv. Petit Havana SR1)	MS ¹	-	1	0.2
Tobacco BY-2 (<i>N. tabacum</i> cv. BY-2 (cultivar Bright Yellow – 2))	MS ¹	0.2		

Table 1. Hormone concentrations and media used for plant cultures. 2,4-D (2,4-Dichlorophenoxyacetic acid), NAA (1-naphthaleneacetic acid). ¹MS: Murashige and Skoog medium (Murashige & Skoog, 1962), ²N6M (LP40): Maize culture medium with 40 mg/L L-proline (Mórocz *et al.*, 1990), ³G1: Rice culture medium (Jenes & Pauk, 1989)

3.3. Cell treatment

3.3.1. Treatment of human HeLa cells with selected compounds

One day after plating, cell cultures were treated with the chemicals at 1 and 10 μM for 1–2 h (short incubation) or one day (long-term incubation) on a 96-well glass bottom microplates (Greiner Bio-One, Kremsmünster, Austria) or LabTek 8-well coverslip-bottom chambers (Nalge Nunc International, Rochester, NY, USA). Photoconversion of chemical C2 was achieved either via successive scanning with 633 nm HeNe laser at 50% laser intensity setting or using the rhodamine filter set excitation (510–550 nm) for 10 s using maximum intensity of HBO 103W/2 (Osram, Munich, Germany) mercury short arc burner. Stability of chemical C2 at low laser intensity was recorded using successive scanning with 633 nm laser at 4% laser intensity setting. Control cultures were treated with 1% DMSO.

3.3.2. Plant cell treatment with fluorochromes

Actively dividing suspension cells (2–4 days old) were used in all of the experiments except in one experiment, where 9-day old culture was used to show cell death in an aging culture. The cell cultures were treated with the chemicals at 1, 10 and 50 μM for various durations in 4-chambered 35 mm glass-bottom dishes (Greiner Bio-One, Kremsmünster, Austria). Dye labeling of Arabidopsis seedlings were done in microcentrifuge tubes using 10 μM Ac chemical for 1 h. LD540 dye was used at 0.3 ng/mL for 15 min. DMSO (1 %, v/v) was used as carrier control in all experiments.

3.4. Colocalization of novel dyes

3.4.1. Co-labeling of chemicals with fluorescent markers on human HeLa cells

DNA intercalating dye Hoechst 33342 was used at 1 μM to stain live cell nuclei. MitoTracker Orange (0.2 μM) and nonyl acridine orange (NAO) (0.5 μM) were used to label mitochondria. Fluorescein diacetate (FDA) was used at 0.1 μM to highlight the living cells. RedDot 1 is supplied commercially as 200 \times concentrated solution and used by diluting 200 \times in culture medium as suggested by the manufacturer. Fixed cells were used for LD colocalization and apoptotic nuclei analysis: Cell fixation was performed using 4% paraformaldehyde in phosphate buffered saline (PBS) for 7 min at ambient temperature. Fixer was removed with 3 \times 5 min PBS washes. For LD colocalization Oil Red O was prepared as 1% (w/v) in isopropanol. Cells were first incubated with the tested fluorochromes for 10 min then Oil Red O was added at a final concentration of 0.01% (w/v) at the center of the chamber. Regions surrounding the isopropanol-exposed central part were analyzed for colocalization. For apoptotic analysis HeLa cells were incubated for 24 h with the chemicals at 10 μM (1 μM for C2 and its photoconverted form which is indicated with an asterisk: C2*). Following PBS washes, cells were fixed and stained with 0.1 $\mu\text{g/mL}$ DAPI for 10 min.

3.4.2. Co-labeling on rice Unggi 9 cells

Nile Red stock solution was prepared in DMSO at 100 ng/ μL concentration. For colocalization experiments, working concentration of 500 ng/mL was used. For viability assays, propidium iodide (PI) at 0.45 μM concentration was added 5 min before microscopy imaging.

3.5. Detecting S-phase of cell cycle in tobacco BY-2 cells using EdU

3.5.1. EdU labeling of BY-2 cells

BY-2 cells were collected (day 0-9 after subculturing) in a 1.5mL microcentrifuge tube and labeled with 10 μ M final concentration of EdU for 30 minutes in its own culture medium at culture growth temperature, on a roller. Cells were settled by centrifuging for 5 minutes at 400xg. Cells were washed once in PBS for 5 minutes and fixed. Cells fixed for 30 minutes in 4% paraformaldehyde in PBS with 0.05% Triton X-100, on a 50rpm shaker. After 30 minutes, fixer was replaced with PBS and shifted to 4°C for further processing.

3.5.2. Detection of EdU using fluorescence microscopy

EdU labeled and fixed BY-2 cells were washed 3×5 minutes in PBS and 1/20th of the total fixed cells were collected in a 0.2mL microfuge tube. Cells were settled by centrifuging for 5 minutes at 400xg and were incubated in 150 μ L of EdU detection cocktail (PBS, 40 mM sodium ascorbate, 0.05% Triton X-100, 4 mM CuSO₄, 10 μ M Alexa Fluor 488 azide) for 30 minutes at room temperature on a roller. Detection cocktail was removed by 2×5 minute PBS washes and cells were labeled for 15 minutes with 0.45 μ M PI and 10 μ M Ac-201. The number of S-phase cells were counted (n=500) by eye considering Alexa Fluor 488 labeled cells as positives for S-phase as opposed to PI labeled cells which gave the total cell count.

3.6. Blocking BY-2 cells in S-phase using hydroxyurea

5 day old BY-2 culture was refreshed 30X with fresh medium and blocked immediately with sterile 5mM hydroxyurea (HU), for a period of 36 hours. A control sample without HU block was maintained with the same refreshment method. After 36 hours, HU block was removed by washing the cells 3×5 minutes with the sterile supernatant of a 36 hour old culture (same age as the blocked culture) and further cultured in the same medium. BY-2 and control cells before and 2 hours after wash were labeled with Ac-201 at 10 μ M concentration for 15 minutes before image acquisition.

3.7. Confocal Laser Scanning Microscopy (CLSM)

CLSM was mainly performed using Olympus Fluoview FV1000 confocal laser scanning microscope (Olympus Life Science Europa GmbH, Hamburg, Germany). Microscope configuration was as follows: Objective lenses: UPLSAPO 20 \times (dry, NA: 0.75), UPLFLN 40 \times (oil, NA: 1.3), LUMPLFL 40 \times (water, NA: 0.80) and UPLSAPO 60 \times (oil, NA: 1.35); sampling speed: 4 μ s/pixel; line averaging: 2 \times ; scanning mode: Sequential unidirectional; excitation: 405 nm (Hoechst 33342, DAPI and blue fluorescence detection of the novel chemicals) 488 nm (NAO, FDA, LD540, Nile Red, spectral scan and green fluorescence detection), 543 nm (Oil Red O, MitoTracker Orange, PI, Nile Red and red fluorescence detection) and 633 nm (RedDot 1 and deep-red fluorescence detection); maximum laser transmissivity values: 2% (405 nm), 5% (488 nm), 50% (543 nm) and 50% (633 nm); emission filters: Blue: 425–475 nm, Green: 500–530 nm; Red: 555–625 nm; Deep-red: 650 nm and above. Spectral imaging was performed using lambda scan mode of Olympus software (20 nm intervals, 10 nm apart).

Before imaging one-day-treated HeLa cells, detector pinhole diameter (1 airy unit) was increased two to three times to capture faint dye fluorescence emissions. Blue-colored dyes which had reduced intensity due to 24 h incubation in culture medium and formaldehyde fixation, was not detectable with the microscope settings used for bright DAPI dye detection. Images were pseudocolored using Olympus Fluoview software (version 4.0 c).

Successive 3D optical sections of fixed BY-2 cells labeled with Ac-201 (LD), Alexa Fluor 488 (EdU) and PI (nuclei) were taken using the $40\times$ (NA: 0.80) water immersion objective and analyzed with Huygens Object Analyzer module of Huygens 3D analysis software (Scientific Volume Imaging B.V, The Netherlands). Microscope configuration was as explained earlier and a step size of $1\text{ }\mu\text{m}$ was used.

Leica SP5 AOBS (Leica, Heidelberg, Germany) confocal laser scanning microscope was used for images presented in Fig. 20. Ac chemicals and chlorophyll fluorescence were excited using 405 and 488 nm lasers and detected between 418-536 nm and 650-750 nm, respectively. Pinhole diameter was set to Airy 1; sampling speed: 700 Hz; line averaging: 1; scanning mode: unidirectional. Single optical sections or successive 3D optical sections of seedlings were taken using HCX PLAPO 63 (NA: 1.2) water immersion objective and analyzed with Leica Application Suite Advanced Fluorescence (LAS AF 2.5) software. “Transparent” 3D projection mode of LAS AF software was used to reconstruct the 3D image using 396 optical sections of a $145\times 145\text{ }\mu\text{m}$ square region encompassing a $39\text{ }\mu\text{m}$ thick cotyledon region. Another set of 396 sections was captured from a smaller cotyledon area (x, y, z: $145\times 24\times 39\text{ }\mu\text{m}$) to be used in Y-axis projection images.

3.8. Three dimensional image analysis and LD quantification

Huygens Professional (version 15.10) software from Scientific Volume Imaging was used for the three dimensional image analysis and LD quantification of BY-2 cells. The Object Analyzer (OA) tool was used for this purpose. Multiple confocal optical z-sections obtained with the Olympus Fluoview FV1000 CLSM were used for the three dimensional image reconstruction and LD quantification of individual cells. The OA's 'auto seed' and 'threshold' functions were used as the template for thresholding all the images before analysis. Using the 'select area' tool, region of interest (ROI) was marked around a single cell on a 2D projection (top view) of a 3D reconstructed bright field image (Fig. 18). Objects outside the ROI were discarded and those left within were all analyzed at once using the 'analyze all' tool. From the various object statistics obtained, the voxel values of each object within the ROI i.e., each cell, was used as the parameter to calculate the total LD volume of each cell.

4. RESULTS AND DISCUSSION

In this chapter, the presentation of experimental results will be immediately followed by their interpretation and discussion, in order to maintain coherence and avoid redundancies. The interpretation and discussion will be in context of the related information available in the literature.

4.1. Novel fluorochrome discovery through combinatorial chemistry

Although SMDs or fluorochromes have various advantages such as their small size and high membrane permeability in comparison to other fluorescent markers, novel fluorochrome discovery or design with a specific target in mind is a time consuming and expensive process (Henrich *et al.*, 2010). Discovering new fluorochromes is significantly advanced by HTS methods, by which novel dyes can be identified in a relatively inexpensive and rapid way by simultaneous testing of a large number of compounds, up to hundreds of thousands, in amounts as low as microliters (Manning *et al.*, 2008).

SMM is a collection of molecules spotted or synthesized on a solid surface in order to examine possible binding partners (Hackler *et al.*, 2003; Darvas *et al.*, 2004; Molnár *et al.*, 2006). This format enables a rapid screen of drug candidates from thousands of small organic compounds that specifically bind to certain proteins marked fluorescently to detect their interaction (Barnes-Seeman *et al.*, 2003; Darvas *et al.*, 2004; Vegas *et al.*, 2007; Shi *et al.*, 2009; Chen *et al.*, 2010; Lee & Park, 2011). While these techniques are routinely used in pharmaceutical research, there are only a limited number of applications in basic science for fluorescent probe discovery (Simeonov *et al.*, 2008). Therefore, we decided to combine SMM

prescreening with CLSM for the discovery of new fluorescent dyes from a chemical library of thousands of diverse compounds.

4.1.1. Small molecule microarray (SMM) prescreening

This part of the work was performed by members of the Laboratory of Functional Genomics in Biological Research Center, Szeged. 14,585 compounds were scanned using a dual channel microarray scanner fitted with green (532 nm wavelength) and red (633 nm wavelength) lasers and suitable emission filters (Figure 4). The screening approach was restricted to dried slides as aqueous analysis would require larger sample volumes to prevent evaporation. Dry analysis not only allows for the fast screening of various SMMs, but has also proved to be practical from the point of storage convenience for future reference.

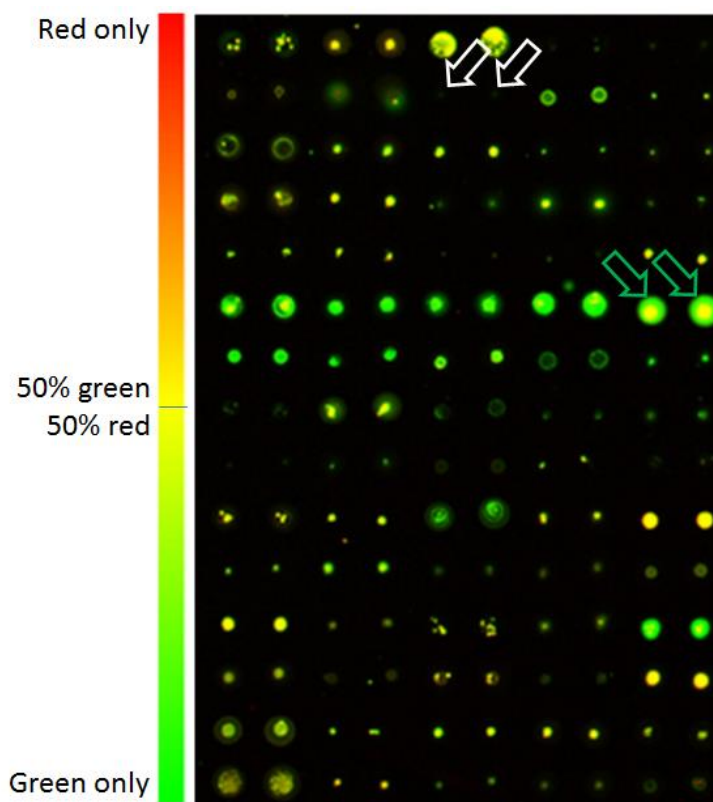


Figure 4. Pseudocolored image of an SMM block excited by 532 and 633 nm lasers. Color of the spots derives from the relative emission intensities at 570 and 670 nm (see gradient at the left hand side of the figure). White arrows point to a double spotted non-fluorescent chemical and green arrows show a duplicate spot of a highly fluorescent compound. (Molnár and Kuntam *et al.*, 2013)

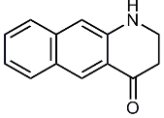
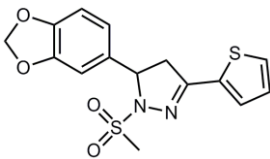
The location of spots in the resulting image was defined and statistical parameters of each feature (signal) and background intensities were extracted. The data was filtered for un-flagged (detected) spots, signal to noise ratio (>2), significance (at least 60% of feature pixels with intensities more than two standard deviations above the background) and signal (background corrected median feature intensity >500) in both 532 and 633 nm wavelengths each. Those molecules which fulfilled all the filtering criteria with two (in case of duplicates) or three (in case of quadruplicates) parallel spots at 523 and/or 633 nm wavelengths were selected for microscopic investigation (see two of the selected compounds in Figure 4).

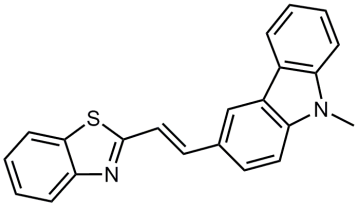
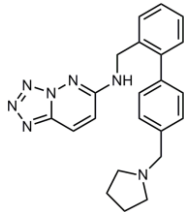
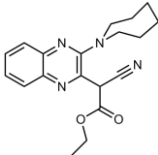
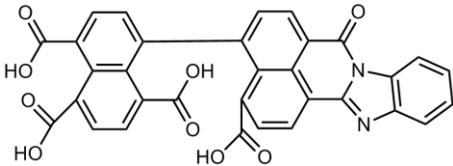
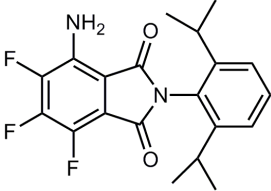
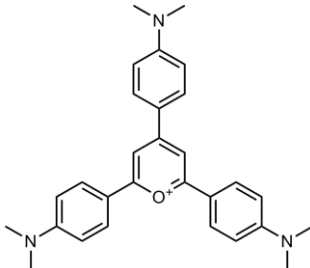
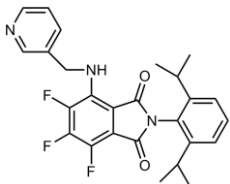
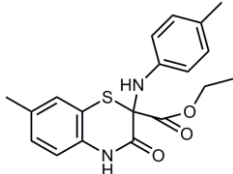
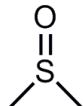
4.1.2. In vivo microscopy studies of the prescreened potential fluorochromes

SMM prescreening yielded 278 fluorescent compounds which were first screened for fluorescence intensity, cell permeability, solubility and toxicity under *in vivo* conditions in human HeLa cells using CLSM. The analysis of the compounds was performed with all four available lasers of the CLSM (405, 488, 543 and 633 nm) even though the autofluorescent compounds were preselected using only the 532 and 633 nm lasers. This was done because certain fluorochromes might have bimodal excitation or emission peaks, such as R-phycoerythrin, which displays an absorption spectrum with distinct peaks at 480 and 565 nm. Furthermore, spectral characteristics of various fluorescent probes may change due to their interaction with organic molecules found in living cells. A well-known example is acridine orange, the nucleic acid intercalating dye which has emission peaks at 530 nm or 640 nm based

on its interaction with DNA or RNA, respectively. Similarly, the spectral properties of some fluorochromes can also be significantly affected by factors such as intracellular pH, ion concentrations and compartmentalization (Haugland *et al.*, 2005).

Chemicals which were cell impermeable, toxic or displayed low solubility were eliminated from further analysis. When tested in living cells, some of the dyes had extremely low fluorescence emission. This may be due to low permeability or interaction with other organic molecules in the culture medium or inside the cells. Such chemicals would require high laser excitation energies to obtain detectable fluorescence which is not desirable in live cell analyses due to their negative effect on cell metabolism and viability. Hence, these chemicals were also disregarded. Following this stringent elimination procedure, we have chosen 11 fluorescent chemicals as novel candidates for live cell imaging (Table 2). Figure 2 shows the four channel emission images of the 11 compounds. We have found five chemicals localized to lipid droplets, three to mitochondria, one to plasma membrane, one to perinuclear/cytoplasmic region and one to mitochondria/nucleolus (Table 2 and Fig. 5). Laser excitation and emission detection thresholds for microscopy imaging were set by using DMSO - treated cells as reference (Fig. 5).

ID	Structure, Localization, Color	ID	Structure, Localization, Color
B5	 Endomembrane/ Nuclear membrane (blue)	D10	 Mitochondria (red)

C4	 <p>Lipid droplets (blue)</p>	E5	 <p>Mitochondria (red)</p>
ID	Structure, Localization, Color	ID	Structure, Localization, Color
C6	 <p>Lipid droplets (blue)</p>	B11	 <p>Plasma membrane (red)</p>
B3	 <p>Lipid droplets (blue-green)</p>	C2	 <p>Mitochondria/nucleolus convertible (deep-red)</p>
B2	 <p>Lipid droplets (blue-green)</p>	C3	 <p>Mitochondria (deep-red)</p>
B4		DMSO	

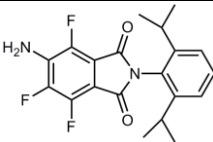
	 <p>Lipid droplets (blue-green)</p>		
--	--	--	--

Table 2. Chemical structures and labeling characteristics of the selected molecules.

All of the chemicals were labeling the target compartment within one hour of incubation at 37 °C when used at 10 μ M concentration. Chemical C2 was not well tolerated by the cells at 10 μ M (as judged by increased cell rounding and cell death), however at concentrations as low as 0.25 μ M, its signal was very bright and detectable. Therefore, its use was limited to a maximum of 1 μ M. We also tested the stability and labeling persistency of these chemicals over time. Apart from chemicals E5, D10 and C3, they were still fluorescent even after one day of incubation at 37 °C (Fig. 6) proving their use for long-term live cell analysis.

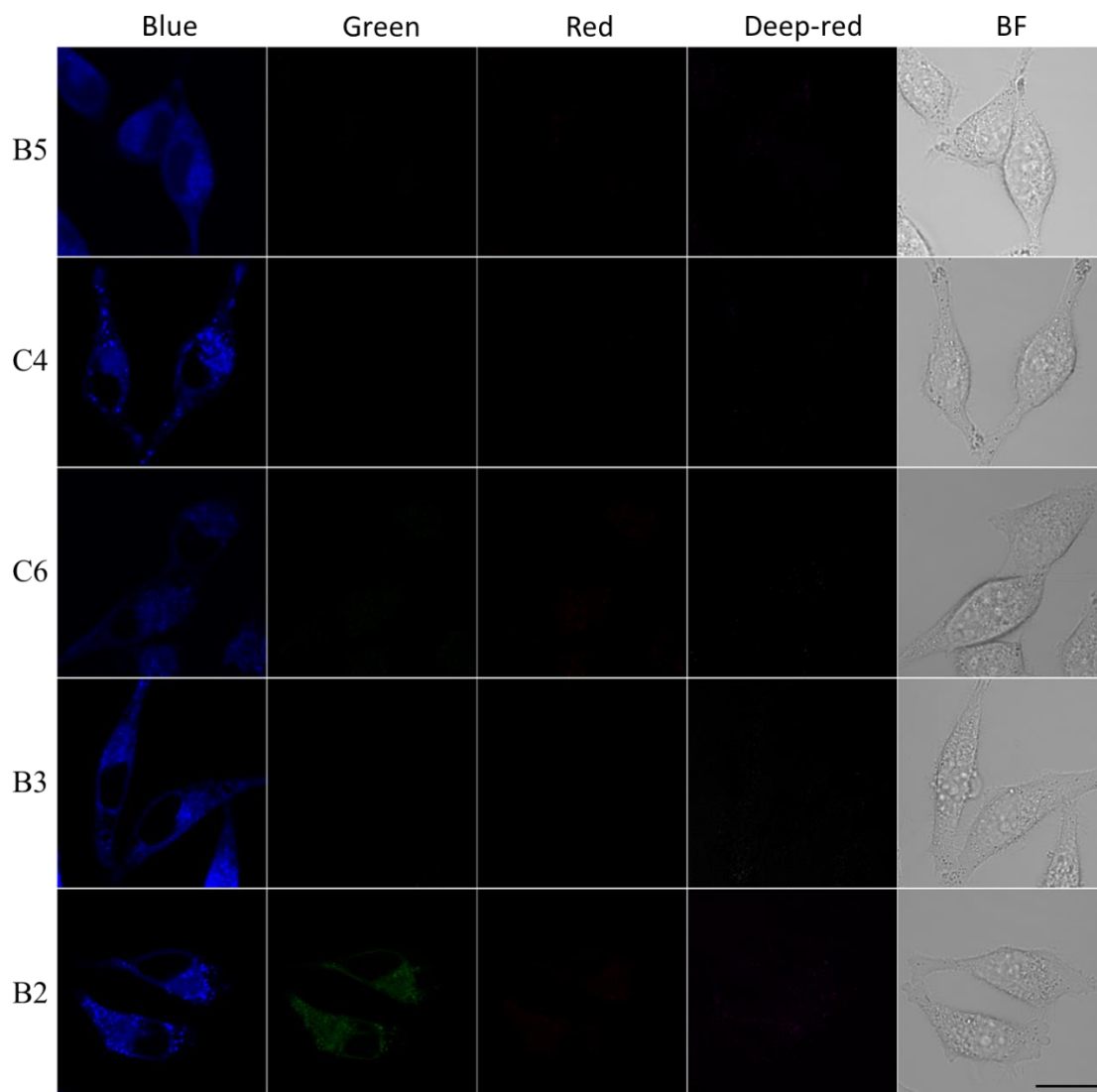


Figure 5. Fluorescence emission and intracellular localization of selected chemicals. Fluorescence emission of the tested chemicals (1 h at 37 °C, 10 μ M) were captured in four channels (Blue: 425–475 nm, Green: 500–530 nm; Red: 555–625 nm; Deep-red: 650 nm and above) using 405, 488, 543 and 633 nm laser excitation. BF: Bright field imaging. Scale bar 10 μ m. (Molnár and Kuntam *et al.*, 2013)

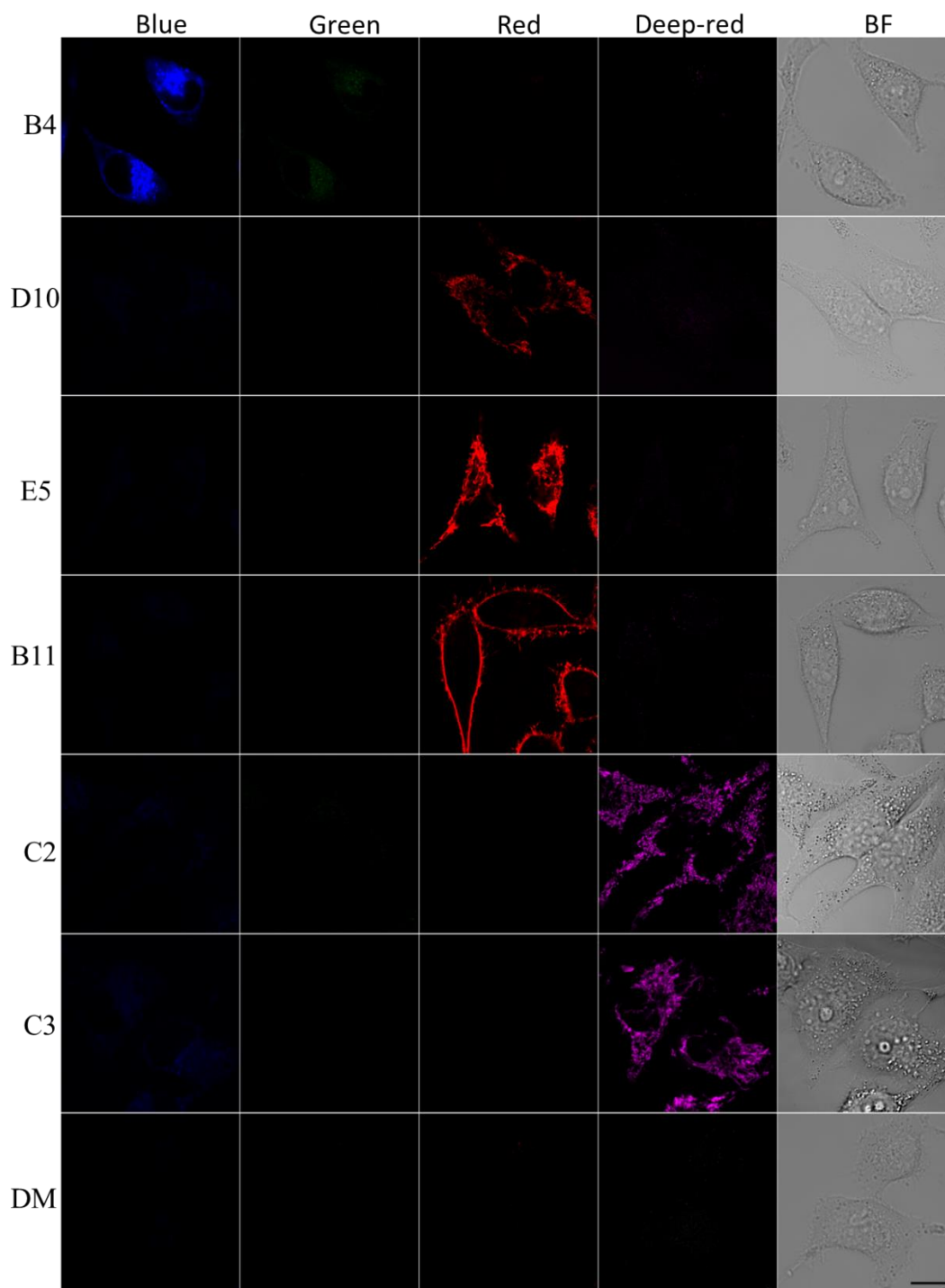


Figure 5 contd. Fluorescence emission and intracellular localization of selected chemicals. Fluorescence emission of the tested chemicals (1 h at 37 °C, 10 μ M each, except C2 which was 1 μ M) were captured in four channels (Blue: 425–475 nm, Green: 500–530 nm; Red: 555–625 nm; Deep-red: 650 nm and above) using 405, 488, 543 and 633 nm laser excitation. Control cells were treated with DMSO. BF: Bright field imaging, DM: DMSO. Scale bar 10 μ m. (Molnár and Kuntam *et al.*, 2013)

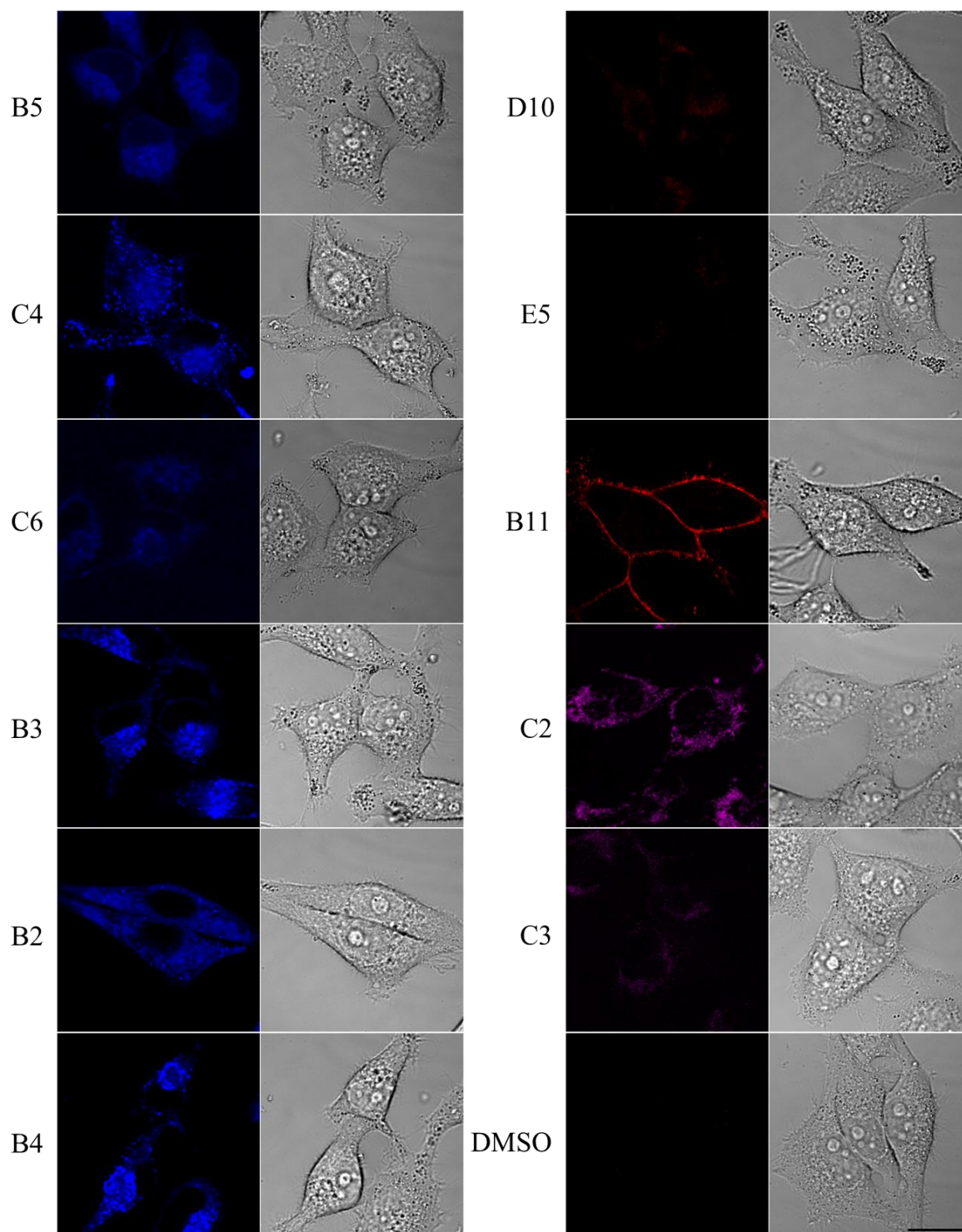


Figure 6. Fluorescence emission of selected chemicals after 24-hours. Fluorescence emissions were captured after 1 day of incubation with selected chemicals, at 37 °C. Only the image of the brightest fluorescence color paired with the corresponding bright field image is shown. Up to three times wider confocal aperture (pinhole) was used for taking images. Scale bar 10 μm . (Molnár and Kuntam *et al.*, 2013)

4.1.3. Intracellular localization confirmation by colocalization with known markers

The intracellular localization of all 11 autofluorescent compounds was determined by colocalization with known fluorescent markers (Fig. 7a–l). A DNA specific nuclear marker dye RedDot 1 was co-labeled with chemical B5, which is localized to the perinuclear region (Fig. 7a). Figure 7b–f show Oil Red O staining of LDs colocalizing with chemicals C4, C6, B2, B3 and B4 on fixed HeLa cells. Chemicals B2, B3 and B4 are derived from our in-house, non-randomly synthesized collection along with some other trifluoroaminophthalimide derivatives, which were further developed as potential anticancer agents (Puskás *et al.*, 2010). Therefore, molecules B2–B4 (Table 2) have the same basic structure in contrast with the other eight fluorochromes, which were obtained from commercially available libraries. All five of the LD-localizing novel fluorescent probes were cell membrane permeable dyes without the necessity of cell fixation, unlike the Oil Red O stain. Hence they allow live analysis of LD localization, mobility and dynamics. Figure 7g–k show five other fluorescent live cell markers discovered in this study.

Chemicals D10, E5, C2 and C3 were all localized to mitochondria. Red-colored D10 and E5 were co-stained with green-colored NAO (Fig. 7g, h) and deep-red colored chemicals C2, C3 with red-colored MitoTracker Orange (Fig. 7j, k). All four resulted in complete colocalization with these mitochondria localized markers.

Chemical B11 was found to localize preferentially to plasma membrane (Figure 7i). Cell borders labeled with this chemical were still visible even after one day of incubation in culture without significant loss of cell viability (Fig. 6). Therefore, this dye can also be used in long-

term live cell labeling and tracking experiments. The whole cell-labeling FDA was co-stained with chemical B11 to confirm its localization (Fig. 7i).

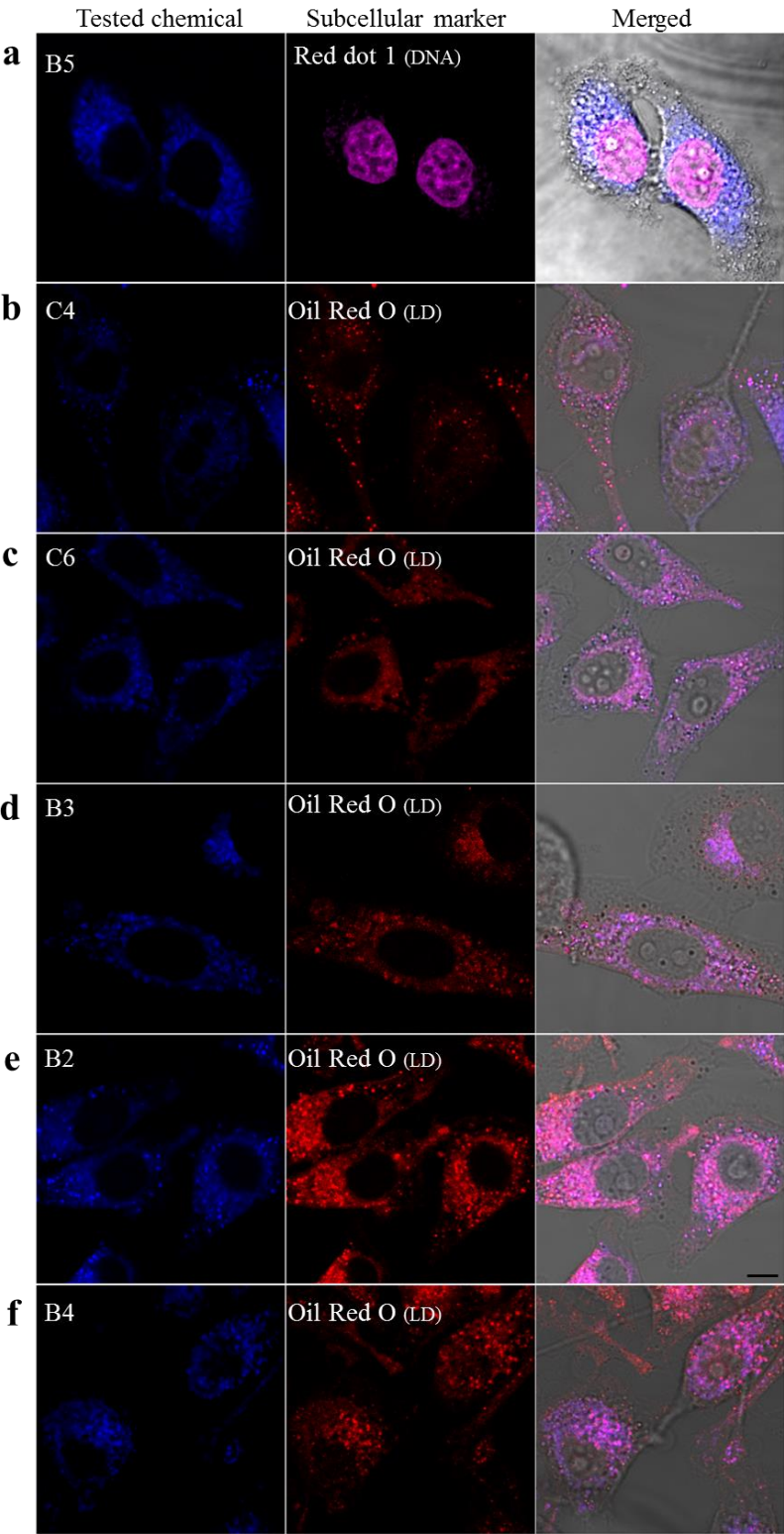


Figure 7. Colocalization of chemicals with fluorescent markers. Localization of the chemicals and the fluorescent markers are indicated on the panels. (b–f) Formaldehyde fixed cells were used for colocalization with Oil Red O. Scale bar 10 μ m. (Molnár and Kuntam *et al.*, 2013)

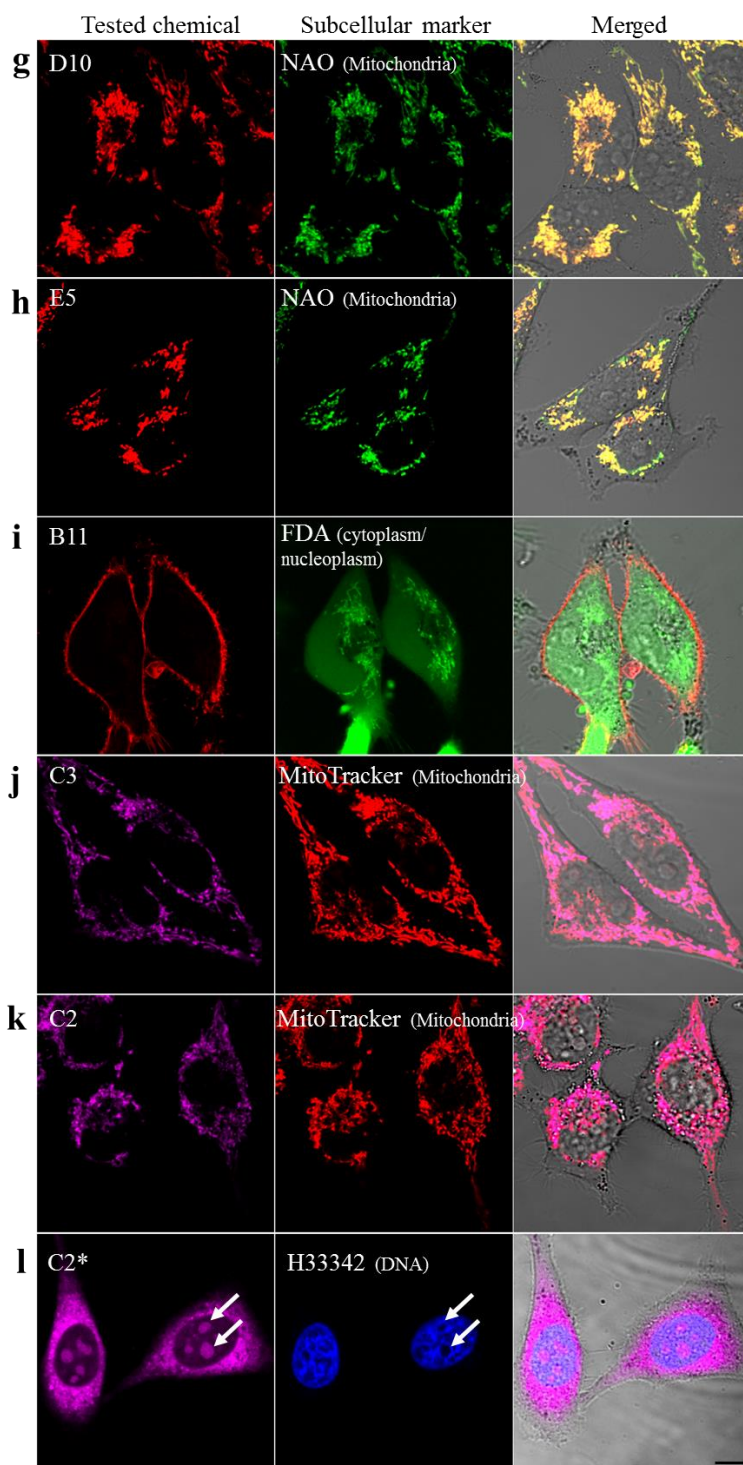


Figure 7 contd. Colocalization of chemicals with fluorescent markers. Localization of the chemicals and the fluorescent markers are indicated on the panels. (l) Successive scanning with

633 nm HeNe laser at 50% laser intensity-induced relocation of chemical C2 to nucleolus/cytoplasm. C2*: Photoconverted form of chemical C2. Arrows indicate two nucleoli. Scale bar 10 μm . (Molnár and Kuntam *et al.*, 2013)

4.1.4. Unusual spectral behavior of chemical C2

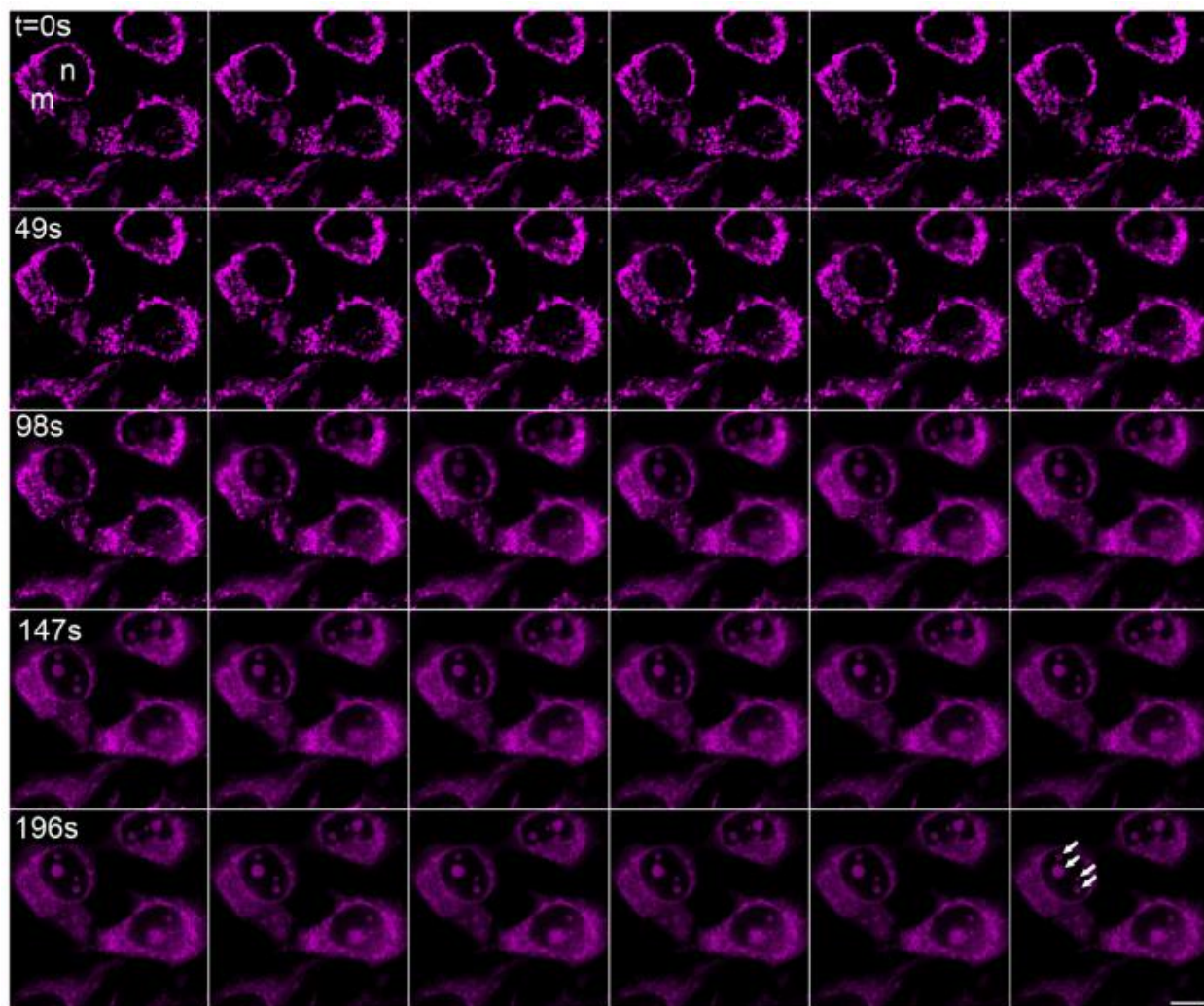


Figure 8. Laser scanning-induced relocation of chemical C2 from mitochondria to cytoplasm and nucleoli. C2-treated (1 μM) HeLa cells were repeatedly scanned with 633 nm HeNe laser at 50% intensity. Each frame is 7 seconds apart. Elapsed time is shown for every 7th frame. Mitochondria (m) and nucleus (n) of a cell are shown at the first frame. The four nucleoli of the same cell are indicated with arrows at the last frame. Bar 10 μm . (Molnár and Kuntam *et al.*, 2013)

We have discovered an unusual spectral behavior of the chemical C2 during our microscopy analyses. Gradual relocation of dye signal from mitochondria to cytoplasm (seen as diffused dye signal all over the cell except in the nucleus) and the nucleolus was observed when labeled cells were repetitively scanned with 633 nm laser at 50% intensity setting as shown in Figure 8. However, such a conversion was not observed when using a lower laser intensity setting (4%) for the 633 nm laser, indicating that the mitochondria-localized C2 dye was not changing its properties by itself and that a certain threshold amount of laser energy was necessary to cause relocation (Fig. 9).

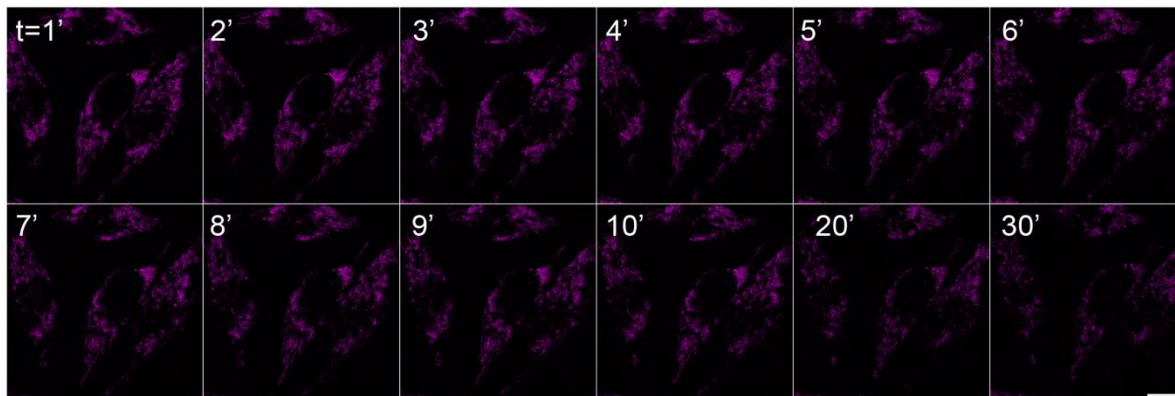


Figure 9. Stability of chemical C2 using low laser intensity settings. 633 nm laser was used at 4% intensity to capture images at indicated time points. Bar 10 μm . (Molnár and Kuntam *et al.*, 2013)

We have observed that photoconversion was also inducible by illumination with the rhodamine filter set of the fluorescence microscope (510–550 nm green excitation). To confirm the nucleolar localization of the photoconverted C2 dye (denoted with an asterisk C2*), we have used co-staining on live cells, 1 h after photoconversion with a vital DNA dye Hoechst 33342 which displays a negative staining pattern at the RNA-rich nucleolar regions (arrows in Fig. 71). We predict that, this chemical may undergo laser-induced structural changes which may cause its

relocalization, like the photoconvertible and photosensitizing fluorescent proteins (Haugland *et al.*, 2005) and hence the photoconversion of C2 might be an irreversible process. A previous work suggests that, upon light stimulation, the pyrylium core of C2 behave as an electron acceptor (Marin *et al.*, 2007) which is capable of oxidizing surrounding donor molecules within the cell (photooxidation). Previously it has been reported that photosensitizing fluorescent probes may cause dye relocalization due to cell death (Alvarez *et al.*, 2011). Similar photosensitization and toxicity might also be the reason for the light-induced relocalization of chemical C2. Reduced viability of chemical C2*-treated cells after 1 day of incubation (Fig. 10 and 11) also supports this possibility and further strengthens our hypothesis that C2* is quite stable and its photoconversion an irreversible process. However, in the absence of laser excitation for the photo-conversion of C2 molecule, it stayed stable in mitochondria for a longer period of time (Fig. 6). Photo-conversion was also not observed with successive laser scanning, using reduced laser intensity (633 nm laser at 4%) (Fig. 9).

4.1.5. Effect of selected chemicals on long-term viability of cells

We have also tested the effect of these chemicals on long-term viability of cultured cells. 4-hydroxytamoxifen (HT), a known apoptosis inducer was used at a concentration of 20 μ M, as a positive control. During a 24-hour period, HeLa cells were treated with chemicals at a concentration of 10 μ M (1 μ M for chemicals C2 and C2*). Viability was assessed using FDA staining. Due to esterase activity, living cells actively convert the non-fluorescent FDA into the bright green fluorescent compound fluorescein (Haugland *et al.*, 2005). Due to varying levels of esterase activity among different cells, varying degree of green fluorescence can be observed in a healthy culture after FDA labeling. Complete absence of fluorescein fluorescence however,

indicates a clear sign of cell death. Figure 10 shows that as compared to DMSO-treated cells, 24-hour treatment with the chemicals did not significantly affect cell viability, except C2* and HT. Hence, it can be inferred that these dyes are also suitable for long-term labeling and tracking experiments. Although C2* did not induce any visible morphological changes during 1-hour post conversion (Fig. 6k), 24h treatment significantly decreased cell viability (arrows on Fig. 10,11 C2* indicate dead cells). Therefore, we concluded that the application of C2* is limited to short term (such as 1 h) colocalization analyses.

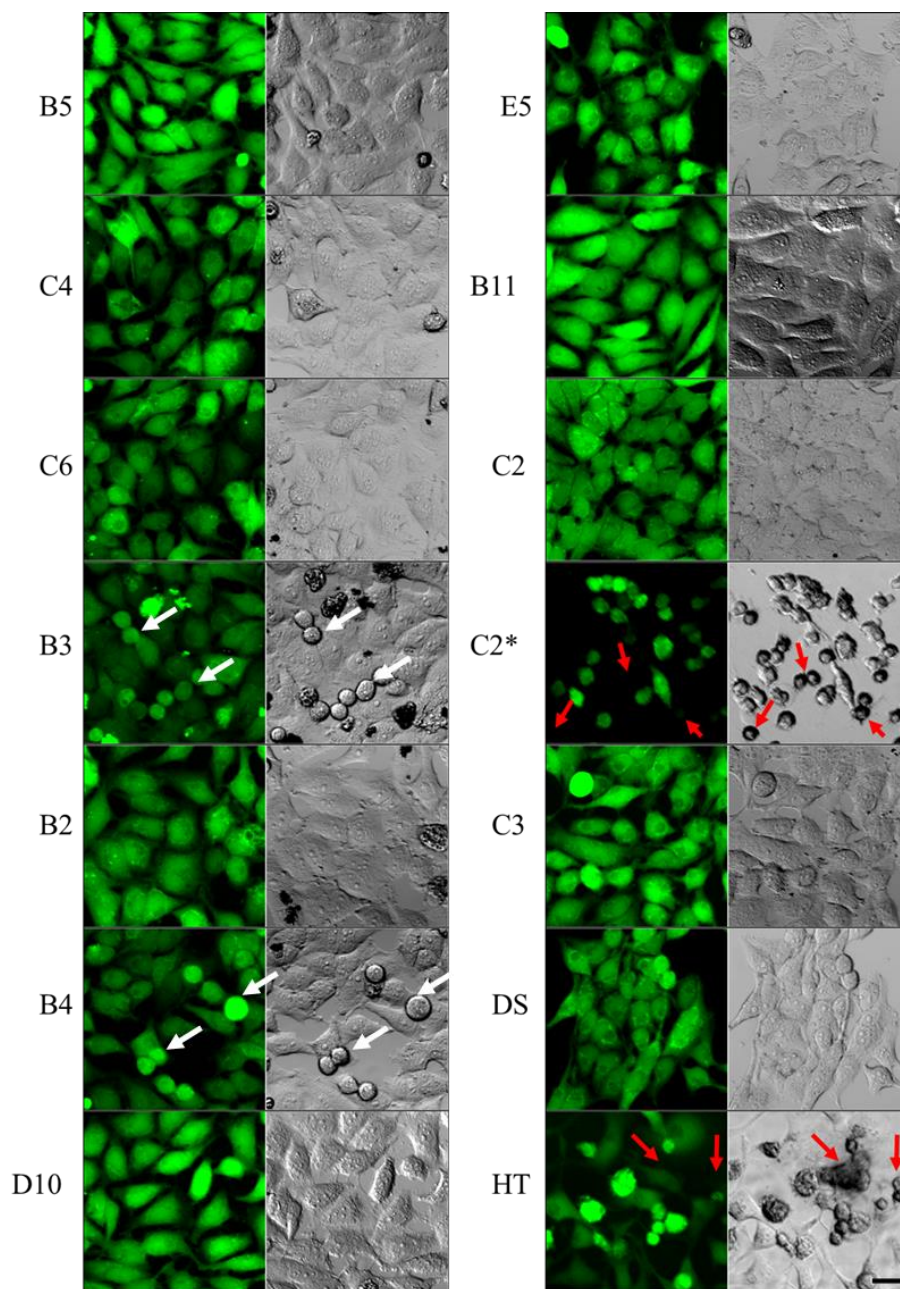


Figure 10. Viability analyses of 24 h-treated HeLa cells. FDA (green) labeling of live cells and their corresponding bright field images (black and white transmitted light images) are shown. Arrows in C2* and HT samples indicate FDA-negative dead cells and clusters. White arrows in panels B3 and B4 indicate FDA-positive, live round up cells in the process of mitosis and cytokinesis. C2*: Photoconverted C2; DS: DMSO. Scale bar 20 μm . (Molnár and Kuntam *et al.*, 2013)

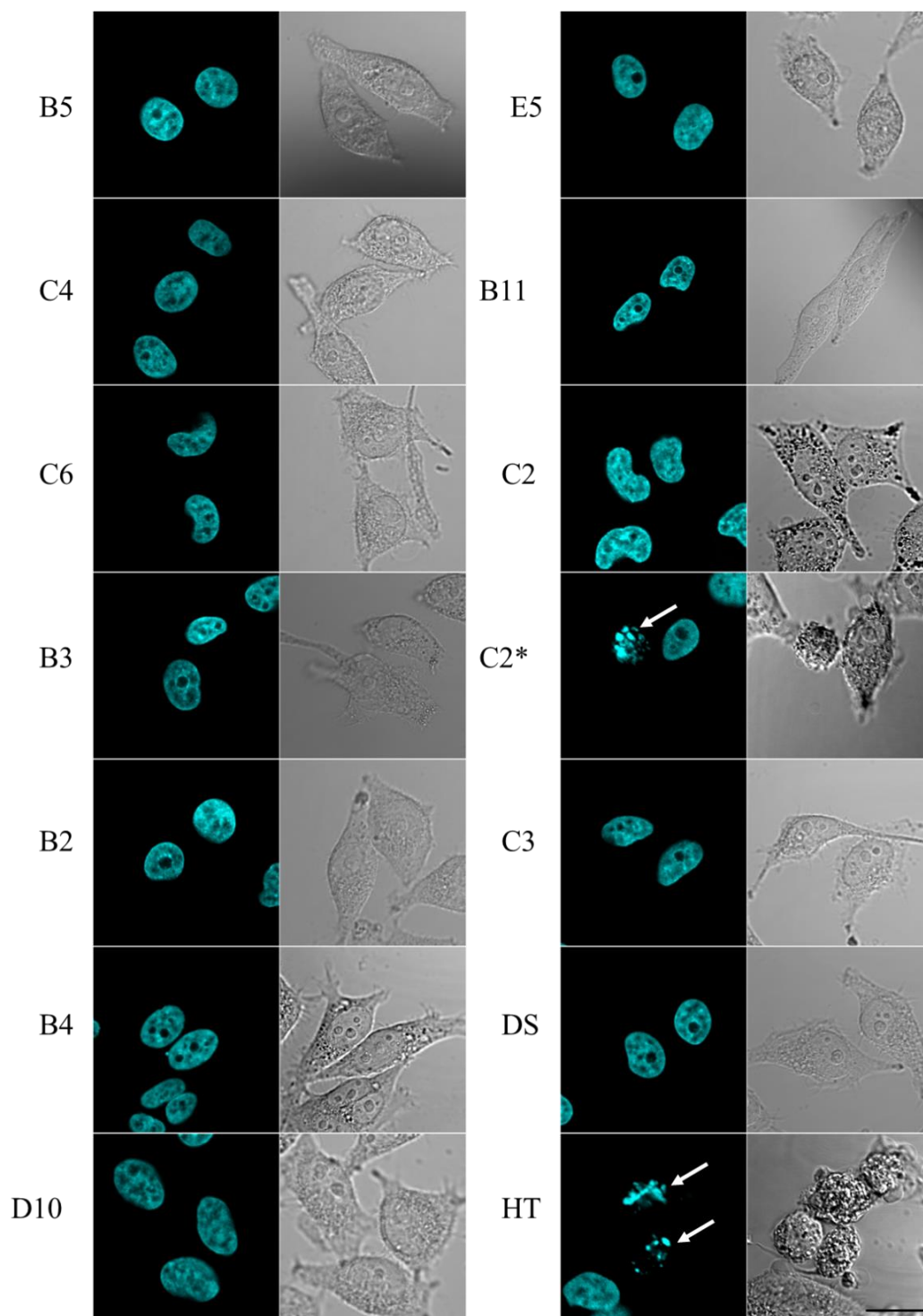


Figure 11. Nuclear morphology analyses of 24 h-treated HeLa cells. DAPI (blue emission nuclear dye) labeling of fixed cells and their corresponding bright field images (black and white transmitted light images) are shown. Arrows in C2* and HT samples show fragmented, apoptotic-like nuclei in C2* and HT samples. C2*: Photoconverted C2; DS: DMSO. Scale bar 20 μm . (Molnár and Kuntam *et al.*, 2013)

The chemicals were also tested for apoptotic nuclei formation as an alternative approach (Fig. 11). Apoptotic cells display distinct nuclear morphological changes such as nuclear blebbing and degradation of nuclear envelope (Johnson *et al.*, 2000). Cells treated with HT at 20 μ M and with the selected chemicals at 10 μ M (1 μ M for C2 and C2*) for 24 h were fixed and stained with DAPI to screen nuclear morphology changes. As this method involves fixation and multiple washes of the fixer, majority of healthy, round up mitotic cells (white arrows in Fig 10 panels B3, B4) and severely apoptotic round up dead cells (Fig 10, panels C2* and HT) were washed off leaving only partially attached apoptotic cells and fully attached healthy cells after DAPI staining of samples. Based on this method, none of the chemicals displayed nuclear abnormalities except C2* and HT for which blebs and micronuclei were frequently observed (Fig. 11).

4.2. Characterizing blue-fluorescent LD markers in plants

Cell membrane permeable live dyes discovered and developed in animal model cultures may not always be practical in intact plant studies due to the presence of the cell wall. For example, blue fluorescent, live cell nuclear dyes used in animal cells such as DAPI, Hoechst 33258 and Hoechst 33342 or several fluorescent pH indicator dyes used in living animal cells cannot be used efficiently in intact live plant cells. During *in vivo* studies, wounding stress inducing microinjection or protoplastation is required for such cell wall impermeable dyes to be delivered into plant cells (Fasano *et al.*, 2001). Furthermore, the small number of LD dyes available for use in intact live plant cells, like BODIPY and Nile Red, have certain drawbacks, especially during multicolor imaging. Nile Red has a very broad emission range which interferes with the chlorophyll fluorescence, limiting its use in green plant tissues and also hinders

multicolor imaging (Miquel *et al.*, 2014). BODIPY 493/503 on the other hand, is known to have lesser photostability and undesirable photoconvertible properties, limiting its use for long-term, repetitive imaging (Ohsaki *et al.*, 2010). Despite the presence of other LD dyes with better photostability such as BODIPY 505/515, LD540 (Spandl *et al.*, 2009) or blue–red colored, dual behaving monodansylpentane (Yang *et al.*, 2012), the problem still remains that they have emission in the green, yellow or red region of the visible spectrum. Taking all of the above mentioned information into consideration, there is a pressing need for the identification of a vital LD dye for plants which is spectrally well separated from the majority of the live fluorescent markers and chlorophyll autofluorescence.

4.2.1. Localization and toxicity of Ac chemicals on plant suspension cultures

In our HeLa cell study, we have discovered in-house synthesized thalidomide analogs localizing to lipid droplets on human cancer cells (Molnár and Kuntam *et al.*, 2013). These dyes were attractive candidates as novel LD fluorescent reporters for studies in plant cells, as they were blue fluorescent and plasma membrane permeable. However, not all animal cell permeable dyes are suitable for use in plant studies due to various reasons, the major one being the presence of cell walls as physical barriers in plant cells. Lower acidity of plant cell walls and plant culture media can also negatively affect fluorescence emission properties of such chemicals in plant experiments. Moreover, biocompatibility and toxicity of these chemicals may also be different for plant cells.

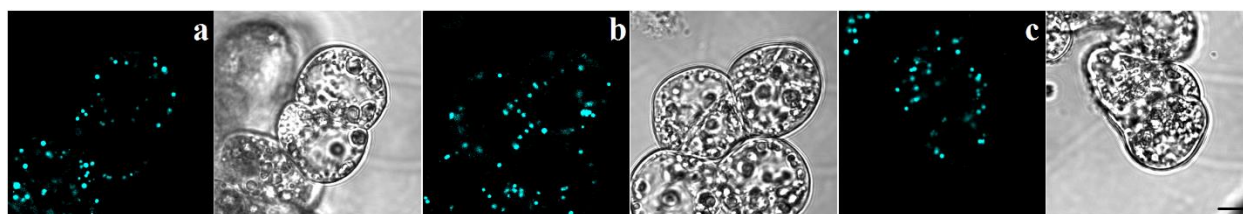


Figure 12. Localization of B2, B3 and C4 dyes on Unggi 9 cells. **a**, **b** and **c** show the intracellular localization of B2, B3 and C4 respectively. All three dyes were used at 10 μ M concentration. Scale bar 20 μ m.

Of the five LD localizing dyes discovered in our previous work (Molnár and Kuntam *et al.*, 2013), only three, B2, B3 and C4 were found to penetrate the cell wall and displayed bright, blue, LD like spotty signals (Fig. 12). However, these novel dyes were available in limited amount and were difficult to synthesize and hence were not further pursued as potential LD dyes for plant studies.

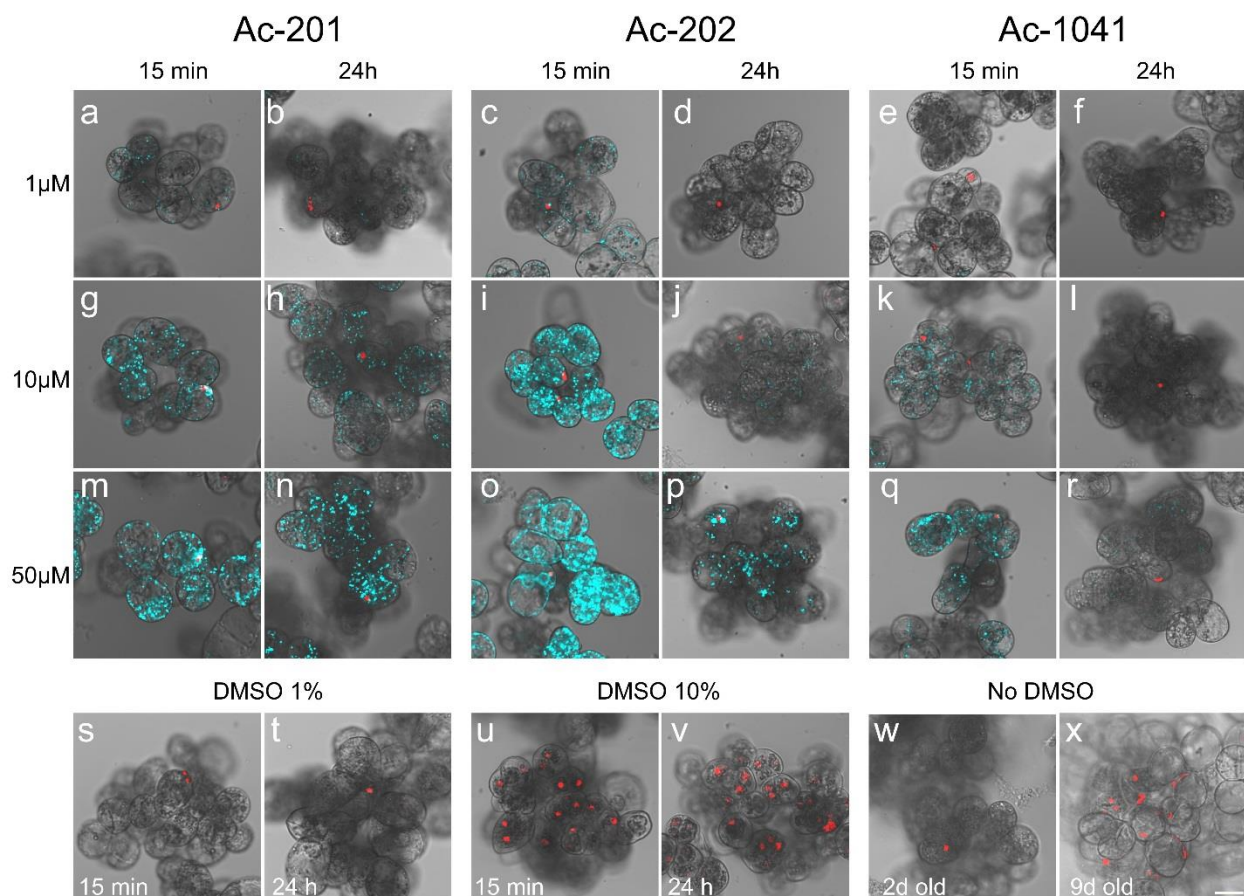


Figure 13. LD labeling efficiency and analysis of cell viability using various treatment durations and doses of Ac chemicals on rice culture. Short (15 min) and long (24 h) treatment durations using 1, 10, 50 μ M of Ac chemicals (a–r) and DMSO (s–v) are shown. Propidium iodide (PI) labeling (in red) indicates nuclei of dead cells. PI labeled untreated 2-day-old and 9-day-old control cultures are shown in w, x. Single plane confocal fluorescence images are shown. Cyan (Ac chemical) and red (PI) fluorescence emissions are merged with transmission images. Identical excitation energy and fluorescence emission sensitivity settings were used for all images. Scale bar 20 μ m (Kuntam *et al.*, 2015).

Chemicals B2 and B3 were derived from our in-house, non-randomly synthesized collection along with some other trifluoroaminophthalimide derivatives (such as Ac-202 and Ac-1041), which were further developed as potential anticancer agents (Puskás *et al.*, 2010). Since the above mentioned dyes (B2 and B3) were not available for analysis, the Ac chemicals which were more abundant, were used in our following studies. In addition to Ac-202 and Ac-1041 chemicals, we have also included Ac-201 (a positional isomer of Ac-202) to test suitability of these chemicals as LD probes in plant cells (Puskás *et al.*, 2010).

Making use of fine rice suspension cultures (*Oryza sativa* L. japonica cv. ‘Unggi 9’) and confocal laser scanning microscopy, we have tested cell wall penetration and labeling efficiency of these chemicals. Using live cell cultures, various concentrations and treatment durations were screened. All three chemicals penetrated cells of rice suspension cultures and displayed bright spotty signals which were uniformly distributed all over the cytoplasm (Fig. 13).

For Ac-201 and Ac-202 intracellular blue spotty signals were detectable even at concentrations as low as 1 μ M, following incubation periods of even 15 minutes (Fig. 13a, c). Ac-1041 labeling was extremely weak when used at this concentration. For long-term experiments 1 μ M concentration was not sufficient, as the signal intensity diminished after 24-hour of incubation for all three chemicals (Fig. 13b, d, f). Higher concentration treatments, such as 10 μ M and 50 μ M, resulted in faster accumulation of bright signals within 15 min (Fig. 13g,

m, i, o, k, q). Ac-201 and Ac-202 were still visible even after 24-hours when used at 10 μ M concentration (Fig. 13h, j). With the use of identical detection settings, it was observed that Ac-202 showed the brightest signal in the rice culture used in our experiments and at least 10 μ M concentration was needed for proper detection of Ac-1041 chemical in short-term experiments (Fig. 13k).

Control cultures treated with 1 % (v/v) of solvent DMSO did not display detectable blue autofluorescence in short-term or long-term experiments (Fig. 13s, t). The chemicals were added directly into cultures growing in rice culture medium (G1) with a starting pH of 5.6. We could detect similar labeling efficiency on both young and old cultures, leading us to deduce that the age of cell culture or pH changes of aging medium did not significantly affect labeling intensity or penetration efficiency of the Ac chemicals. Furthermore, no detectable precipitation or background fluorescence was observed because of the direct addition of chemicals into liquid growth medium, even at 50 μ M concentration (Fig. 13a–r).

We have incubated Ac chemical-treated cells with PI, a membrane impermeable, red fluorescent nucleic acid dye to assess the effect of these chemicals on cell viability and plasma membrane integrity. PI immediately enters dead cells and stains nucleic acids bright red due to compromised plasma membranes (Truernit & Haseloff, 2008). No significant increase in PI labeling was observed with the use of Ac chemicals at 1–50 μ M concentration range, even after 24-hour treatment (see for example Fig. 13n, p, r). Bright field (transmission) microscopy images of the treated cells were also comparable to control, DMSO-treated cultures with no/very rarely observable abnormalities such as cell swelling, shrinking, color change or clumping in treated cultures (Fig. 13a–t, bright field images).

DMSO is used as solvent for Ac chemicals in our experiments and the level of DMSO concentration was always kept at or below 1 % (v/v). In control experiments, at 1 % DMSO concentration, cell viability was not affected significantly (Fig. 13s, t, red PI labeling). However, significant increase in cell mortality (as judged by PI staining) of cultured cells was seen at 10 % (v/v) DMSO (Fig. 13u, v, note numerous red nuclei). Mortality increase due to high DMSO treatment was immediately evident even after 15 min (Fig. 13u). Untreated young cultures showed low level of cell death, similar to 1 % DMSO-treated cultures (Fig. 13w). As the culture gets older, the number of dead clusters increases (Fig. 13x). On that account, only young cultures (2–4 days old) were used in all experiments. Overall, these data suggest that all three dyes could be efficiently excited using the 405 nm laser, commonly available on laser scanning confocal fluorescence microscope setups. When used below 50 μ M concentration and without exceeding 1 % DMSO as final solvent concentration, Ac chemicals do not have any significant toxicity issues in plant cell cultures even during long-term experiments.

4.2.2. Ac chemicals and Nile Red colocalization

In order to assess whether the intracellular bright granules highlighted by Ac chemicals are LDs or not, Nile Red, a red fluorescent, live cell probe for LDs was used (Greenspan *et al.*, 1985). All three Ac chemicals we found to colocalize completely with Nile Red, suggesting that Ac chemicals are specifically recognizing LDs in plant cells (Fig. 14a–c). Both blue and red emission range images were captured in single dye labeling experiments to assess the degree of channel crosstalk and autofluorescence (Fig. 14d). No signal from the Ac chemicals could be observed in the red detection range (Fig. 14d, second column, southwest, northwest and

northeast sectors) and Nile Red was not detectable in blue detection range that is used to detect Ac chemicals (Fig. 14d, first column, south sector). DMSO (1 %, v/v) did not induce any autofluorescence either in blue or red detection ranges (Fig. 14d, first and second columns, southeast sectors).

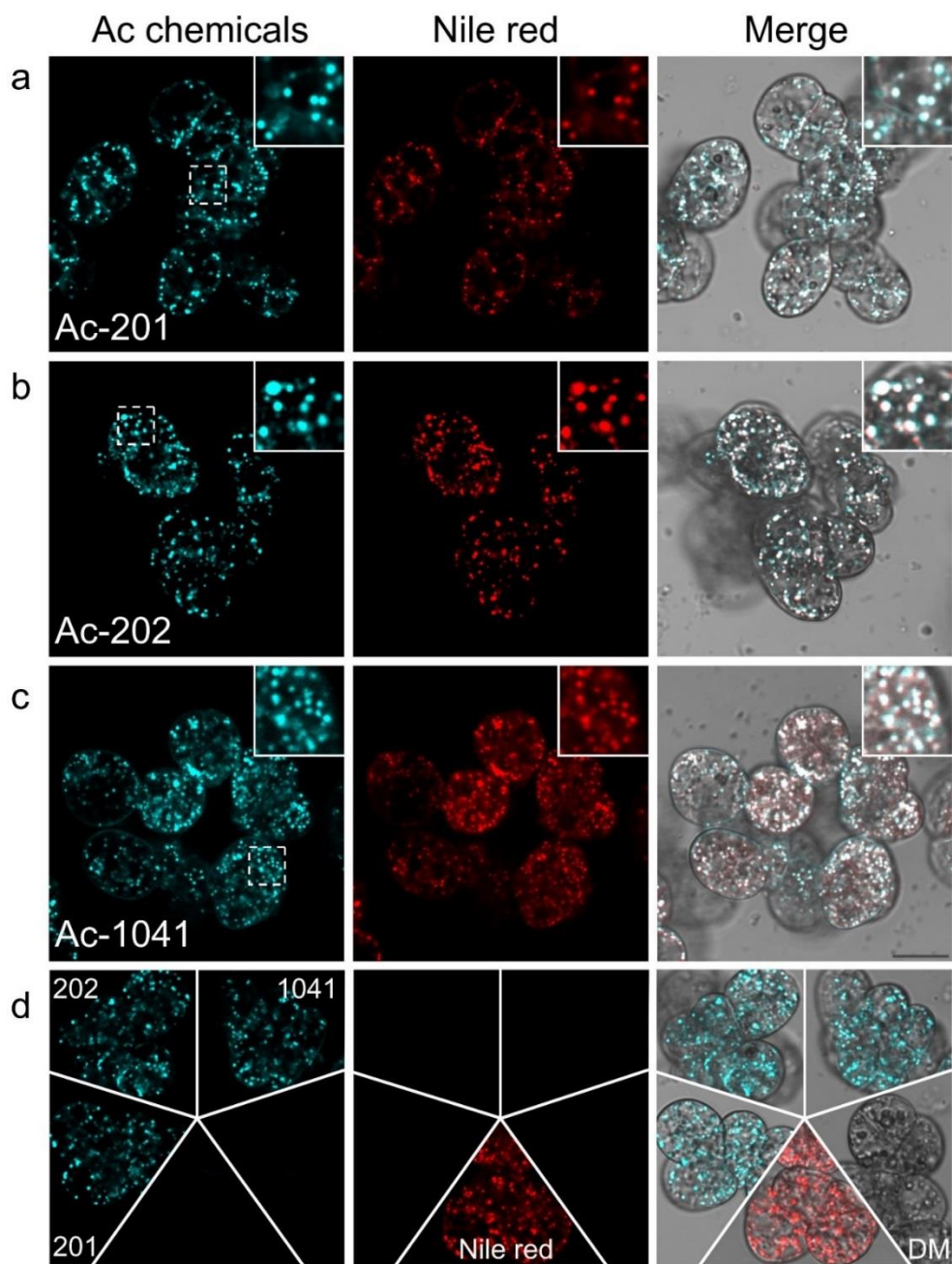


Figure 14. Ac chemicals and Nile Red, an LD specific dye colocalize completely in cultured rice cells *in vivo*. Ac chemicals (cyan) and Nile Red (red) single optical section images are overlaid onto bright field images on the last column (a–c). Insets show enlarged images of rectangular selection areas. Due to differences in emission intensities of Ac chemicals, varying detector sensitivities were used for capturing each image. Lowest detector sensitivity was used for Ac-202 which was followed by Ac-201 and Ac-1041/DMSO. To assess the degree of crosstalk between blue and red channels, single dye labeled control cells were imaged in both channels and displayed as composite images d. DMSO (DM) is used as solvent control. Scale bar is 20 μm (Kuntam *et al.*, 2015)

4.2.3. Spectral emission characteristics of Ac chemicals

Ac chemicals present a significant advantage over dyes such as Nile Red and the BODIPY derivative LD540 (Spandl *et al.*, 2009) which are routinely used as live cell LD probes. They have a specific advantage in multi-color experiments and in experiments involving green tissues with interfering red chlorophyll fluorescence. To further analyze comparatively the *in vivo* fluorescence emission characteristics of Ac chemicals, we have used a microscopy technique called spectral imaging, also known as lambda scan (Haraguchi *et al.*, 2002). This imaging technique allows quantitative determination of emission characteristics of a fluorochrome inside a living cell under physiological conditions.

Blue–cyan range fluorescence emission spectra of Ac chemicals, yellow-green colored LD540 and orange-red colored Nile Red fluorescence, acquired using spectral imaging of respectively stained rice cell cultures are shown in Figure 15. Peak intensity was observed for images captured at 460–480 nm detection interval for all the Ac chemicals (Fig. 15, spectral image series). A wider emission curve extending into shorter blue wavelengths of the spectrum was observed for the dye Ac-202. Although Ac-201 and Ac-202 are positional isomers with very similar chemical structures (Puskás *et al.*, 2010), their emission characteristics were not identical. Ac-202 displayed a more asymmetric emission curve with a pronounced shoulder at around 430 nm.

Nile Red, on the other hand, displayed emission across the middle of the visible spectrum peaking at 580–600 nm interval. This broad emission range significantly overlaps with yellow, orange and red fluorescent proteins widely used in *in vivo* studies (Fig. 15, rectangular labels on chart). Furthermore, for studies requiring proper discrimination of LDs and chloroplasts in green tissues, Nile Red is not a suitable dye.

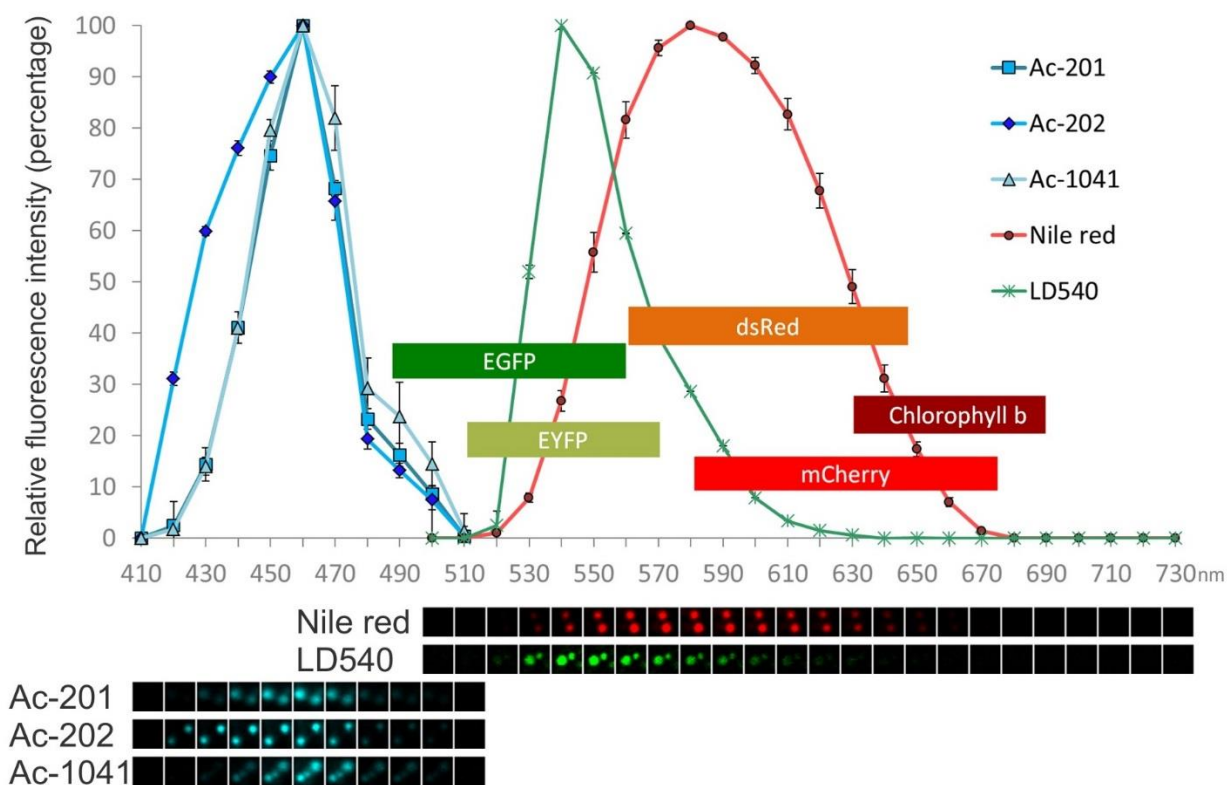


Figure 15. Comparison of spectral emission characteristics of Ac chemicals, LD540 and Nile Red using spectral imaging and live cell microscopy on rice cell cultures. Average fluorescence emission intensities of dye labeled LDs are plotted following spectral imaging with a confocal microscope. Emission ranges (above 20 % intensity) of EGFP (Enhanced green fluorescent protein), EYFP (Enhanced yellow fluorescent protein), dsRed, mCherry and chlorophyll b are indicated as colored rectangles to show the degree of spectral overlap with Nile Red and LD540 emission. Representative spectral image series of LDs stained with Ac dyes (detection: 410–510 nm), Nile Red and LD540 (detection: 500–730 nm) are shown at the bottom aligned with the abscissa of the chart (wavelength in nm). LDs of three different cells were used for calculating

averages and standard deviations. Each image frame below the chart is 4.4 μm wide (Kuntam *et al.*, 2015).

Its emission range overlaps with the chlorophyll autofluorescence requiring careful selection of bandpass emission filters (or tuning of spectral detectors) (Fig. 15). In contrast to Nile Red, LD540 dye which has a narrow emission around 540 nm should not present a significant issue of interference with chlorophyll fluorescence. On the other hand, emission of LD540 spans the same region as EYFP fluorescence and partially overlaps with green- (e.g. EGFP) and orange-colored probes (Fig. 15). Therefore, specific detection and discrimination of LD540 dye in multicolor experiments necessitates the use of specific filters and/or carefully adjusted microscopy parameters (Spandl *et al.*, 2009). Ac chemicals with their spectrally well-isolated blue fluorescence can be confidently and easily isolated from green- and red-colored dyes and fluorescent proteins without significant crosstalk issues (Fig. 16).

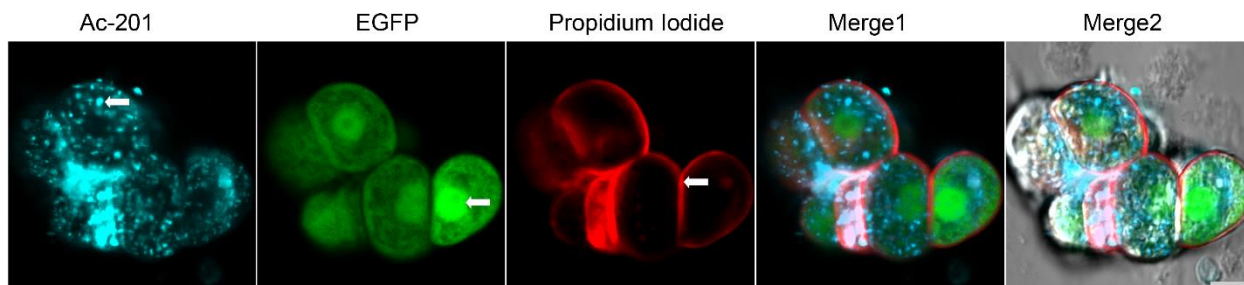


Figure 16. Detection of LDs (Ac-201, 10 μM , 15 minutes), EGFP and cell borders/cell walls (PI, 0.45 μM , 15 minutes) on live rice cell cultures (*O. sativa* L. ssp. japonica cv. 'Nipponbare') stably expressing untagged EGFP protein (PI is getting trapped in cell walls of live cells and can be used as live cell wall labeling marker). Arrows mark representative high signal intensity regions in cyan, green and red channels. Note the absence of channel crosstalk in these regions. Three-color merged image (Merge 1) was overlaid onto bright field image at the last panel (Merge 2). Scale bar is 10 μm (Kuntam *et al.*, 2015).

4.2.4. LD detection on various plant cultures

Different plant species may display different dye penetration and labeling characteristics due to differences in cell wall structure, cellular architecture and metabolism. Therefore, to assess their behavior, we tested Ac chemicals on several monocot and dicot plant cultures. Under identical treatment (10 μ M, 15 min) and image-capturing conditions, the most intense labeling with Ac dyes was observed with alfalfa cultures (*M. sativa* ssp. varia A2) (Fig. 17a–c).

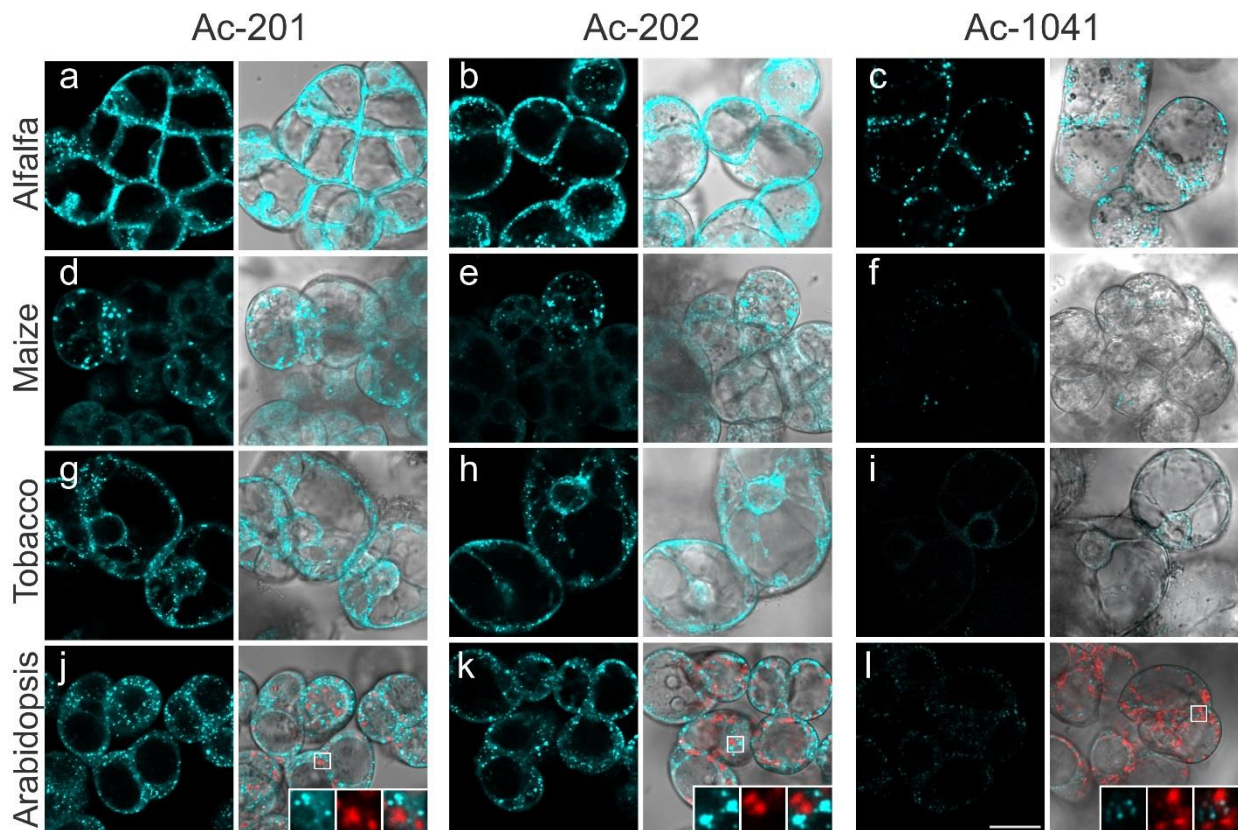


Figure 17. LD detection in various plant cultures using Ac chemicals. LD labeling with Ac-201, Ac-202 and Ac-1041 chemicals (10 μ M, 15 min) was tested on **a–c** alfalfa (*M. sativa* ssp. varia A2), **d–f** maize (*Z. mays*, cv. H1233), **g–i** tobacco (*N. tabacum* cv. Petit Havana SR1) and **j–l** chlorophyll-containing Arabidopsis (*A. thaliana* ecotype Landsberg erecta, MM1) cell cultures. Merged images of chemical fluorescence (cyan), chlorophyll (red) and bright field (grayscale) are shown. Insets show 3 \times magnified close-up images of representative selected regions (white rectangles in **j–l**). Note complete color separation between cyan and red channels in insets. Scale bar 20 μ m (Kuntam *et al.*, 2015).

Also, high cytoplasmic background was noticed in alfalfa cultures labeled with Ac-201 and Ac-202, but not Ac-1041. Ac-1041 labeling on alfalfa was composed of fine, discrete spots with minimal background, making this chemical more suitable for LD studies in this particular plant culture (Fig. 17c). To further provide proof that labeling the cells with higher concentration of the dyes was not the reason for the observed high cytoplasmic background with Ac-201/202, alfalfa cultures were treated with lower concentration (1 μ M) of all three Ac dyes for 15 minutes (Fig. 18). As can be observed from the images, even at low concentrations and low incubation times, faint cytoplasmic background could be observed in Ac-201 and 202 but not in Ac-1041.

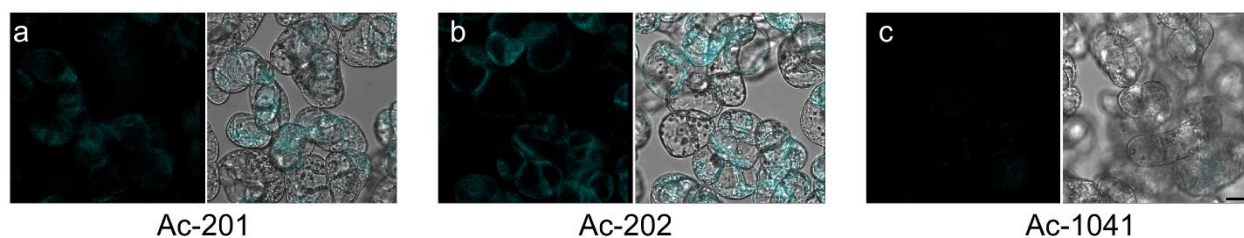


Figure 18. Application of low concentration of Ac chemicals on alfalfa cultures. Ac-201 (a), Ac-202 (b) and Ac-1041 (c) were used at 1 μ M concentration for 15min. Faint cytoplasmic background was observed in Ac-201/202 but not Ac-1041. Scale bar is 20 μ m (Kuntam *et al.*, 2015).

For all other cultures tested, Ac-1041 when used at 10 μ M with a 15-minute incubation period, showed detectable but very weak signal (Fig. 17f, i, l and insets in l). Maize culture (*Z. mays*, cv. H1233) used in our experiments displayed a surprisingly high LD heterogeneity when labeled with Ac 201/202 dyes. Within a single cluster several LD rich cells with multiple big and bright fluorescent spots were clearly distinguishable from neighboring cells with minimal LD labeling (Fig. 17d, e). Considering the fact that we could see fine LDs and a faint cytoplasmic dye background in all of the cells, we could deduce that this observed striking difference was not due to lack of dye penetration to some cells (Fig. 17d, e compare with f).

To further provide evidence that the observed heterogeneity in Figure 17 was not due to issues related to single optical section imaging, we have captured multiple optical z-sections of maize cell clusters labeled with Ac-201 dye and quantified average fluorescence intensities of individual cells (data not shown). Fluorescence intensity differences of more than 3 times could be measured between certain cells. We speculate this difference in LD heterogeneity might be due to cells in different phases of the cell cycle (Kwok & Wong, 2005).

We also observed equal, efficient labeling of LDs with both Ac-201 and Ac-202 dyes on tobacco SR1 culture (*N. tabacum* cv. Petit Havana SR1). Cells displayed very fine LD labeling, enriched in the perinuclear region, cytoplasm and cytoplasmic strands. Similar to alfalfa and tobacco cultures, Arabidopsis culture (*A. thaliana* ecotype Landsberg erecta, MM1) also displayed homogenous LD labeling within a given cell cluster with Ac-201/202 chemicals (Fig. 17j–l). No emission crosstalk issues were encountered while imaging these chlorophyll containing Arabidopsis cells labeled with Ac chemicals. We could clearly isolate spectrally well-separated, blue Ac chemical-labeled LDs from red chloroplasts (Fig. 17j–l, insets).

4.2.5. LD labeling on intact Arabidopsis seedlings

Plant suspension cultures, made up of relatively small clusters with only a few layers of mostly homogenous cells, are easier to be labeled with live cell dyes. On the other hand, tissues and organs of plants with multiple layers of diverse cells present penetration barriers for dyes during *in vivo* use.

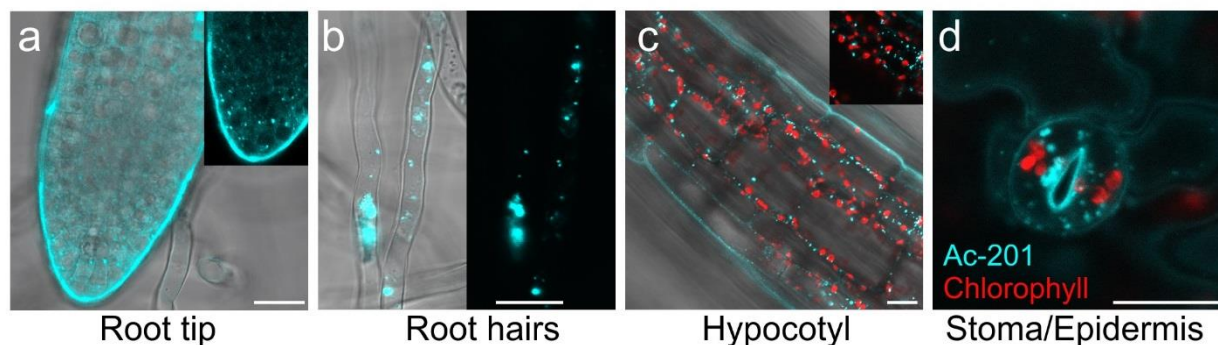


Figure 19. LD labeling on seedlings using Ac chemicals. Arabidopsis (ecotype Columbia-0) seedlings were incubated 1 h (10 μ M) with Ac-201. *In vivo* LD detection on various plant parts are shown. Scale bar 20 μ m (Kuntam *et al.*, 2015).

To investigate the full potential of Ac chemicals as LD dyes for plants, we further tested them in germinating Arabidopsis seedlings. As shown in Figure 19 and 20, both Ac-201 and Ac-202 dyes were equally suitable for use in various organs and tissues of intact seedlings. Dense root meristem region, with multiple layers of actively dividing cells (Fig. 19a and inset), fine root hairs (Fig. 19b), hypocotyl (Fig. 19c) and epidermis of cotyledon (Fig. 19d) labeled with Ac-201 were all showing fine spots of LD indicating successful probe penetration and LD labeling. In root tip labeling experiments, we have observed larger and more abundant LD labeling in columella cells as compared to meristematic and quiescent center cells. This difference might be due to the differences in the metabolic activity or identity of these different cell types. It is possible that the degradation of LDs might be slower in the columella cells leading to the coalescence of smaller LDs to form bigger LDs. As opposed to that, rapidly dividing meristematic cells and stem cells with higher metabolic rates might be catabolizing the LDs at a faster rate, giving them lesser time to coalesce and form bigger LDs. For the quiescent center, slower synthesis of neutral lipids may be the cause of the size difference of LDs.

Similar to the Arabidopsis MM1 culture, blue fluorescent Ac chemical labeled LD detection in chlorophyll containing green tissues such as hypocotyl (Fig. 19c) and cotyledon

regions (Fig. 19d, 20) was particularly advantageous. Efficient penetration and bright fluorescence emission of these dyes facilitated the use low excitation energies. This was particularly advantageous in 3D confocal optical sections and reconstructions, wherein multiple successive image capturing is necessary. Images presented in Figure 20a and b, were reconstructed from images captured by laser scanning of 396 consecutive optical sections without significant dye bleaching (see also Fig. 20c for additional 396 scans of a subset area).

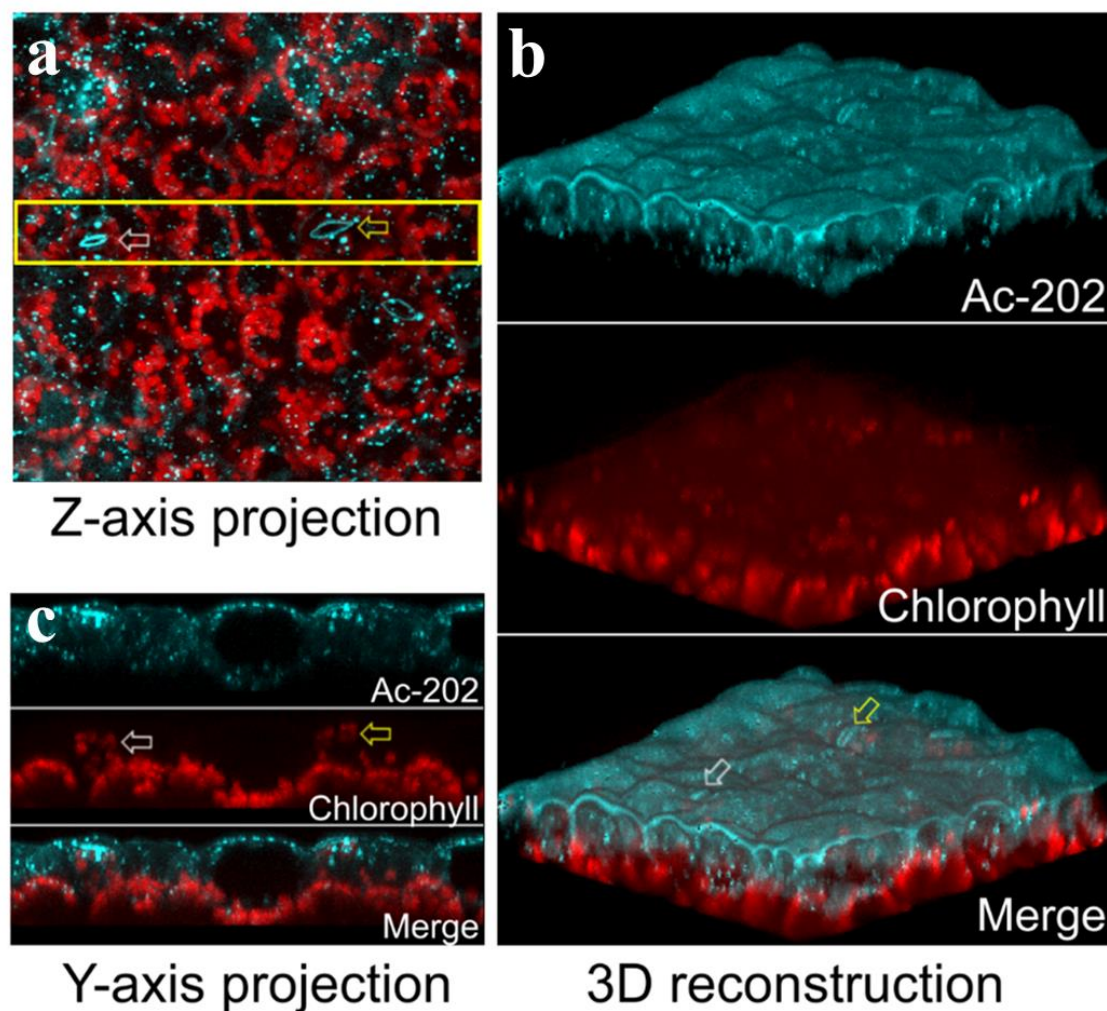


Figure 20. LD labeling on Arabidopsis cotyledon using Ac-202. Arabidopsis cotyledon treated with 10 μ M Ac-202 for 1 h was optically sectioned using laser scanning confocal microscope. Z-axis projection (image merging) of 396 optical sections of cotyledon epidermis/upper parenchyma region is shown in (e). Three-dimensional reconstruction of merged z-axis images in (e) is shown in (f). For better visualization of 3D morphology, image in (f) is contrast enhanced

to amplify faint cell wall fluorescence of epidermal cells. Y-axis projection (side view) of additional 396 scans shown in (g) was obtained by fast scanning of a smaller area (yellow rectangular area in e). White and yellow arrows mark two stomata which also indicate orientation of 3D image. Interstomatal distance (center to center) is 74 μm (Kuntam *et al.*, 2015).

In order to lessen image smudging due to mobile LDs, a smaller area was rescanned in 3D using faster scanning parameters. Figure 20c shows the y-axis projection (side view) of the selected area (yellow rectangle in Fig. 20a) using additional 396 optical sections from the same cotyledon area. Note that a total of approximately 800 times repeated laser scanning of the same area did not cause significant signal bleaching of Ac-202 fluorescence.

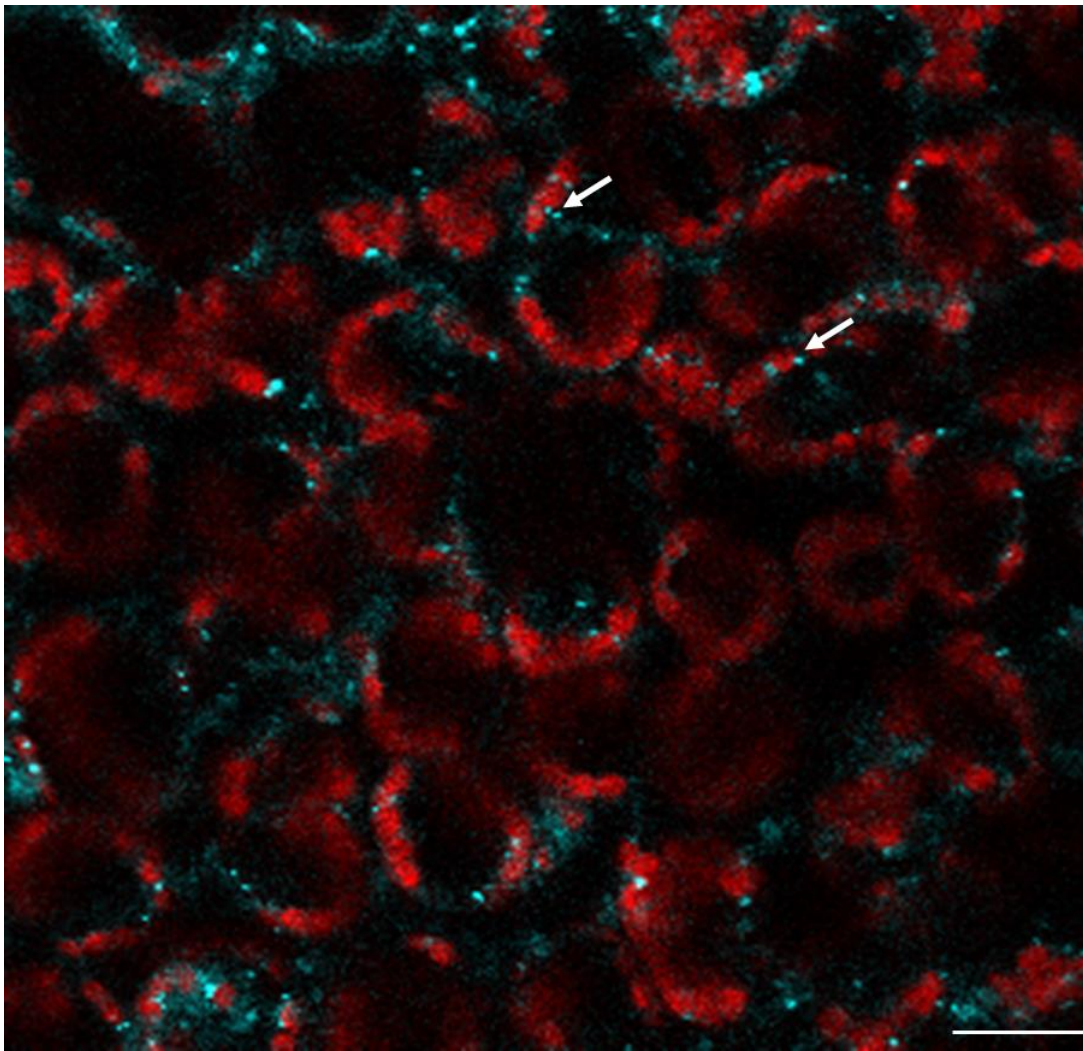


Figure 21. Optical z-section of Arabidopsis cotyledon labelled with Ac-202. Arabidopsis cotyledon treated with 10 μ M Ac-202 for 1 h was optically sectioned using laser scanning confocal microscope. Shown is a single representative optical sections showing LD labelling in parenchymal cells (white arrows). Scale bar 15 μ m

As demonstrated by these 3D confocal optical sections (Fig. 20b, c), epidermis of Arabidopsis cotyledon was found to contain significantly more LDs than the parenchyma region. This difference was not due to lack of dye penetration to parenchyma region as evidenced by the presence of LD labeling between and around the chloroplasts of parenchyma cells (Fig. 21).

Effective LD labeling was also observed with Ac-1041 in root hair and hypocotyl region (Fig. 22), but in dense and multilayered tissues (such as root tip) it was weaker in intensity as compared to Ac-201/202. Differentiated cells usually have a large central vacuole which occupies most of the volume of the cell confining the cytoplasm to a thin layer. Hence the organelles of the cells (like LDs and ER) are pressed against the cell wall. The LD labelling of hypocotyl cells in Figure 22b appears to be labelling the cell wall/plasma membrane but it is arising mostly from the several LDs in the cytoplasm confined to a smaller area. In addition, faint cell wall autofluorescence of hypocotyl cells may also play an additional role in this border labelling.

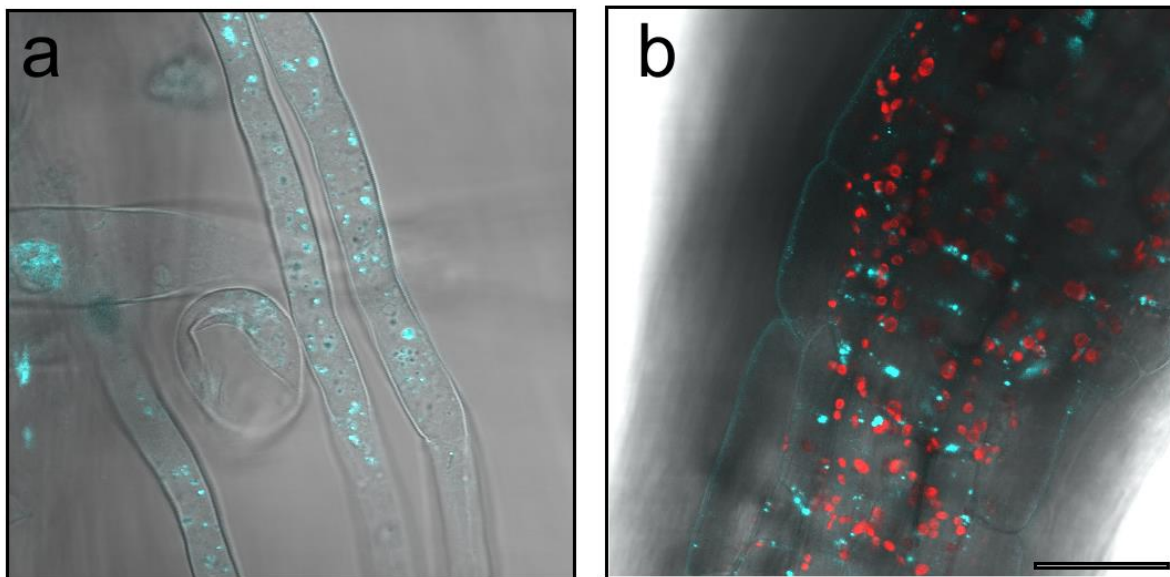


Figure 22. Ac-1041(10 μ M, 1hr) labeling on Arabidopsis seedlings. Root hairs (**a**) and hypocotyl (**b**). Ac-1041 (cyan) and chlorophyll (red) images are overlaid onto bright field images in (**b**). Scale bar 20 μ m (Kuntam *et al.*, 2015).

4.3. Monitoring LD behavior during plant cell cycle

In the past decade it has become clear that, while there are specialized lipid storing tissues, essentially all cell types have the ability to store LDs, even if they are dynamic and short lived (Walther & Farese, 2009; Chapman & Ohlrogge, 2012; Denis J Murphy, 2012). Furthermore, along with an increasing appreciation for the prevalence of LDs throughout biological systems, a broader range of functions associated with LDs has been reported including stress response and pathogen resistance (Coca & San Segundo, 2010), dormancy release in shoot apical meristems (Rinne *et al.*, 2001), dormancy process in root nodules, photoperiod signaling

(Grefen *et al.*, 2008), lipid homeostasis, hormone metabolism/ signaling and a specialized role in anther development (Hsieh & Huang, 2004).

In the past years, the neutral lipid content (sequestered mostly in LDs) of cells has been linked to cell cycle progression (Guckert & Cooksey, 1990; Gocze & Freeman, 1994; Kwok & Wong, 2005). The major TAG lipase in budding yeast, Tgl4p, is phosphorylated and activated by cyclin-dependent kinase 1/cell division cycle protein 28 (Cdk1p/Cdc28p) (Kurat *et al.*, 2009). Lipolysis of TAG contributes to bud formation in late G1 phase of the cell cycle and lack of lipolysis delays the same bud formation. Other earlier work has shown that the intensity of neutral lipids of MA-10 Leydig tumor cells labeled with BODIPY 493/503, was a function of the cell cycle (Gocze & Freeman, 1994). Neutral lipid biosynthesis has also been reported to be coordinated with cell cycle progression in heterotrophic dinoflagellate protists (Kwok & Wong, 2005). Thus, there appears to be links between cell cycle progression and neutral lipid turnover, but they are just beginning to be appreciated, and the role of LDs in these processes is yet to be elaborated.

4.3.1. LD variability in BY-2 cells across the culture's growth curve

Although GFP-tagged proteins have been used in many studies to study LDs (Pol *et al.*, 2001; Targett-Adams *et al.*, 2003; Boström *et al.*, 2005), the function of the proteins used for the visualization is not always defined and hence their expression itself might modify the behavior of the LDs in unpredictable ways. LDs are known to harbor a variety of associated proteins on their surface and based on the composition of proteins, form functional and morphological LD subpopulations (Wolins *et al.*, 2005). Lipids tagged with fluorescence groups might also have adverse effects on physiological processes (Gocze & Freeman, 1994). Taking this into account,

the LD dyes we had effectively characterized in our previous studies were perfect tools to be utilized for quantitative LD studies.

Microscopy in three spatial dimensions is necessary to quantify the total LD content of a cell because the LDs are dynamic enough that, individual LD movement in or out of the focal plane will result in erroneous results. This is particularly true of small droplets. BY-2 cells are useful for tracking such dynamics because they provide a well-defined volume in which quantitative confocal microscopy can be performed owing to their tendency to grow in chains (Nagata *et al.*, 1992).

Fixed BY-2 cell samples were labeled with Ac-201 (LD), Alexa Fluor 488 azide (labeling incorporated EdU) and PI (nucleus). Multiple confocal optical z-sections of cells with visible, well defined cell borders were obtained (Fig. 23). Identical imaging parameters were maintained throughout the image acquisition process over the course of the experiment. The LDs of individual cells were further analyzed quantitatively using the Huygens Professional image analysis software from Scientific Volume Imaging.

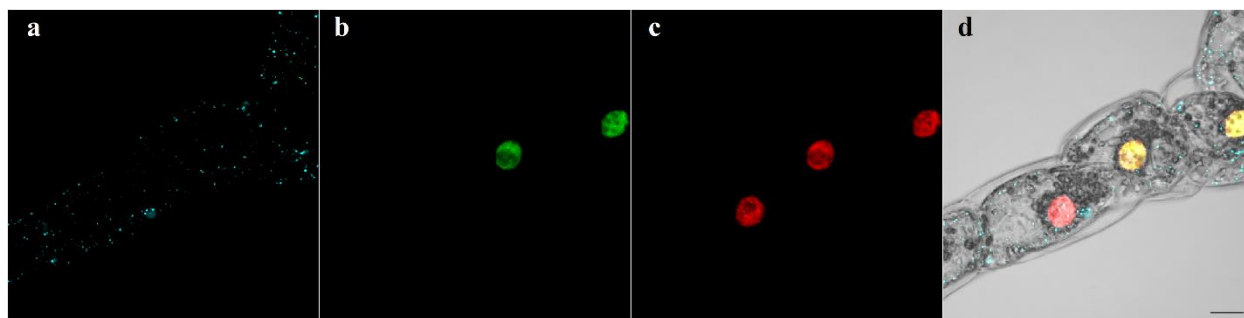
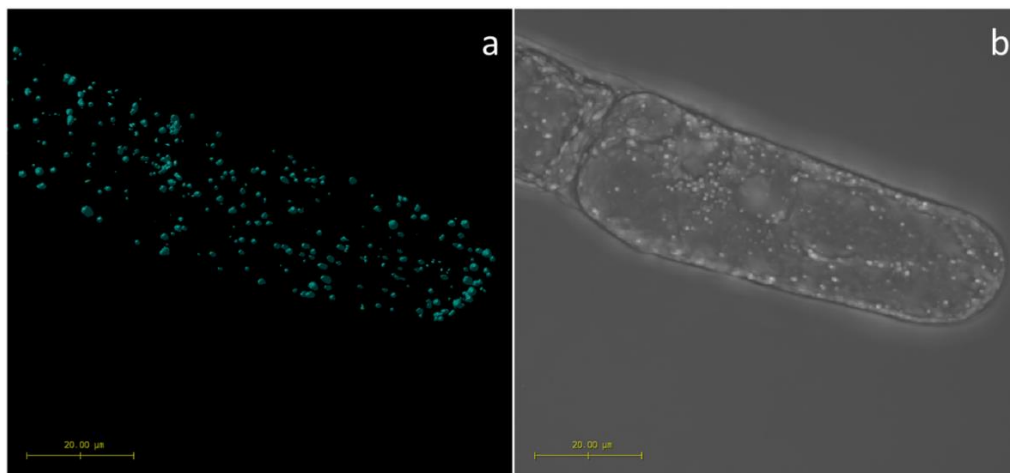


Figure 23. Detection of LD (**a**, Ac-201, 10 μ M), S-phase nuclei (**b**, Alexa Fluor 488) and nuclei (**c**, PI) on fixed BY-2 cells. (**d**) All three channel images were merged and overlaid onto the bright field image. Scale bar 20 μ m.

We were interested in the voxel values of individual LDs within a cell. Voxel is short for volume pixel and is the 3D equivalent of a 2D pixel, representing the smallest value on a

rectangular grid in three-dimensional space. The volume of an object can be described in voxels by extracting the polygon iso-surface rendering of the object which follows the contours of given threshold values. Iso-surface is the surface that envelops all the voxels in a 3D rendering of an image. If the voxels are distributed in groups that are not spatially connected, many different non connected surfaces are obtained and each non connected surface is labeled as an independent object (e.g. individual lipid droplets within a cell Fig. 24c). Utilizing the OA tool of the Huygens Professional image analysis software, the total LD volume of individual cells (n=50) was calculated for each day, starting with day 0 (day of medium refreshment of a 7d old culture) and continued till day 9 (nine days after culture refreshment) (Fig. 25). Furthermore, to correlate the total LD content with cell cycle progression, the percentage of S-phase cells in all (0-9 days) samples were also calculated (n=500). The total LD content of each day in correlation with the number of S-phase and M-phase cells for that day is shown in Figure 25.



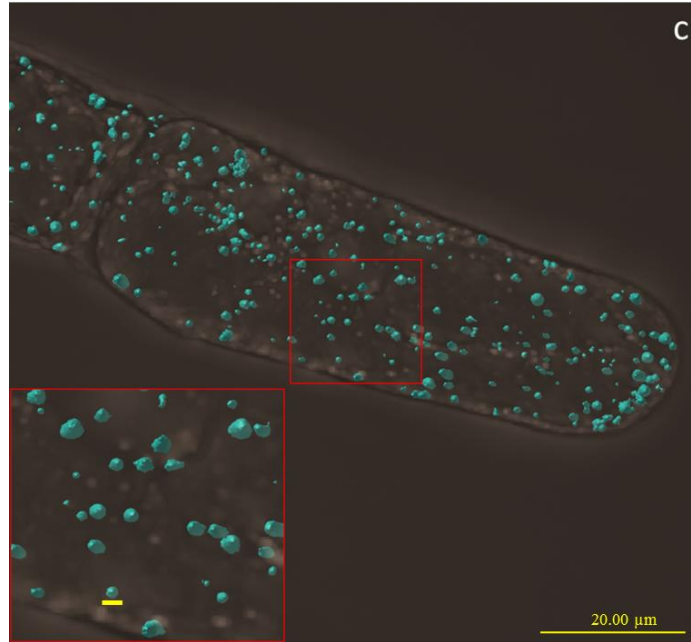


Figure 24. 3D reconstruction of BY-2 cells using the Huygens Object Analyzer. (a) 2D projection (top view) of LD labeling on BY-2 cells. (b) 2D projection of bright field image (c) 3D reconstruction of LD labeling. Inset shows enlarged image of rectangular selection area. Scale bar of inset 1 μm .

As can be observed from the graph, the total LD volume of the cells seem to be cycling through the different days of the growth curve of BY-2 culture. A striking discovery for us was the significant drop of LD volume on day 2 in comparison to the low M-phase and high S-phase cells in that day. This could also be observed to a lesser degree on day4. With these results, we could hypothesize that there might be a possible interrelationship between total volume of LD and the different cell cycle phases.

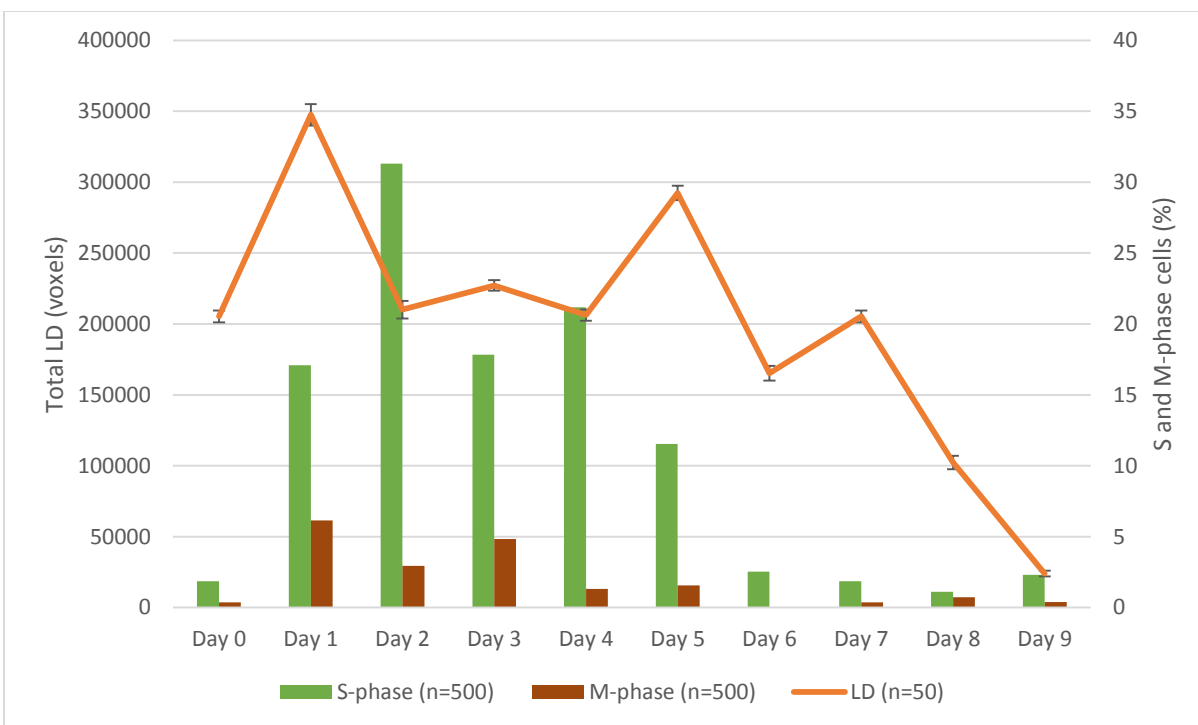


Figure 25. Total LD, S-phase and mitotic index count of BY-2 cells across their growth curve. Total LD volume was determined by calculating voxel values of individual LDs/cell/sample (n=50). Percentage of cells in S and M-phase/sample calculated using EdU and PI labelled cells respectively (n=500). Day 0: day of culture refreshment and every day is 24 h apart.

4.3.2. LD in hydroxyurea-synchronized BY-2 cells

To further investigate the correlation between total LD volume and cell division cycle, BY-2 cells were blocked in S-phase with 5mM HU for a period of 36 hours and then the HU block was removed by successive conditioned media washes that lasted for a total of 45 minutes. Before wash and 2 hours after wash, BY-2 cells were labeled with 10 μ M concentration of Ac-201 for 15 minutes and imaged using CLSM. Figure 26 (a, b) show control and HU blocked BY-2 cells before wash. As can be observed from the images, there was a marked difference in the LD content of the control and HU blocked cells. The HU blocked cells had markedly less LD in comparison to control cells, which showed abundant LD labeling.

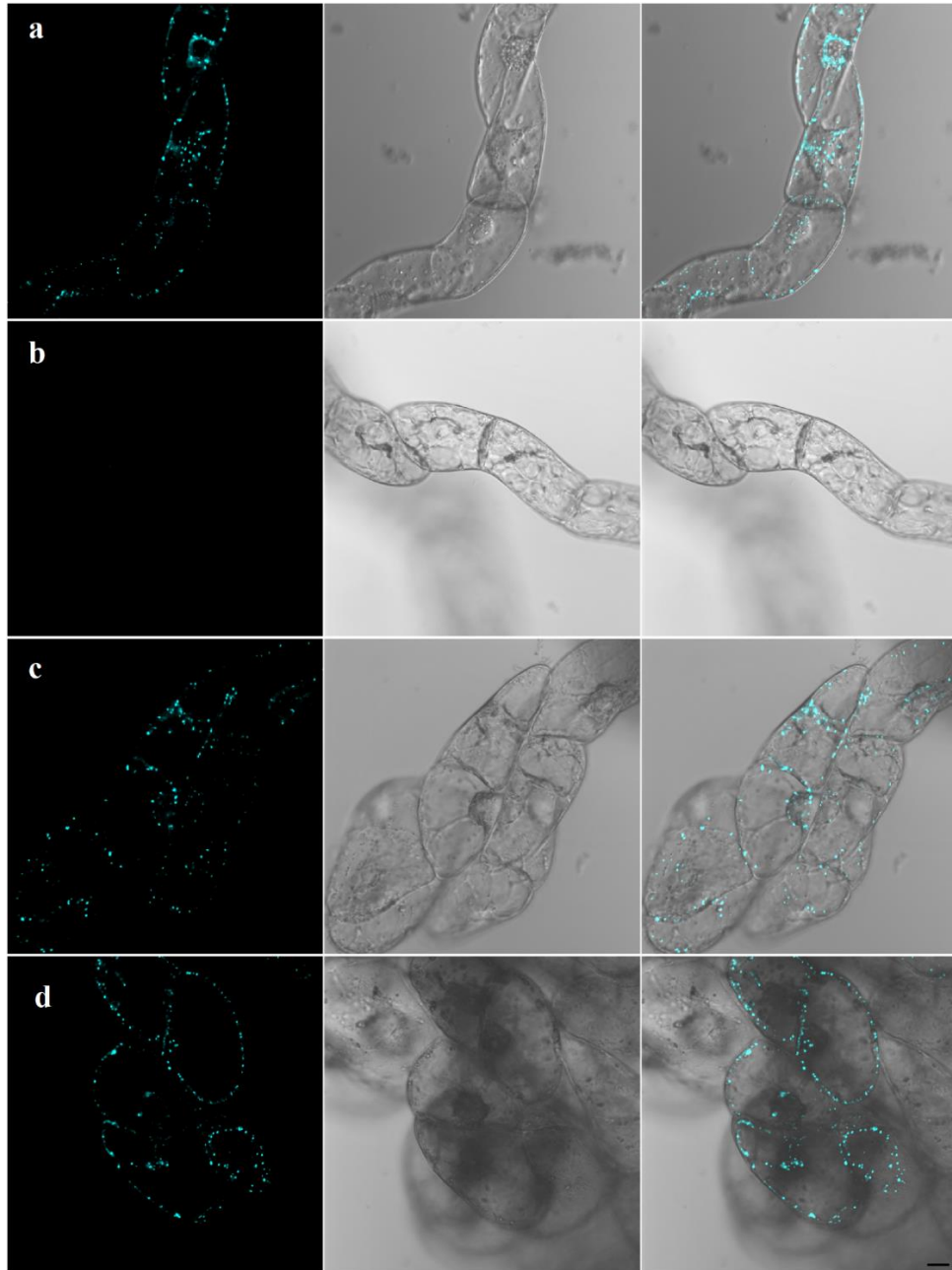


Figure 26. Re-emergence of Ac-201 labeled LDs after HU removal in BY-2 cells. LD labeling of control cells 36h after refreshment (**a**), 5mM HU blocked, before HU wash (**b**), control cells 2h after conditioned media (CM) wash (**c**), and HU blocked, 2h after CM wash (**d**). Scale bar 20 μm .

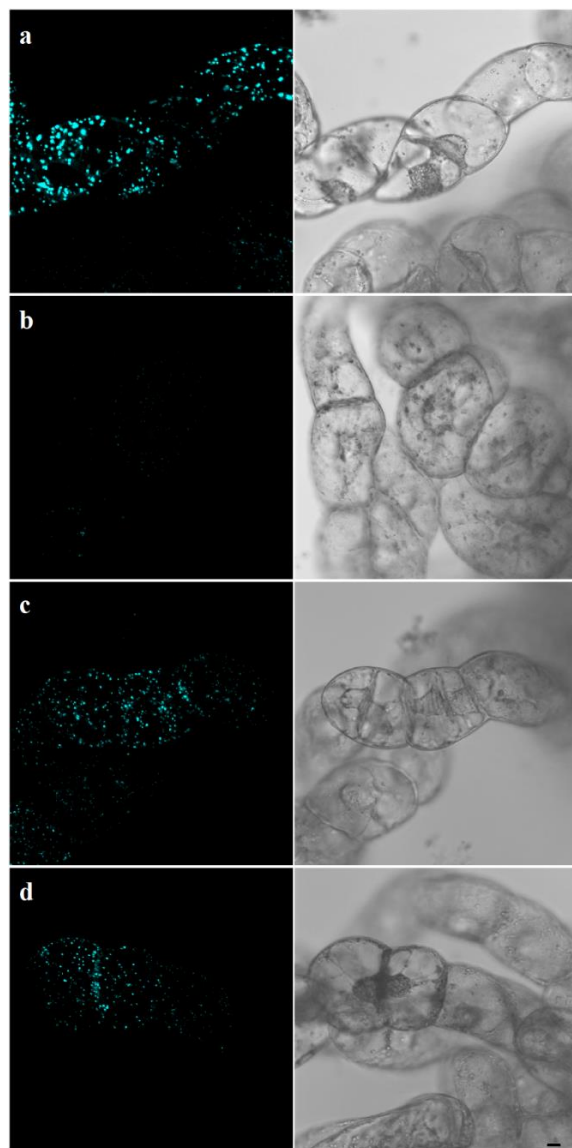


Figure 27. Re-emergence of Ac-201 labeled LDs after HU removal confirmed with multiple optical z-sections. LD labeling of control cells 36h after refreshment (**a**), 5mM HU blocked, before HU wash (**b**), control cells 2h after conditioned media (CM) wash (**c**), and HU blocked, 2h after CM wash (**d**). Scale bar 20 μ m.

To further prove that this difference was not due to single optical section imaging, multiple z-optical section images were acquired (Fig 27 a, b). From these images it was apparent that there is a definite difference in the LD content of control and HU blocked cells with the HU blocked cells having only very few LDs.

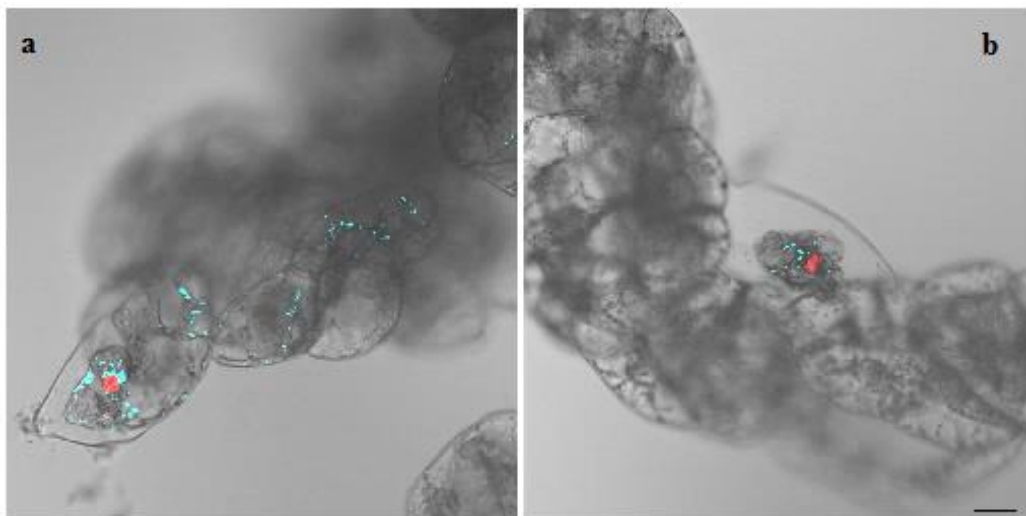


Figure 28. Comparing cell viability of control and HU treated culture. PI labeled control and 5mM HU treated cells shown in (a) and (b). PI viability of control and HU treated cells were 96.21% (± 0.2) and 94.79% (± 0.3), respectively. Ac-201 and PI fluorescence emission merged with transmission images. Scale bar 20 μm .

To make sure that the LD content difference seen between the samples was not due to cell death caused by HU block, the HU blocked and control cells were simultaneously labeled with nuclear dye PI, which cannot penetrate intact, living cells (Fig 28). We did not find a marked difference between the PI labeling of control and HU blocked cells. With this, we could infer that the LD labeling difference between the samples was not caused by cell death induced by HU block.

Two hours after HU block removal, control cells and HU block removed cells were also labeled with Ac-201 at 10 μM concentration for 15 minutes. Same imaging parameters as those used for before wash samples were employed while acquiring images through CLSM (Fig 26 c, d). As can be seen from the images, we could observe a reemergence of LD in HU block removed cells. As with the before wash cells, multiple z-optical sections were obtained for both

the control and HU block removed cells (Fig. 27 c, d). The reemergence of the LDs was also confirmed in these multiple optical sectioning images, as well.

Coordination between lipid metabolism and cell cycle progression is necessary for the faultless duplication and enlargement of cellular components. A disharmonic regulation of the highly dynamic balance between LD synthesis and breakdown would result in cells with either excessive LD accumulation or fast depletion of available LD stocks. We have observed a significant decrease in LD content of cells blocked in S-phase using HU. We hypothesize that the reason for this drastic drop of LDs in HU blocked cells is mostly due to depletion of available LD reserves for energy and/or neutral lipid requiring processes during prolonged S-phase block without allowing cells to activate and/or duplicate LD synthesis-related genes in G2 phase of the cell cycle following replication. It is less likely that HU intercalates and inhibits Ac-201 dye fluorescence, as we have seen LD labeling in the presence of HU during PI viability experiments (Fig. 27b).

Aphidicolin-based tobacco BY-2 culture synchronizations reported by Magyar *et al.*, (2005) and Kumagai-Sano *et al.*, (2007) indicate that the cells are mostly in S or G2 phase of the cell division cycle 2 h after removal of this G1/S border blocking reagent. Since HU blocks the cells in a later phase (early S-phase) than aphidicolin, we predict that in our experiments, a significant portion of cells must be already in G2 phase 2h (with HU washes and LD labelling durations, nearly 3h) after HU removal. On the other hand, we cannot rule out the possibility that HU, as a replicative stress inducer, may be the culprit or has an additional role of reduced LD amounts during prolonged HU incubation. The relationship between LDs and stress response has already been shown during pathogen attack and drought stress in plants (Coca & San Segundo, 2010; Anjum *et al.*, 2011), therefore the replicative stress imposed by HU should also be taken

into account to interpret these results. Nonetheless, to better dissect the relationship between LDs and cell division cycle, precise amounts of cells in each cell cycle phase – especially G2 content, need to be followed using flow cytometry in a full synchronization experiment. Alternatively, to eliminate the possible stress effect of synchronization reagents (e.g: HU or aphidicolin), LD amount-growth curve analyses can be followed by taking frequent samples, such as every 6 to 8 hours after culture refreshment. Nevertheless, our results based on daily samplings of an unstressed, semi-synchronously dividing cultures point towards a possible cyclic interrelationship between LDs and the cell division cycle of plant cells. Employing novel LD dyes and confocal microscopy in live plant cells, we postulate that our results have a significant potential to lay the groundwork for better understanding of LD regulation during plant cell division cycle.

5. CONCLUSIONS

The present study resulted in the discovery of several novel fluorochromes, which were further characterized in both animal and several plant cell types. The main results of the work can be summarized as follows:

- Of the 278 chemicals screened, we have discovered 11 novel fluorochromes labeling various, specific intracellular compartments using human HeLa cells as a model organism. Their labeling was confirmed by co-labeling each fluorochrome with a known marker. The fluorochromes were further studied for their optimum working concentrations. Each fluorochrome was assayed for its toxicity to assess its use for long-term live cell experiments.
- Three of the fluorochromes (B2, B3 and C4) were found to be plant cell wall permeable and labeling LDs. Owing to their unavailability in large quantities, these dyes were not pursued as potential LD dyes. Ac chemicals derived from the same pool of our in-house synthesized trifluoroaminophthalimide derivatives as B2 and B3 were used in our further studies. All three Ac chemicals tested (201, 202 and 1041) were plant cell wall permeable and confirmed to be labeling LDs by co-labeling with known LD marker Nile Red. The dyes were assessed for their toxicity and found to be non-toxic at concentrations up to 50 μ M, hence suitable for long-term live cell analysis such as studying their mobility dynamics.
- Spectral emission characteristics of the Ac chemicals using lambda scan were studied. All three dyes with their narrow emission range, displayed a peak intensity at 460-480 nm, well isolated from green and red colored dyes and fluorescent proteins, providing the much needed flexibility for multi-color imaging.

- Ac chemicals were tested on several monocot and dicot plant cultures; Ac 201/202 displayed high background in alfalfa cultures whereas Ac 1041 showed discrete LD labeling. The staining intensity and/or penetration of Ac 1041 was less favorable in other plant cultures. Spectral emission and labeling intensity differences between the highly similar Ac chemicals suggest that, additional modifications might yield even better LD probes with superior characteristics.
- Ac chemicals were also tested for their labeling properties on intact green tissues. Ac-201 and 202 were found to penetrate deep multilayered tissues of intact seedlings. Both underground and aboveground tissues of seedlings showed several LDs stained with Ac chemicals. Repetitive laser scanning during collection of multiple z-axis optical sections on stained cotyledons did not cause significant signal fading of Ac chemicals. It was found that the epidermal cells of Arabidopsis cotyledons have more LDs as compared to parenchyma cells.
- Employing the novel LD dyes, the LD abundance and variability in BY-2 cells across their growth curve were studied. It was observed that the total LD volume of the cells was cycling through the different days of the growth curve of BY-2 culture. Furthermore, we could observe a significant drop of LD volume on day 2 in comparison to the reduced M-phase and elevated S-phase cells in that day.
- BY-2 cells blocked in S-phase using 5mM HU had a considerable decrease in LDs as compared to control cells. Two hours after HU block removal, we could observe a reemergence of LDs.

REFERENCES

- Adeyo, O., Horn, P. J., Lee, S., Binns, D. D., Chandrahas, A., Chapman, K. D., & Goodman, J. M. (2011). The yeast lipin orthologue Pah1p is important for biogenesis of lipid droplets. *Journal of Cell Biology*, 192(6), 1043–1055. <http://doi.org/10.1083/jcb.201010111>
- Agard, N. J., Baskin, J. M., Prescher, J. A., Lo, A., & Bertozzi, C. R. (2006). A Comparative Study of Bioorthogonal Reactions with Azides. *ACS Chemical Biology*, 1(10), 644–648. <http://doi.org/10.1021/cb6003228>
- Alvarez, M., Villanueva, Á., Acedo, P., Cañete, M., & Stockert, J. C. (2011). Cell death causes relocalization of photosensitizing fluorescent probes. *Acta Histochemica*, 113(3), 363–368. <http://doi.org/10.1016/j.acthis.2010.01.008>
- Anjum, S. A., Xie, X.-Y., Wang, L.-C., Saleem, M. F., Man, C., & Lei, W. (2011). Morphological, physiological and biochemical responses of plants to drought stress. *African Journal of Agricultural Research*, 6(9), 2026–2032. <http://doi.org/10.5897/AJAR10.027>
- Arumuganathan, K., Slattery, J. P., Tanksley, S. D., & Earle, E. D. (1991). Preparation and flow cytometric analysis of metaphase chromosomes of tomato. *TAG. Theoretical and Applied Genetics. Theoretische Und Angewandte Genetik*, 82(1), 101–11. <http://doi.org/10.1007/BF00231283>
- Ayaydin, F., Kotogány, E., Abrahám, E., & Horváth, G. V. (2011). Synchronization of *Medicago sativa* cell suspension culture. *Methods in Molecular Biology (Clifton, N.J.)*, 761, 227–38. http://doi.org/10.1007/978-1-61779-182-6_15
- Barnes-Seeman, D., Park, S. B., Koehler, A. N., & Schreiber, S. L. (2003). Expanding the Functional Group Compatibility of Small-Molecule Microarrays: Discovery of Novel Calmodulin Ligands. *Angewandte Chemie International Edition*, 42(21), 2376–2379. <http://doi.org/10.1002/anie.200351043>
- Bass, H. W., Wear, E. E., Lee, T. J., Hoffman, G. G., Gumber, H. K., Allen, G. C., ... Hanley-Bowdoin, L. (2014). A maize root tip system to study DNA replication programmes in somatic and endocycling nuclei during plant development. *Journal of Experimental Botany*. <http://doi.org/10.1093/jxb/ert470>
- Bazin, J., Khan, G. A., Combier, J. P., Bustos-Sanmamed, P., Debernardi, J. M., Rodriguez, R., ... Lelandais-Brière, C. (2013). MiR396 affects mycorrhization and root meristem activity in the legume *Medicago truncatula*. *Plant Journal*, 74(6), 920–934. <http://doi.org/10.1111/tpj.12178>
- Best, M. D. (2009). Click chemistry and bioorthogonal reactions: Unprecedented selectivity in the labeling of biological molecules. *Biochemistry*. <http://doi.org/10.1021/bi9007726>
- Bewersdorf, J., Farese, R. V., & Walther, T. C. (2011). A new way to look at fat. *Nature Methods*, 8(2), 132–133. <http://doi.org/10.1038/nmeth0211-132>
- Bickel, P. E., Tansey, J. T., & Welte, M. A. (2009). PAT proteins, an ancient family of lipid droplet proteins that regulate cellular lipid stores. *Biochimica et Biophysica Acta* -

- Molecular and Cell Biology of Lipids*. <http://doi.org/10.1016/j.bbalip.2009.04.002>
- Boström, P., Rutberg, M., Ericsson, J., Holmdahl, P., Andersson, L., Frohman, M. A., ... Olofsson, S. O. (2005). Cytosolic lipid droplets increase in size by microtubule-dependent complex formation. *Arteriosclerosis, Thrombosis, and Vascular Biology*, 25(9), 1945–1951. <http://doi.org/10.1161/01.ATV.0000179676.41064.d4>
- Bouaid, A., Diaz, Y., Martinez, M., & Aracil, J. (2005). Pilot plant studies of biodiesel production using *Brassica carinata* as raw material. *Catalysis Today*, 106(1), 193–196. <http://doi.org/10.1016/j.cattod.2005.07.163>
- Carle, S. A., Bates, G. W., & Shannon, T. A. (1998). Hormonal control of gene expression during reactivation of the cell cycle in tobacco mesophyll protoplasts. *Journal Of Plant Growth Regulation*. *Fal*, 17(4), 221–230.
- Chapman, K. D., Dyer, J. M., & Mullen, R. T. (2012). Biogenesis and functions of lipid droplets in plants: Thematic Review Series: Lipid Droplet Synthesis and Metabolism: from Yeast to Man. *Journal of Lipid Research*, 53(2), 215–26. <http://doi.org/10.1194/jlr.R021436>
- Chapman, K. D., & Ohlrogge, J. B. (2012). Compartmentation of triacylglycerol accumulation in plants. *Journal of Biological Chemistry*. <http://doi.org/10.1074/jbc.R111.290072>
- Chen, J., Armstrong, A. H., Koehler, A. N., & Hecht, M. H. (2010). Small Molecule Microarrays Enable the Discovery of Compounds That Bind the Alzheimer's A β Peptide and Reduce its Cytotoxicity. *Journal of the American Chemical Society*, 132(47), 17015–17022. <http://doi.org/10.1021/ja107552s>
- Cheng, J., Fujita, A., Ohsaki, Y., Suzuki, M., Shinohara, Y., & Fujimoto, T. (2009). Quantitative electron microscopy shows uniform incorporation of triglycerides into existing lipid droplets. *Histochemistry and Cell Biology*, 132(3), 281–291. <http://doi.org/10.1007/s00418-009-0615-z>
- Chudakov, D. M., Lukyanov, S., & Lukyanov, K. A. (2007). Tracking intracellular protein movements using photoswitchable fluorescent proteins PS-CFP2 and Dendra2. *Nature Protocols*, 2(8), 2024–2032. <http://doi.org/10.1038/nprot.2007.291>
- Coca, M., & San Segundo, B. (2010a). AtCPK1 calcium-dependent protein kinase mediates pathogen resistance in Arabidopsis. *The Plant Journal*, 63(3), 526–540. <http://doi.org/10.1111/j.1365-313X.2010.04255.x>
- Coca, M., & San Segundo, B. (2010b). AtCPK1 calcium-dependent protein kinase mediates pathogen resistance in Arabidopsis. *The Plant Journal*, 63, 526–540. <http://doi.org/10.1111/j.1365-313X.2010.04255.x>
- Cooper, M. S., Hardin, W. R., Petersen, T. W., & Cattolico, R. A. (2010). Visualizing “green oil” in live algal cells. *Journal of Bioscience and Bioengineering*, 109(2), 198–201. <http://doi.org/10.1016/j.jbiosc.2009.08.004>
- Darvas, F., Dorman, G., Krajcsi, P., Puskas, L. G., Kovari, Z., Lorincz, Z., & Urge, L. (2004). Recent advances in chemical genomics. *Curr Med Chem*, 11(23), 3119–3145.
- Darzynkiewicz, Z., Traganos, F., Zhao, H., Halicka, H. D., & Li, J. (2011). Cytometry of DNA

- replication and RNA synthesis: Historical perspective and recent advances based on “click chemistry.” *Cytometry Part A*. <http://doi.org/10.1002/cyto.a.21048>
- de Kroon, A. I. P. M. (2007). Metabolism of phosphatidylcholine and its implications for lipid acyl chain composition in *Saccharomyces cerevisiae*. *Biochimica et Biophysica Acta - Molecular and Cell Biology of Lipids*. <http://doi.org/10.1016/j.bbalip.2006.07.010>
- DiDonato, D., & Brasaemle, D. L. (2003). Fixation Methods for the Study of Lipid Droplets by Immunofluorescence Microscopy. *Journal of Histochemistry & Cytochemistry*, 51(6), 773–780. <http://doi.org/10.1177/002215540305100608>
- Diermeier-Daucher, S., Clarke, S. T., Hill, D., Vollmann-Zwerenz, A., Bradford, J. A., & Brockhoff, G. (2009). Cell type specific applicability of 5-ethynyl-2'-deoxyuridine (EDU) for dynamic proliferation assessment in flow cytometry. *Cytometry Part A*, 75(6), 535–546. <http://doi.org/10.1002/cyto.a.20712>
- Digel, M., Eehalt, R., & F??llekrug, J. (2010). Lipid droplets lighting up: Insights from live microscopy. *FEBS Letters*. <http://doi.org/10.1016/j.febslet.2010.03.035>
- Ding, Y., Yang, L., Zhang, S., Wang, Y., Du, Y., Pu, J., ... Liu, P. (2012). Identification of the major functional proteins of prokaryotic lipid droplets. *Journal of Lipid Research*, 53(3), 399–411. <http://doi.org/10.1194/jlr.M021899>
- Dolbeare, F., Gratzner, H., Pallavicini, M. G., & Gray, J. W. (1983). Flow cytometric measurement of total DNA content and incorporated bromodeoxyuridine. *Proceedings of the National Academy of Sciences of the United States of America*, 80(18), 5573–7. <http://doi.org/10.1073/pnas.80.18.5573>
- Doležel, J., Číhalíková, J., Weiserová, J., & Lucretti, S. (1999). Cell cycle synchronization in plant root meristems. *Methods in Cell Science*, 21(2-3), 95–107. <http://doi.org/10.1023/A:1009876621187>
- Dudits, D., Abrahám, E., Miskolczi, P., Ayaydin, F., Bilgin, M., & Horváth, G. V. (2011). Cell-cycle control as a target for calcium, hormonal and developmental signals: the role of phosphorylation in the retinoblastoma-centred pathway. *Annals of Botany*, 107(7), 1193–202. <http://doi.org/10.1093/aob/mcr038>
- Eastmond, P. J. (2006). SUGAR-DEPENDENT1 encodes a patatin domain triacylglycerol lipase that initiates storage oil breakdown in germinating Arabidopsis seeds. *The Plant Cell*, 18(3), 665–675. <http://doi.org/10.1105/tpc.105.040543>
- Elledge, S. J., Hartwell, L. H., Weinert, T. A., Rusch, H. P., Sachsenmaier, W., Behrens, K., ... Elledge, S. J. (1996). Cell cycle checkpoints: preventing an identity crisis. *Science (New York, N.Y.)*, 274(5293), 1664–72. <http://doi.org/10.1126/science.274.5293.1664>
- Farese, R. V., & Walther, T. C. (2009). Lipid Droplets Finally Get a Little R-E-S-P-E-C-T. *Cell*. <http://doi.org/10.1016/j.cell.2009.11.005>
- Fasano, J. M., Swanson, S. J., Blancaflor, E. B., Dowd, P. E., Kao, T. H., & Gilroy, S. (2001). Changes in root cap pH are required for the gravity response of the Arabidopsis root. *The Plant Cell*, 13(4), 907–921. <http://doi.org/10.1105/tpc.13.4.907>

- Ferullo, D. J., Cooper, D. L., Moore, H. R., & Lovett, S. T. (2009). Cell cycle synchronization of *Escherichia coli* using the stringent response, with fluorescence labeling assays for DNA content and replication. *Methods*, 48(1), 8–13. <http://doi.org/10.1016/j.ymeth.2009.02.010>
- Fowke LC, C. A. (1994). Plant protoplast techniques. In O. K. Harris N (Ed.), *Plant Cell Biology. A Practical Approach* (pp. 177–196). IRL Press, Oxford.
- Frédéric Beaudoin, J. A. N. (n.d.). Targeting and membrane-insertion of a sunflower oleosin in vitro and in *Saccharomyces cerevisiae* : the central hydrophobic domain contains more than one signal sequence, and directs oleosin insertion into the endoplasmic reticulum membrane using a signal . *Planta*, 215(2), 293–303. <http://doi.org/10.1007/s00425-002-0737-1>
- Frey-Wyssling, A., Grieshaber, E., & Mühlethaler, K. (1963). Origin of spherosomes in plant cells. *Journal of Ultrastructure Research*, 8(5-6), 506–516. [http://doi.org/10.1016/s0022-5320\(63\)80052-0](http://doi.org/10.1016/s0022-5320(63)80052-0)
- Fujimoto, T., Ohsaki, Y., Cheng, J., Suzuki, M., & Shinohara, Y. (2008). Lipid droplets: A classic organelle with new outfits. *Histochemistry and Cell Biology*. <http://doi.org/10.1007/s00418-008-0449-0>
- Gáspár, I., & Szabad, J. (2009). In vivo analysis of MT-based vesicle transport by confocal reflection microscopy. *Cell Motility and the Cytoskeleton*, 66(2), 68–79. <http://doi.org/10.1002/cm.20334>
- Ghosh, S., Sen, J., Kalia, S., & Guha-Mukherjee, S. (1999). Establishment of synchronization in carrot cell suspension culture and studies on stage specific activation of glyoxalase I. *Methods in Cell Science*, 21(2-3), 141–148. <http://doi.org/10.1023/A:1009836923004>
- Gidda, S. K., Shockey, J. M., Rothstein, S. J., Dyer, J. M., & Mullen, R. T. (2009). Arabidopsis thaliana GPAT8 and GPAT9 are localized to the ER and possess distinct ER retrieval signals: Functional divergence of the dilysine ER retrieval motif in plant cells. *Plant Physiology and Biochemistry*, 47(10), 867–879. <http://doi.org/10.1016/j.plaphy.2009.05.008>
- Giepmans, B. N. G., Adams, S. R., Ellisman, M. H., & Tsien, R. Y. (2006). The fluorescent toolbox for assessing protein location and function. *Science (New York, N.Y.)*, 312(5771), 217–24. <http://doi.org/10.1126/science.1124618>
- Gocze, P. M., & Freeman, D. A. (1994). Factors underlying the variability of lipid droplet fluorescence in MA-10 Leydig tumor cells. *Cytometry*, 17(2), 151–158. <http://doi.org/10.1002/cyto.990170207>
- Goodman, J. M. (2009). Demonstrated and inferred metabolism associated with cytosolic lipid droplets. *Journal of Lipid Research*, 50(11), 2148–2156. <http://doi.org/10.1194/jlr.R001446>
- Gratzner, H. G. (1982). Monoclonal antibody to 5-bromo- and 5-iododeoxyuridine: A new reagent for detection of DNA replication. *Science (New York, N.Y.)*, 218(4571), 474–475. <http://doi.org/10.1126/science.7123245>
- Greenspan, P., Mayer, E. P., & Fowler, S. D. (1985). Nile red: A selective fluorescent stain for intracellular lipid droplets. *Journal of Cell Biology*, 100(3), 965–973. <http://doi.org/10.1083/jcb.100.3.965>

- Grefen, C., Städele, K., Růžicka, K., Obrdlík, P., Harter, K., & Horák, J. (2008). Subcellular localization and in vivo interactions of the *Arabidopsis thaliana* ethylene receptor family members. *Molecular Plant*, 1, 308–320. <http://doi.org/10.1093/mp/ssm015>
- Guckert, J. B., & Cooksey, K. E. (1990). Triglyceride accumulation and fatty acid profile changes in *Chlorella* (Chlorophyta) during high pH-induced cell cycle inhibition. *Journal of Phycology*. <http://doi.org/10.1111/j.0022-3646.1990.00072.x>
- Hackler, L., Dormán, G., Kele, Z., Üрге, L., Darvas, F., & Puskás, L. G. (2003). Development of chemically modified glass surfaces for nucleic acid, protein and small molecule microarrays. *Molecular Diversity*, 7(1), 25–36. <http://doi.org/10.1023/B:MODI.0000006534.36417.06>
- Haraguchi, T., Shimi, T., Koujin, T., Hashiguchi, N., & Hiraoka, Y. (2002). Spectral imaging fluorescence microscopy. *Genes to Cells*, 7(9), 881–887. <http://doi.org/10.1046/j.1365-2443.2002.00575.x>
- Haugland, R.P.; Spence, M.T.Z.; Johnson, I.D.; Basey, A. (2005). *The Handbook: A Guide to Fluorescent Probes and Labeling Technologies* (10th ed.). Eugene, OR, USA: Molecular Probes.
- Hayashi, K., Hasegawa, J., & Matsunaga, S. (2013). The boundary of the meristematic and elongation zones in roots: endoreduplication precedes rapid cell expansion. *Scientific Reports*, 3, 2723. <http://doi.org/10.1038/srep02723>
- Henrich, S., Salo-Ahen, O. M. H., Huang, B., Rippmann, F., Cruciani, G., & Wade, R. C. (2010). Computational approaches to identifying and characterizing protein binding sites for ligand design. *Journal of Molecular Recognition*, 23(2), 209–219. <http://doi.org/10.1002/jmr.984>
- Hope, R. G., Murphy, D. J., & McLauchlan, J. (2002). The Domains Required to Direct Core Proteins of Hepatitis C Virus and GB Virus-B to Lipid Droplets Share Common Features with Plant Oleosin Proteins. *Journal of Biological Chemistry*, 277(6), 4261–4270. <http://doi.org/10.1074/jbc.M108798200>
- Hsieh, K., & Huang, A. H. C. (2004). Endoplasmic reticulum, oleosins, and oils in seeds and tapetum cells. *Plant Physiology*, 136, 3427–3434. <http://doi.org/10.1104/pp.104.051060>
- Hua, H., & Kearsy, S. E. (2011). Monitoring DNA replication in fission yeast by incorporation of 5-ethynyl-2'-deoxyuridine. *Nucleic Acids Research*, 39(9), e60. <http://doi.org/10.1093/nar/gkr063>
- Ichihashi, Y., Kawade, K., Usami, T., Horiguchi, G., Takahashi, T., & Tsukaya, H. (2011). Key proliferative activity in the junction between the leaf blade and leaf petiole of *Arabidopsis*. *Plant Physiology*, 157(3), 1151–62. <http://doi.org/10.1104/pp.111.185066>
- Jacquier, N., Choudhary, V., Mari, M., Toulmay, A., Reggiori, F., & Schneider, R. (2011). Lipid droplets are functionally connected to the endoplasmic reticulum in *Saccharomyces cerevisiae*. *Journal of Cell Science*, 124(Pt 14), 2424–37. <http://doi.org/10.1242/jcs.076836>
- Jenes, B., & Pauk, J. (1989). Plant regeneration from protoplast derived calli in rice (*Oryza sativa* L.) using dicamba. *Plant Science*, 63(2), 187–198. [http://doi.org/10.1016/0168-9452\(89\)90244-6](http://doi.org/10.1016/0168-9452(89)90244-6)

- Johnson, V. L., Ko, S. C., Holmstrom, T. H., Eriksson, J. E., & Chow, S. C. (2000). Effector caspases are dispensable for the early nuclear morphological changes during chemical-induced apoptosis. *Journal of Cell Science*, 113 (Pt 1), 2941–2953.
- Kaiser, C. L., Kamien, A. J., Shah, P. A., Chapman, B. J., & Cotanche, D. A. (2009). 5-ethynyl-2'-deoxyuridine labeling detects proliferating cells in the regenerating avian cochlea. *Laryngoscope*, 119(9), 1770–1775. <http://doi.org/10.1002/lary.20557>
- Kakar, K., Zhang, H., Scheres, B., & Dhonukshe, P. (2013). CLASP-mediated cortical microtubule organization guides PIN polarization axis. *Nature*, 495(7442), 529–33. <http://doi.org/10.1038/nature11980>
- Kalantari, F., Bergeron, J. J. M., & Nilsson, T. (2010). Biogenesis of lipid droplets--how cells get fatter. *Molecular Membrane Biology*, 27(8), 462–468. <http://doi.org/10.3109/09687688.2010.538936>
- Kapros, T., Nemeth, K., Wu, S. C., Dudits, D., & Center, B. R. (1992). Differential Expression of Histone H3 Gene Variants during Cell Cycle and Somatic Embryogenesis in Alfalfa. *Plant Physiol.*, 98, 621–625. <http://doi.org/10.1104/pp.98.2.621>
- Kelliher, T., & Walbot, V. (2011). Emergence and patterning of the five cell types of the Zea mays anther locule. *Developmental Biology*, 350(1), 32–49. <http://doi.org/10.1016/j.ydbio.2010.11.005>
- Kolb, H. C., & Sharpless, K. B. (2003). The growing impact of click chemistry on drug discovery. *Drug Discov. Today*, 8(24), 1128–1137. [http://doi.org/10.1016/S1359-6446\(03\)02933-7](http://doi.org/10.1016/S1359-6446(03)02933-7)
- Kotogány, E., Dudits, D., Horváth, G. V., & Ayaydin, F. (2010). A rapid and robust assay for detection of S-phase cell cycle progression in plant cells and tissues by using ethynyl deoxyuridine. *Plant Methods*, 6(1), 5. <http://doi.org/10.1186/1746-4811-6-5>
- Kühnlein, R. P. (2012). Thematic review series: Lipid droplet synthesis and metabolism: from yeast to man. Lipid droplet-based storage fat metabolism in Drosophila. *Journal of Lipid Research*, 53(8), 1430–6. <http://doi.org/10.1194/jlr.R024299>
- Kumagai-Sano, F., Hayashi, T., Sano, T., & Hasezawa, S. (2006). Cell cycle synchronization of tobacco BY-2 cells. *Nature Protocols*. <http://doi.org/10.1038/nprot.2006.381>
- Kumagai-Sano, F., Hayashi, T., Sano, T., & Hasezawa, S. (2007). Cell cycle synchronization of tobacco BY-2 cells. *Nature Protocols*, 1(6), 2621–2627. <http://doi.org/10.1038/nprot.2006.381>
- Kuntam, S., Puskás, L. G., & Ayaydin, F. (2015). Characterization of a new class of blue-fluorescent lipid droplet markers for live-cell imaging in plants. *Plant Cell Reports*, 34(4), 655–665. <http://doi.org/10.1007/s00299-015-1738-4>
- Kurat, C. F., Wolinski, H., Petschnigg, J., Kaluarachchi, S., Andrews, B., Natter, K., & Kohlwein, S. D. (2009). Cdk1/Cdc28-Dependent Activation of the Major Triacylglycerol Lipase Tgl4 in Yeast Links Lipolysis to Cell-Cycle Progression. *Molecular Cell*, 33(1), 53–63. <http://doi.org/10.1016/j.molcel.2008.12.019>

- Kuznetsova, M. A., & Sheval', E. V. (2013). Detection of replication sites in the nuclei of plant cells using semithin sections. *Tsitologiya*, 55(5), 324–7.
- Kwok, A. C., & Wong, J. T. (2005). Lipid biosynthesis and its coordination with cell cycle progression. *Plant Cell Physiol*, 46(12), 1973–1986.
- Lea, W. a., & Simeonov, A. (2011). Fluorescence polarization assays in small molecule screening. *Expert Opinion on Drug Discovery*, 6(1), 17–32.
<http://doi.org/10.1517/17460441.2011.537322>
- Lee, H. Y., & Park, S. B. (2011). Surface modification for small-molecule microarrays and its application to the discovery of a tyrosinase inhibitor. *Molecular bioSystems*, 7(2), 304–310.
<http://doi.org/10.1039/c0mb00122h>
- Leif, R. C., Stein, J. H., & Zucker, R. M. (2004). A short history of the initial application of anti-5-BrdU to the detection and measurement of S phase. *Cytometry*, 58A(1), 45–52.
<http://doi.org/10.1002/cyto.a.20012>
- Li, Q., Kim, Y., Namm, J., Kulkarni, A., Rosania, G. R., Ahn, Y.-H., & Chang, Y.-T. (2006). RNA-selective, live cell imaging probes for studying nuclear structure and function. *Chemistry & Biology*, 13(6), 615–623. <http://doi.org/10.1016/j.chembiol.2006.04.007>
- Limsirichaikul, S., Niimi, A., Fawcett, H., Lehmann, A., Yamashita, S., & Ogi, T. (2009). A rapid non-radioactive technique for measurement of repair synthesis in primary human fibroblasts by incorporation of ethynyl deoxyuridine (EdU). *Nucleic Acids Research*, 37(4).
<http://doi.org/10.1093/nar/gkp023>
- Long, A. P., Mannes Schmidt, A. K., Verbrugge, B., Dortch, M. R., Minkin, S. C., Prater, K. E., ... Dalhaimer, P. (2012). Lipid Droplet De Novo Formation and Fission Are Linked to the Cell Cycle in Fission Yeast. *Traffic*, 13(5), 705–714. <http://doi.org/10.1111/j.1600-0854.2012.01339.x>
- Lopez-Serra, L., Lengronne, A., Borges, V., Kelly, G., & Uhlmann, F. (2013). Budding yeast Wapl controls sister chromatid cohesion maintenance and chromosome condensation. *Current Biology*, 23(1), 64–69. <http://doi.org/10.1016/j.cub.2012.11.030>
- Lynes, E. M., & Simmen, T. (2011). Urban planning of the endoplasmic reticulum (ER): How diverse mechanisms segregate the many functions of the ER. *Biochimica et Biophysica Acta - Molecular Cell Research*, 1813(10), 1893–1905.
<http://doi.org/10.1016/j.bbamcr.2011.06.011>
- Magyar, Z., Mészáros, T., Miskolczi, P., Deák, M., Fehér, a, Brown, S., ... Dudits, D. (1997). Cell cycle phase specificity of putative cyclin-dependent kinase variants in synchronized alfalfa cells. *The Plant Cell*, 9(2), 223–235. <http://doi.org/10.1105/tpc.9.2.223>
- Magyar, Z., Veylder, L. De, Atanassova, A., Bakó, L., Inzé, D., & Bögre, L. (2005). The Role of the Arabidopsis E2FB Transcription Factor in Regulating Auxin-Dependent Cell Division. *THE PLANT CELL ONLINE*, 17(9), 2527–2541. <http://doi.org/10.1105/tpc.105.033761>
- Manning, H. C., Lander, A., McKinley, E., & Mutic, N. J. (2008). Accelerating the development of novel molecular imaging probes: A role for high-throughput screening. *J Nucl Med*, 49(9), 1401–1404. <http://doi.org/10.2967/jnumed.108.053009>

- Marin, M. L., Miguel, A., Santos-Juanes, L., Arques, A., Amat, A. M., & Miranda, M. A. (2007). Involvement of triplet excited states in the electron transfer photodegradation of cinnamic acids using pyrylium and thiapyrylium salts as photocatalysts. *Photochemical & Photobiological Sciences*, 6(8), 848–852. <http://doi.org/10.1039/b702752d>
- Martin, S., & Parton, R. G. (2006). Lipid droplets: a unified view of a dynamic organelle. *Nature Reviews. Molecular Cell Biology*, 7(5), 373–378. <http://doi.org/10.1038/nrm1912>
- Maxfield, F. R., & Tabas, I. (2005). Role of cholesterol and lipid organization in disease. *Nature*, 438(7068), 612–621. <http://doi.org/10.1038/nature04399>
- McFie, P. J., Stone, S. L., Banman, S. L., & Stone, S. J. (2010). Topological orientation of acyl-CoA:diacylglycerol acyltransferase-1 (DGAT1) and identification of a putative active site histidine and the role of the n terminus in dimer/tetramer formation. *The Journal of Biological Chemistry*, 285(48), 37377–87. <http://doi.org/10.1074/jbc.M110.163691>
- Melo, R. C. N., D'Avila, H., Wan, H.-C., Bozza, P. T., Dvorak, A. M., & Weller, P. F. (2011). Lipid bodies in inflammatory cells: structure, function, and current imaging techniques. *The Journal of Histochemistry and Cytochemistry: Official Journal of the Histochemistry Society*, 59(5), 540–56. <http://doi.org/10.1369/0022155411404073>
- Menges, M., & Murray, J. A. H. (2002). Synchronous Arabidopsis suspension cultures for analysis of cell-cycle gene activity. *Plant Journal*, 30(2), 203–212. <http://doi.org/10.1046/j.1365-313X.2002.01274.x>
- Miquel, M., Trigui, G., d'Andréa, S., Kelemen, Z., Baud, S., Berger, A., ... Dubreucq, B. (2014). Specialization of oleosins in oil body dynamics during seed development in Arabidopsis seeds. *Plant physiology* (Vol. 164). <http://doi.org/10.1104/pp.113.233262>
- Molnár, E., Hackler, L., Jankovics, T., Üрге, L., Darvas, F., Fehér, L. Z., ... Puskás, L. G. (2006). Application of Small Molecule Microarrays in Comparative Chemical Proteomics. *QSAR & Combinatorial Science*, 25(11), 1020–1026. <http://doi.org/10.1002/qsar.200640080>
- Molnár, E., Kuntam, S., Cingaram, P. K. R., Peksel, B., Suresh, B., Fábíán, G., ... Puskás, L. G. (2013). Combination of small molecule microarray and confocal microscopy techniques for live cell staining fluorescent dye discovery. *Molecules (Basel, Switzerland)*, 18(8), 9999–10013.
- Moran, R., Darzynkiewicz, Z., Staiano-Coico, L., & Melamed, M. R. (1985). Detection of 5-bromodeoxyuridine (BrdUrd) incorporation by monoclonal antibodies: role of the DNA denaturation step. *J Histochem Cytochem*, 33(8), 821–827. <http://doi.org/10.1177/33.8.3860561>
- Mórocz, S., Donn, G., Nérneth, J., & Dudits, D. (1990). An improved system to obtain fertile regenerants via maize protoplasts isolated from a highly embryogenic suspension culture. *TAG. Theoretical and Applied Genetics. Theoretische Und Angewandte Genetik*, 80(6), 721–6. <http://doi.org/10.1007/BF00224183>
- Müller, M., & Schins, J. M. (2002). Imaging the thermodynamic state of lipid membranes with multiplex CARS microscopy. *Journal of Physical Chemistry B*, 106(14), 3715–3723.

<http://doi.org/10.1021/jp014012y>

- Murashige, T., & Skoog, F. (1962). A revised medium for rapid growth and bioassays with tobacco tissue cultures. *Physiologia Plantarum*. <http://doi.org/10.1021/jf9040386>
- Murphy, D. J. (1993). Structure, function and biogenesis of storage lipid bodies and oleosins in plants. *Progress in Lipid Research*, 32(3), 247–80.
- Murphy, D. J. (2001). The biogenesis and functions of lipid bodies in animals, plants and microorganisms. *Progress in Lipid Research*. [http://doi.org/10.1016/S0163-7827\(01\)00013-3](http://doi.org/10.1016/S0163-7827(01)00013-3)
- Murphy, D. J. (2012). The dynamic roles of intracellular lipid droplets: From archaea to mammals. *Protoplasma*. <http://doi.org/10.1007/s00709-011-0329-7>
- Murphy, D. J. (2012). The dynamic roles of intracellular lipid droplets: from archaea to mammals. *Protoplasma*, 249(3), 541–85. <http://doi.org/10.1007/s00709-011-0329-7>
- Nagata, T.; Nemoto, Y.; and Hasezawa, S. (1992). Tobacco BY-2 cell line as the “HeLa” cell in the cell biology of higher plants. In *International Review of Cytology* (132nd ed., pp. 1–29). Academic Press.
- Nakayama, H., Yamaguchi, T., & Tsukaya, H. (2012). Acquisition and Diversification of Cladodes: Leaf-Like Organs in the Genus Asparagus. *The Plant Cell*, 24(3), 929–940. <http://doi.org/10.1105/tpc.111.092924>
- Nan, X., Cheng, J.-X., & Xie, X. S. (2003). Vibrational imaging of lipid droplets in live fibroblast cells with coherent anti-Stokes Raman scattering microscopy. *Journal of Lipid Research*, 44(11), 2202–2208. <http://doi.org/10.1194/jlr.D300022-JLR200>
- Napier, J. A., Stobart, A. K., & Shewry, P. R. (1996). The structure and biogenesis of plant oil bodies: the role of the ER membrane and the oleosin class of proteins. *Plant Molecular Biology*, 31(5), 945–56.
- Notaguchi, M., Wolf, S., & Lucas, W. J. (2012). Phloem-mobile Aux/IAA transcripts target to the root tip and modify root architecture. *Journal of Integrative Plant Biology*, 54(10), 760–772. <http://doi.org/10.1111/j.1744-7909.2012.01155.x>
- Oheim, M. (2011). Advances and challenges in high-throughput microscopy for live-cell subcellular imaging. *Expert Opinion on Drug Discovery*, 6(12), 1299–1315. <http://doi.org/10.1517/17460441.2011.637105>
- Ohsaki, Y., Shinohara, Y., Suzuki, M., & Fujimoto, T. (2010). A pitfall in using BODIPY dyes to label lipid droplets for fluorescence microscopy. *Histochemistry and Cell Biology*, 133(4), 477–480. <http://doi.org/10.1007/s00418-010-0678-x>
- Pang, W.-J., Bai, L., & Yang, G.-S. (2006). Relationship Among H-FABP Gene Polymorphism, Intramuscular Fat Content, and Adipocyte Lipid Droplet Content in Main Pig Breeds with Different Genotypes in Western China. *Acta Genetica Sinica*, 33(6), 515–524. [http://doi.org/10.1016/S0379-4172\(06\)60080-2](http://doi.org/10.1016/S0379-4172(06)60080-2)
- Park, S. H., & Blackstone, C. (2010). Further assembly required: construction and dynamics of

- the endoplasmic reticulum network. *EMBO Reports*, 11(7), 515–521.
<http://doi.org/10.1038/embor.2010.92>
- Peres, A., Ayaydin, F., Nikovics, K., Gutie, C., Gutierrez, C., Horvath, G. V., ... Feher, A. (1999). Partial synchronization of cell division in cultured maize (*Zea mays* L.) cells: differential cyclin, cdc2, histone, and retinoblastoma transcript accumulation during the cell cycle. *Journal of Experimental Botany*, 50(337), 1373–1379.
<http://doi.org/10.1093/jxb/50.337.1373>
- Perilli, S., Perez-perez, J. M., Mambro, R. Di, Peris, L., Díaz-triviño, S., Bianco, M. Del, ... Del Bianco, M. (2013). RETINOBLASTOMA-RELATED protein stimulates cell differentiation in the Arabidopsis root meristem by interacting with cytokinin signaling. *The Plant Cell*, 25(11), 4469–78. <http://doi.org/10.1105/tpc.113.116632>
- Pol, A., Luetterforst, R., Lindsay, M., Heino, S., Ikonen, E., & Parton, R. G. (2001). A caveolin dominant negative mutant associates with lipid bodies and induces intracellular cholesterol imbalance. *Journal of Cell Biology*, 152(5), 1057–1070.
<http://doi.org/10.1083/jcb.152.5.1057>
- Purkrtova, Z., Le Bon, C., Kralova, B., Ropers, M.-H., Anton, M., & Chardot, T. (2008). Caleosin of *Arabidopsis thaliana* : Effect of Calcium on Functional and Structural Properties. *Journal of Agricultural and Food Chemistry*, 56(23), 11217–24.
<http://doi.org/10.1021/jf802305b>
- Puskás, L. G., Fehér, L. Z., Vizler, C., Ayaydin, F., Rásó, E., Molnár, E., ... Kitajka, K. (2010). Polyunsaturated fatty acids synergize with lipid droplet binding thalidomide analogs to induce oxidative stress in cancer cells. *Lipids in Health and Disease*, 9, 56.
<http://doi.org/10.1186/1476-511X-9-56>
- Quastler, H., & Sherman, F. G. (1959). Cell population kinetics in the intestinal epithelium of the mouse. *Experimental Cell Research*, 17(3), 420–438. [http://doi.org/10.1016/0014-4827\(59\)90063-1](http://doi.org/10.1016/0014-4827(59)90063-1)
- Rengachari, S., Bezerra, G. A., Riegler-Berket, L., Gruber, C. C., Sturm, C., Taschler, U., ... Oberer, M. (2012). The structure of monoacylglycerol lipase from *Bacillus* sp. H257 reveals unexpected conservation of the cap architecture between bacterial and human enzymes. *Biochimica et Biophysica Acta*, 1821(7), 1012–21.
<http://doi.org/10.1016/j.bbalip.2012.04.006>
- Rinne, P. L., Kaikuranta, P. M., & van der Schoot, C. (2001). The shoot apical meristem restores its symplasmic organization during chilling-induced release from dormancy. *The Plant Journal : For Cell and Molecular Biology*, 26(3), 249–64.
- Robenek, H., Buers, I., Robenek, M. J., Hofnagel, O., Ruebel, A., Troyer, D., & Severs, N. J. (2011). Topography of Lipid Droplet-Associated Proteins: Insights from Freeze-Fracture Replica Immunogold Labeling. *Journal of Lipids*, 2011, 1–10.
<http://doi.org/10.1155/2011/409371>
- Ron, M., Dorrity, M. W., de Lucas, M., Toal, T., Hernandez, R. I., Little, S. A., ... Brady, S. M. (2013). Identification of Novel Loci Regulating Interspecific Variation in Root Morphology and Cellular Development in Tomato. *Plant Physiology*, 162(2), 755–768.

<http://doi.org/10.1104/pp.113.217802>

- Salic, A., & Mitchison, T. J. (2008). A chemical method for fast and sensitive detection of DNA synthesis in vivo. *Proceedings of the National Academy of Sciences of the United States of America*, 105(7), 2415–20. <http://doi.org/10.1073/pnas.0712168105>
- Schmidt, M. A., & Herman, E. M. (2008). Suppression of soybean oleosin produces micro-oil bodies that aggregate into oil body/ER complexes. *Molecular Plant*, 1(6), 910–24. <http://doi.org/10.1093/mp/ssn049>
- Schubert, I., Schubert, V., & Fuchs, J. (2011). No evidence for “break-induced replication” in a higher plant - but break-induced conversion may occur. *Frontiers in Plant Science*, 2(April), 8. <http://doi.org/10.3389/fpls.2011.00008>
- She, W., Grimanelli, D., Rutowicz, K., Whitehead, M. W. J., Puzio, M., Kotlinski, M., ... Baroux, C. (2013). Chromatin reprogramming during the somatic-to-reproductive cell fate transition in plants. *Development*, 140(19), 4008–19. <http://doi.org/10.1242/dev.095034>
- Shi, H., Liu, K., Xu, A., & Yao, S. Q. (2009). Small molecule microarray-facilitated screening of affinity-based probes (AfBPs) for gamma-secretase. *Chemical Communications*, (33), 5030–5032. <http://doi.org/10.1039/b910611a>
- Shockey, J. M., Gidda, S. K., Chapital, D. C., Kuan, J.-C., Dhanoa, P. K., Bland, J. M., ... Dyer, J. M. (2006). Tung tree DGAT1 and DGAT2 have nonredundant functions in triacylglycerol biosynthesis and are localized to different subdomains of the endoplasmic reticulum. *The Plant Cell*, 18(9), 2294–313. <http://doi.org/10.1105/tpc.106.043695>
- Simeonov, A., Jadhav, A., Thomas, C. J., Wang, Y., Huang, R., Southall, N. T., ... Inglese, J. (2008). Fluorescence spectroscopic profiling of compound libraries. *Journal of Medicinal Chemistry*, 51(8), 2363–2371. <http://doi.org/10.1021/jm701301m>
- Somwar, R., Roberts, C. T., & Varlamov, O. (2011). Live-cell imaging demonstrates rapid cargo exchange between lipid droplets in adipocytes. *FEBS Letters*, 585, 1946–1950. <http://doi.org/10.1016/j.febslet.2011.05.016>
- Spandl, J., White, D. J., Peychl, J., & Thiele, C. (2009). Live cell multicolor imaging of lipid droplets with a new dye, LD540. *Traffic*, 10, 1579–1584. <http://doi.org/10.1111/j.1600-0854.2009.00980.x>
- Sparkes, I. a, Frigerio, L., Tolley, N., & Hawes, C. (2009). The plant endoplasmic reticulum: a cell-wide web. *The Biochemical Journal*, 423(2), 145–155. <http://doi.org/10.1042/BJ20091113>
- Stroobants, C., Sossountzov, L., & Miginiac, E. (1990). DNA synthesis in excised tobacco leaves after bromodeoxyuridine incorporation: immunohistochemical detection in semi-thin spurr sections. *The Journal of Histochemistry and Cytochemistry: Official Journal of the Histochemistry Society*, 38(5), 641–647. <http://doi.org/10.1177/38.5.2185311>
- Targett-Adams, P., Chambers, D., Gledhill, S., Hope, R. G., Coy, J. F., Girod, A., & McLauchlan, J. (2003). Live cell analysis and targeting of the lipid droplet-binding adipocyte differentiation-related protein. *Journal of Biological Chemistry*, 278(18), 15998–16007. <http://doi.org/10.1074/jbc.M211289200>

- Tauchi-Sato, K., Ozeki, S., Houjou, T., Taguchi, R., & Fujimoto, T. (2002). The surface of lipid droplets is a phospholipid monolayer with a unique Fatty Acid composition. *The Journal of Biological Chemistry*, 277(46), 44507–12. <http://doi.org/10.1074/jbc.M207712200>
- Terskikh, A., Fradkov, A., Ermakova, G., Zeraisky, A., Tan, P., Kajava, A. V., ... Siebert, P. (2000). “Fluorescent timer”: protein that changes color with time. *Science*, 290(5496), 1585–1588. <http://doi.org/10.1126/science.290.5496.1585>
- Thiele, C., & Spandl, J. (2008). Cell biology of lipid droplets. *Current Opinion in Cell Biology*. <http://doi.org/10.1016/j.ceb.2008.05.009>
- Tresch, S., Schmotz, J., & Grossmann, K. (2011). Probing mode of action in plant cell cycle by the herbicide endothall, a protein phosphatase inhibitor. *Pesticide Biochemistry and Physiology*, 99(1), 86–95. <http://doi.org/10.1016/j.pestbp.2010.11.004>
- Truernit, E., & Haseloff, J. (2008). A simple way to identify non-viable cells within living plant tissue using confocal microscopy. *Plant Methods*, 4(1), 15. <http://doi.org/10.1186/1746-4811-4-15>
- Tsien, R. Y. (2005). Building and breeding molecules to spy on cells and tumors. In *FEBS Letters* (Vol. 579, pp. 927–932). <http://doi.org/10.1016/j.febslet.2004.11.025>
- Tsien, R. Y. (2009). Constructing and exploiting the fluorescent protein paintbox (Nobel Lecture). *Angewandte Chemie (International Ed. in English)*, 48, 5612–5626. <http://doi.org/10.1002/anie.200901916>
- Vegas, A. J., Bradner, J. E., Tang, W., McPherson, O. M., Greenberg, E. F., Koehler, A. N., & Schreiber, S. L. (2007). Fluorophore-based small-molecule microarrays for the discovery of histone deacetylase inhibitors. *Angewandte Chemie - International Edition*, 46(42), 7960–7964. <http://doi.org/10.1002/anie.200703198>
- Walther, T. C., & Farese, R. V. (2009). The life of lipid droplets. *Biochimica et Biophysica Acta - Molecular and Cell Biology of Lipids*. <http://doi.org/10.1016/j.bbalip.2008.10.009>
- Wang, M. L., Leitch, A. R., Schwarzacher, T., Heslop-Harrison, J. S., & Moore, G. (1992). Construction of a chromosome-enriched HpaII library from flow-sorted wheat chromosomes. *Nucleic Acids Research*, 20(8), 1897–1901. <http://doi.org/10.1099/mic.0.052282-0>
- Wanner, G., Formanek, H., & Theimer, R. R. (1981). The ontogeny of lipid bodies (sphaerosomes) in plant cells - Ultrastructural evidence. *Planta*, 151(2), 109–123. <http://doi.org/10.1007/BF00387812>
- Wanner, G., & Theimer, R. R. (1978). Membranous appendices of sphaerosomes (oleosomes) : Possible role in fat utilization in germinating oil seeds. *Planta*, 140(2), 163–9. <http://doi.org/10.1007/BF00384916>
- Warren, M., Puskarczyk, K., & Chapman, S. C. (2009). Chick embryo proliferation studies using EdU labeling. *Developmental Dynamics*, 238(4), 944–949. <http://doi.org/10.1002/dvdy.21895>
- Watanabe, T., Thayil, A., Jesacher, A., Grieve, K., Debarre, D., Wilson, T., ... Srinivas, S.

- (2010). Characterisation of the dynamic behaviour of lipid droplets in the early mouse embryo using adaptive harmonic generation microscopy. *BMC Cell Biology*, 11, 38. <http://doi.org/10.1186/1471-2121-11-38>
- Watson, P. a, Hanauske-Abel, H. H., Flint, a, & Lalande, M. (1991). Mimosine reversibly arrests cell cycle progression at the G1-S phase border. *Cytometry*, 12(3), 242–246. <http://doi.org/10.1002/cyto.990120306>
- Weissleder, R., & Pittet, M. J. (2008). Imaging in the era of molecular oncology. *Nature*, 452(7187), 580–589. <http://doi.org/10.1038/nature06917>
- Wilson, E. B. (1896). *The cell in development and inheritance*. New York : The Macmillan company,. <http://doi.org/10.5962/bhl.title.46211>
- Wolins, N. E., Quaynor, B. K., Skinner, J. R., Schoenfish, M. J., Tzekov, A., & Bickel, P. E. (2005). S3-12, adipophilin, and TIP47 package lipid in adipocytes. *Journal of Biological Chemistry*, 280(19), 19146–19155. <http://doi.org/10.1074/jbc.M500978200>
- Xiong, Y., McCormack, M., Li, L., Hall, Q., Xiang, C., & Sheen, J. (2013). Glucose-TOR signalling reprograms the transcriptome and activates meristems. *Nature*, 496(7444), 181–6. <http://doi.org/10.1038/nature12030>
- Xu, D., Huang, W., Li, Y., Wang, H., Huang, H., & Cui, X. (2012). Elongator complex is critical for cell cycle progression and leaf patterning in Arabidopsis. *Plant Journal*, 69(5), 792–808. <http://doi.org/10.1111/j.1365-313X.2011.04831.x>
- Yang, H.-J., Hsu, C.-L., Yang, J.-Y., & Yang, W. Y. (2012). Monodansylpentane as a blue-fluorescent lipid-droplet marker for multi-color live-cell imaging. *PloS One*, 7(3), e32693. <http://doi.org/10.1371/journal.pone.0032693>
- Young, C. W., & Hodas, S. (1964). Hydroxyurea: Inhibitory Effect on DNA Metabolism. *Science*, 146(3648), 582–1174. <http://doi.org/10.1126/SCIENCE.146.3648.1172>
- Yun, S.-W., Leong, C., Zhai, D., Tan, Y. L., Lim, L., Bi, X., ... Chang, Y.-T. (2012). Neural stem cell specific fluorescent chemical probe binding to FABP7. *Proceedings of the National Academy of Sciences*, 109(26), 10214–10217. <http://doi.org/10.1073/pnas.1200817109>
- Zanghellini, J., Wodlei, F., & von Grünberg, H. H. (2010). Phospholipid demixing and the birth of a lipid droplet. *Journal of Theoretical Biology*, 264(3), 952–61. <http://doi.org/10.1016/j.jtbi.2010.02.025>
- Zhu, Y., Weng, M., Yang, Y., Zhang, C., Li, Z., Shen, W. H., & Dong, A. (2011). Arabidopsis homologues of the histone chaperone ASF1 are crucial for chromatin replication and cell proliferation in plant development. *Plant Journal*, 66(3), 443–455. <http://doi.org/10.1111/j.1365-313X.2011.04504.x>

ACKNOWLEDGEMENTS

I would like to convey my sincere appreciation and heartfelt gratitude to Dr. Ferhan Ayaydin, for giving me the opportunity to do my PhD under his supervision. He has always been patient, positive and encouraging through all my success and failures. I would like to thank him for his timely critical suggestions, help and reviews. My many thanks to Zsuzsanna Kószó, for all her help and technical assistance.

I also would like to convey my deepest gratitude to Dr. László G. Puskás and Dr. Eszter Molnár for their contribution to this work, help and support.

I would like to thank Prof. Dr. Imre Vass and the Institute of Plant Biology (Biological Research Centre, Hungarian Academy of Sciences, Szeged) for providing Ph.D. fellowship during my studies.

My sincere appreciation and thankfulness towards Dr. Zoltán Magyar and Dr. András Viczián for kindly agreeing to be my referees, for their constructive criticism and diligent comments, which have greatly helped improve the quality of my thesis.

The completion of this project could not have been accomplished without the support of my friends here in Szeged and the ITC family. I also would like to take this opportunity to express my immense gratitude to all the administrative staff of the Institute of Plant Biology and BRC, especially Máriann Karolyi and Timea Varga. My many thanks to Dr. Pradeep Kumar Reddy Cingaram for all his help throughout this project.

Finally, to my parents and my brother, for their endless support and love, which has been my greatest encouragement and motivation towards the completion of my PhD.

SUMMARY

Plant cells store neutral lipids in distinct cytosolic organelles called lipid droplets (LDs). LDs are made up of a neutral lipid core surrounded by a phospholipid monolayer, with a series of proteins bound to/embedded in their surface. LD biogenesis in plants is thought to occur in the ER, where they are assembled in specialized ER microdomains. In the past, LDs were mostly regarded as static carbon depots, but in recent years evidence has emerged pointing towards the presence of dynamic LDs in different cell and also broadening their role in plants including functions such as stress response and pathogen resistance. But much is still unknown about this dynamic organelle.

Furthermore, the neutral lipid content (contained mostly in LDs) of cells has been linked to cell cycle progression. Earlier work has shown that the intensity of neutral lipids of MA-10 Leydig tumor cells labeled with BODIPY 493/503, was a function of the cell cycle. Neutral lipid biosynthesis has also been reported to be coordinated with cell cycle progression in the protist dinoflagellates. Taking the above into account, live cell analysis would be particularly important to unravel the role of LDs in dynamic events such as cell division cycle progression.

In recent years, there have been significant advances in the use of live cell imaging systems with the emergence of a variety of novel imaging tools. Combining a reliable LD marker with these tools can create a versatile scheme for exploring LD biology. However, many commercially available live cell LD dyes such as Nile Red and BODIPY 493/503 have certain drawbacks such as broad emission range and lesser photostability. Other vital LD dyes with better photostability, such as BODIPY 505/515 and LD540, fluoresce in the green to orange region of the visible spectrum, hindering multi-color imaging. Therefore, the identification of a vital dye that can stain LDs while being spectrally well separated from most green, orange and

red fluorescence reporters will be a great asset for live cell imaging in studying LD biology. However, designing a fluorochrome with a specific target in mind (e.g. LD localizing dyes) is a tedious and expensive process. Through the course of this work, a method was developed to combine SMM prescreening and CLSM in order to discover novel cell staining fluorescent dyes. Eleven novel fluorochromes were discovered labeling specific intracellular compartments using human HeLa cells as the model organism. Their labeling was confirmed by co-labeling with known markers and were further studied for optimum working concentrations and toxicity, to assess their use for long-term live cell experiments.

Three of the fluorochromes from the above discovered fluorochromes were found to be plant cell wall permeable and labeling LDs. Ac chemicals (Ac-201, 202 and 1041) derived from the same pool of in-house synthesized trifluoroaminophthalimide derivatives were used in our further studies due to their availability in larger quantities. We have found that all three Ac dyes are cell wall permeable and localize to LDs. All are 405 nm violet laser excitable, compatible with most conventional fluorescence and confocal fluorescence microscopes and emit in the blue range, hence, can be easily combined with different fluorescent reporters for multicolor live cell imaging. We have found that these fluorochromes are highly photostable withstanding multiple successive imaging without photoconversion or fading and are non-toxic and stable enough for long-term analyses. Taken together; our findings demonstrate that these new chemicals provide a novel approach for microscopy analysis of LDs in live plant cells.

Employing these novel LD dyes, LD variability during growth of tobacco cell cultures was studied. It was observed that the total LD volume of the cells were cycling through the different days of the growth curve. Furthermore, we have observed a significant drop of LD volume on day 2 in comparison to the reduced M-phase and high S-phase cells in that day, which

hinted towards a relationship between LD amounts and the cell cycle. To further study this phenomenon, BY-2 cells were blocked in S-phase using hydroxyurea (HU). It was found that there was a considerable decrease in the amount of LDs in blocked cells as compared to control. Two hours after HU block removal, we could observe a reemergence of LDs. While the possible effect of HU as a replicative stress inducer should also be taken into consideration in these experiments, the observation of cyclic LD amount changes during growth curve point towards a possible interrelationship between LDs and the cell division cycle of plant cells. Employing novel LD dyes and microscopy in live plant cells, we postulate that our results have a significant potential to lay the groundwork for better understanding of LD regulation during plant cell division cycle.

ÖSSZEFOGLALÁS

A növényi sejtek olajcseppecskékben avagy lipid dropleteknek (LD-k) nevezett, citoszólikus organellumokban tárolnak neutrális lipideket. Az LD-k magját neutrális lipidek alkotják melyeket egy foszfolipid egyesrétegű burok vesz körül melybe különböző fehérjék ágyazódnak vagy felszínéhez tapadnak. A növényi LD biogenéziséről azt tartják, hogy az endoplazmatikus retikulumban (ER-ben) zajlik le és az LD-k speciális ER mikrodoménékből származnak. Régebben az olajcseppecskéknek csupán szén-raktározó szerepet tulajdonítottak, de az elmúlt években ismertté vált a dinamikus LD-k jelenléte, valamint növényekben igazolták, hogy különböző funkciók ellátását is végzik például stresszválaszok során és patogének elleni rezisztencia alakulásában. Mindemellett, csekély információval rendelkezünk ezekről a dinamikus organellumokról.

A sejtek neutrális lipid tartalma (melyek túlnyomórésze az LD-kben tárolt formában van jelen) továbbá összefüggésbe hozott a sejtosztódási ciklussal is. Egy korábbi tanulmány kimutatta, hogy a BODIPY 493/503–jelölt MA-10 Leydig tumorsejtekben a neutrális lipidek mennyisége sejtciklus függő. A neutrális lipidek bioszintéziséről is leírták, hogy sejtciklus által koordinált dinoflagelláta protistákban zajlik. Mindezeket figyelembe véve, kézenfekvő az LD-k élő sejtben történő vizsgálatának szükségessége, különösen olyan dinamikus folyamatok esetében mint a sejtciklus.

Az elmúlt években jelentős fejlődés történt az élő sejt képalkotási technikákban, és számos új képalkotási eszköz jelent meg. Ezeket az eszközöket, ha kiemelkedő tulajdonsággal rendelkező LD markerekkel kombinálhatjuk, egy vizsgálati sémát hozhatunk létre az LD-k biológiájának kutatására. A legtöbb élő sejtben alkalmazható LD-jelölő festék, mint a Nile Red és a BODIPY 493/503, olyan hátrányos tulajdonságokkal rendelkezik, mint például a széles

emissziós tartomány és alacsony fotostabilitás. Más LD festékek melyek jobb fotostabilitással bírnak, mint például BODIPY 505/515 és LD540, a látható spektrum zöld és narancs tartományában átfedve világítanak, akadályozva ezzel a többszínű képalkotást. Így olyan LD-festékek felfedezése szükséges melyek egy időben specifikus jelölői az LD-knek és spektrálisan is jól elkülönülnek a legtöbb zöld, narancs vagy piros fluoreszcens jelölőmolekulától. Ezek különösen hasznosak lehetnek az LD biológiájának tanulmányozásában élő sejteken belül. Specifikus célobjektumra tervezni fluorokrómot (például LD-lokalizált festéket) azonban egy nagyon összetett és költséges folyamat. A jelen munkában egy olyan módszert fejlesztettünk ki amely kombinálja a kismolekula microarray előszűrési módszert konfokális pásztázó mikroszkópiával, abból a célból, hogy újszerű, élő sejteket festő fluoreszcens markereket azonosítsunk. A módszerünkkel tizenegy új fluorokrómot fedeztünk fel melyek a human HeLa sejtek különböző sejten belüli szervecskéit festik meg. A felfedezett markerek specifikitását ismert markerekkel igazoltuk, majd optimalizálva a koncentrációjukat és toxicitásukat, hosszú távú élő sejtanálízisre való alkalmasságukat vizsgáltuk.

A vizsgált fluorokróмок közül, hármat találtunk melyek áthatolnak a növényi sejt falon és alkalmasak a sejten belüli LD-k specifikus megjelölésére. További kísérleteinkben olyan azonos forrásból szintetizált trifluoro-amino-ftálimid származékokból származó Ac vegyületeket (Ac-201, 202 és 1041) használtunk melyek nagyobb mennyiségben voltak elérhetőek. Azt találtuk, hogy ezek közül mindhárom képes áthatolni a növényi sejt falon és megfesteni az LD olajcseppecskéket. Mindhárom fluorokróm 405 nm hullámhosszú fényel gerjeszthető, ami kompatibilis a legtöbb fluoreszcens és konfokális mikroszkóppal, valamint a kék tartományban bocsátanak ki fényt, így könnyen kombinálhatóak és egyidőben használhatók többszínű élősejtes képanálízisre más fluoreszcens riporter markerekkel. Azt találtuk, hogy ezeknek a

fluorokrómoknak nagy a fotostabilitásuk és többszörös egymás utáni képfelvételt bírnak el fotokonverzió vagy kifakulás nélkül, valamint, nem toxikusak és alkalmasak a hosszú távú sejtanálízishez. Összesítve, eredményeink bizonyították, hogy ezek az új vegyületek egy új megközelítést tesznek lehetővé a növényi LD-k élő sejtekben való mikroszkópiás vizsgálatában.

Ezeket az újonnan felfedezett LD festékeket használva vizsgáltuk dohány sejtkultúrákban az LD-k változását a növekedés során. Azt figyeltük meg, hogy a sejtek össz-LD térfogata ciklikusan változott a növekedés közben. Észrevettük továbbá, hogy a növekedési fázis második napján az össz-LD térfogat ugrásszerűen lecsökken, ellentétben az S-fázisú sejtek számának növekedésével. Ez arra engedett következtetni, hogy összefüggés áll fenn a sejtciklus és LD-k mennyisége között. Tovább vizsgálva ezt a jelenséget, hidroxüreával (HU) blokkoltuk a BY-2 sejteket S-fázisban. Azt találtuk, hogy jelentősen csökkent az LD-k mennyisége a blokkolt sejtekben a kontrollhoz viszonyítva. Megfigyelhettük két órával a HU eltávolítása után az LD-k újbóli megjelenését és mennyiségének növekedését, mely végül a kezeletlen, kontroll sejtekben mért szinttel volt összevethető. Eredményeink egy határozott összefüggést tárnak fel az LD-k és a növényi sejtosztódás ciklusa között. Jelenlegi ismereteink szerint, ez a munka írja le először a növényi LD és sejtciklus közötti, lehetséges ciklikus összefüggést, újonnan kifejlesztett LD-specifikus festékeket és élő növényi mikroszkópiás sejtanalízist alkalmazva.

PUBLICATION LIST (MTMT ID: 10048547)

1. **Soujanya Kuntam**, László G. Puskás, Ferhan Ayaydin (2015) Characterization of a new class of blue-fluorescent lipid droplet markers for live-cell imaging in plants. **Plant Cell Rep**, 34:655-665. IF: 3.071
2. **Soujanya Kuntam** and Ferhan Ayaydin (2015) Detection of S-phase of cell division cycle in plant cells and tissues by using 5-ethynyl-2'-deoxyuridine (EdU). In: Plant Microtechniques and Protocols, Springer International Publishing, pp 311-322.
3. Eszter Molnár*, **Soujanya Kuntam***, Pradeep Kumar Reddy Cingaram, Begüm Peksel, Bhavyashree Suresh, Gabriella Fábián, Liliána Z. Fehér, Attila Bokros, Ágnes Medgyesi, Ferhan Ayaydin, László G. Puskás (2013) Combination of small molecule microarray and confocal microscopy techniques for live cell staining fluorescent dye discovery. **Molecules**, 18:9999-10013. IF: 2.416

(* EM and SK contributed equally to this work)